EFFEROCYTOSIS DRIVES TUMOR GROWTH VIA MYELOID-INTRINSIC NLRP3/CASPASE-1/IL-1B SIGNALING AXIS

By

Cara Noel Lang

Dissertation

Submitted to the Faculty of the

Graduate School of Vanderbilt University

in partial fulfillment of the requirements

for the degree of

DOCTOR OF PHILOSOPHY

in

Molecular Pathology and

Immunology

December 17, 2022

Nashville, Tennessee

Approved:

Jeff Rathmell, Ph.D.

C. Henrique Serezani, Ph.D.

Vivian Weiss, M.D., Ph.D.

Ben Park, M.D., Ph.D.

Young Kim, M.D., Ph.D.

In memory of my dad who didn't get the chance to see me finish my Ph.D., but who I know would be endlessly proud.

ACKNOWLEDGMENTS

It is true when they say that it takes a village to raise a Ph.D. I am eternally thankful for everyone who has helped me get to this point. I would first like to thank my advisor, Dr. Young Kim, and my adoptive advisor, Dr. Henrique Serezani. Young, thank you for mentoring me throughout my first four years of graduate school. Thank you for always pushing me to investigate difficult questions while still giving me the freedom to explore my interests. Your mentorship allowed me to grow independently while still being there when I needed guidance. I am grateful for every opportunity you gave me to grow as a scientist over the years. Henrique, thank you for adopting me after Young left. Over this last year, you have always had my best interests in mind and have provided so much great advice. Throughout graduate school you helped me to become a better scientist by teaching me to always question my data and reagents. You have also helped to shape my thesis with your expert advice on everything inflammasome. Thank you so much for your mentorship and help getting me over the finish line.

I would also like to thank my thesis committee, Dr. Jeff Rathmell, Dr. Vivian Weiss, and Dr. Ben Park for their mentorship. Each of you played an important role in guiding my thesis. Your questioning during our meetings helped to build my critical thinking and reasoning skills and has helped me become a better scientist. I would especially like to thank Vivian for always making time to meet with me for both scientific and life advice.

Next, I'd like to acknowledge the Vanderbilt Program in Molecular Medicine (VPMM) for giving me the opportunity to gain clinical trial experience. I'd especially like to thank my clinical advisor, Dr. Mike Gibson. Mike thank you for allowing me to follow you around in clinic and teaching me so much about medical oncology. Mike, you also helped me to become a better scientific presenter by helping me to focus on the broader picture and clinical relevance

of my work.

I am extremely thankful for everyone who has been a part of the Kim lab. I would like to thank Dr. Mike Korrer for the huge role that he played in my graduate school experience. Mike, thank you for teaching me everything immunology. Thank you so much for always being available when I needed advice and answering any question no matter how stupid. Thank you for challenging me scientifically. More importantly, thank you for being such a great friend along the way. I would also like to thank Dr. Sohini Roy for being the best scientific collaborator, answering all my myeloid cell questions, and all your help with our paper. Diana Graves, Gabriel Rodriguez, and David Taylor thank you for your friendship, help and support along the way, and for always being available to commiserate about graduate school. Hanwen Feng, thank you for being the best undergraduate researcher and always being game to help with any experiment and learn new techniques. Brandee Brown and Jim Koch thank you both for keeping the lab up and running and making sure I had everything I needed for experiments. Brandee thank you for all your help with sample collection and processing. I would also like to thank all the patients who provided these samples. You are the reason we do this research in the first place and without you this would not be possible.

I would also like to thank the Barry Baker family who not only funded my research but also my salary throughout graduate school. Without your generous gift none of this work would have been possible.

Next, I'd like to thank my undergraduate research advisors that showed me how much I loved science and helped me know that a Ph.D. was the right path. I'd like to thank Dr. Tim Evans who first saw my potential to become a great scientist and showed me the path to get there. Dr. Jill Henning, thank you for igniting my love for immunology. Thanks to Dr. Rebecca Webb and Dr. Lisa Bell-Loncella for being the best advisors and offering great advice even years after I

graduated. I'd also like to thank Dr. Rita Mihailescu at Duquesne University, Dr. Shawn Lupold at the Johns Hopkins University, and Dr. Joseph Kissil at the Scripps Research Institute for allowing me to join your labs for a summer. I learned so much during those summers and am so thankful for your mentorship.

Sarah and Veronika, I don't know if I can put into words how much your friendship means to me. You two are truly my friend soulmates. Thank you for always being there for me in both sad and happy times and helping me through every obstacle. Jenna and Yvonne, thank you for being my PMI sounding board, and for helping me through quals, MPT talks, committee meetings, and now my defense. Thank you to my amazing friend support system back in Pennsylvania. Jamie, Jess, Christy, Nicole, Chelsea, and Ethan, thank you all for being lifelong friends regardless of the distance that separated us. Thank you for always being available to talk and for making time to see me every time I visited home. Thank you for sticking by my side throughout all my major life events over the last 5 years.

Next, I'd like to thank Dr. Taylor Swift. She has been the one artist to help me through everything in my life, including graduate school. Her music was on a constant loop while spending long hours doing experiments in lab, analyzing data, and writing this dissertation. I am honored that we both received our doctorates in the same year.

When I got married last year, I gained the most amazing bonus family. I would like to thank the Wilsons for the endless love and support throughout this journey. Karen and Ron thank you for always thinking of me and checking in to make sure I'm doing okay. Kevin thank you for being my go-to tech advisor when my laptop or phone breaks and I need help picking a new one. Also thank you for helping Ryan fix our Wi-Fi because this thesis would not have happened without that. Amanda thank you for keeping life fun and never saying no to a trip to visit us in Nashville. Thank you to the entire Wilson extended family for always checking in on me and

asking to hear about my research.

I also want to thank my best friend in the entire world, my mom. Thank you for your endless support throughout graduate school and my entire life. Thank you for always being there to listen to me complain or deal with my attitude when I'm stressed. Thank you for being my go-to person whenever I need advice on anything. Thanks for offering your opinions even when I don't ask for them because I always listen anyway. I would not be the person I am today without you and words cannot express how grateful I am for you. I would also like to thank my dad to whom this dissertation is dedicated. While he is no longer with us today, I know he is continuously looking down on me with endless pride. Thank you for shaping me to become the person I am today. Everything I do is for you.

Lastly, I would like to thank my family. To my dog Nelli, thank you for bringing me endless joy and entertainment. Thank you for greatly improving my mental health just by being in my life. To my husband Ryan, I can't thank you enough for everything you have supported me through. Thank you for dealing with my stress crying and constant graduate school related anxiety. Thank you for being there through all the good and the bad. I'm so lucky to have you in my life and I can't wait to see where we go from here.

TABLE OF CONTENTS

LIST OF TABLES

Table **Page**

LIST OF FIGURES

Figure **Page**

LIST OF ABBREVIATIONS

AC	apoptotic cells
AIF1	allograft inflammatory factor 1
AIM2	absent in melanoma 2
ANOVA	analysis of variance
AP-1	activator protein 1
ASC	apoptosis-associated speck-like protein containing a CARD
ATP	adenosine triphosphate
Axl	tyrosine protein kinase receptor
BAI-1	brain-specific angiogenesis inhibitor 1
BMDM	bone marrow derived macrophages
C1QC	complement component 1Q
CANTOS	canakinumab anti-inflammatory thrombosis outcome study
CAR	chimeric antigen receptor
Casp	caspase
CCL/CCR	C-C motif chemokine ligand/receptor
cDC	conventional dendritic cell
CFP	complement factor properdin
CFSE	carboxyfluorescein succinimidyl ester
CRISPR	clustered regularly interspaced short palindromic repeats
CTL	cytotoxic T lymphocyte
CTLA-4	cytotoxic T lymphocyte associated protein 4
CXCR/L	C-X-C motif chemokine receptor/ligand
DAMP	damage associated molecular pattern
DAPI	4′,6-diamidino-2-phenylindole
DC	dendritic cell
DNA	deoxyribonucleic acid
ECM	extracellular matrix
EGFR	epidermal growth factor receptor
ELISA	enzyme-linked immunosorbent assay
FDA	Food and Drug Administration
FPR1	formyl peptide receptor 1
Gal3	galectin-3
Gas6	growth arrest-specific gene 6
GI	gastrointestinal

GM-CSF	granulocyte-macrophage colony-stimulating factor
GO	gene ontology
GSDMD	gasdermin D
GSEA	gene set enrichment analysis
HDAC	histone deacetylase
HER2	human epidermal growth factor receptor 2
Hif-1α	hypoxia inducible factor 1 subunit alpha
HIV	human immunodeficiency virus
HNSCC	head and neck squamous cell carcinoma
HSV	herpes simplex virus
IFI16	interferon gamma inducible protein 16
IFN-γ	interferon gamma
IL	interleukin
INHBA	inhibin subunit beta A
IPA	ingenuity pathway analysis
IRF4	interferon regulatory factor 4
ISG15	ubiquitin-like molecule interferon-stimulated gene 15
KIT	proto-oncogene, receptor tyrosine kinase
KLRC1	killer cell lectin like receptor C1
KO	knockout
LAG3	lymphocyte activating 3
LILRA4	leukocyte immunoglobulin-like receptor subfamily A
LPS	lipopolysaccharide
LST1	leukocyte-specific transcript 1
LYZ	lysozyme
MDSC	myeloid derived suppressor cell
MerTK	Mer proto-oncogene tyrosine kinase
MHC	major histocompatibility complex
MOC	mouse oral squamous cell carcinoma
MoMacDC	mononuclear phagocytes
MS4A1	membrane spanning 4-domains A1
MyD88	myeloid differentiation primary response 88
NF-κB	nuclear factor κB
NIH	National Institutes of Health
NK	natural killer cells

NLRC4	Nod-like receptor family CARD domain containing 4
NLRP	nucleotide-binding domain-like receptor protein 3
OSM	oncostatin M
PAMP	pathogen activated molecular pattern
PBMC	peripheral blood mononuclear cell
PBS	phosphate buffered saline
PCA	principal component analysis
PD-1/PD-L1	programmed death-1/ligand
pDC	plasmacytoid dendritic cell
PI	propidium iodide
PI3	phosphoinositide 3
PRR	pattern recognition receptor
PS	phosphatidylserine
PYCARD	gene for ASC
RBC	red blood cell
RNA	ribonucleic acid
S1P	sphingosine-1-phosphate
scRNA-seq	single cell RNA sequencing
SD	standard deviation
SEM	standard error of the mean
SERPINA1	serpin peptidase inhibitor, clade a member 1
SIRPα	signal-regulatory protein alpha
SPP1	secreted phosphoprotein 1
STING	stimulator of interferon genes
TAM	tumor associated macrophage
TCGA	The Cancer Genome Atlas
TGF-β	transforming growth factor beta
Th	T helper cell
TIM-4	T cell transmembrane, immunoglobulin, and mucin
TIMP1	tissue inhibitor of metalloproteinases 1
TLR	toll-like receptor
TME	tumor microenvironment
TNF-α	tumor necrosis factor alpha
Treg	T regulatory cell
tSNE	t-distributed stochastic neighbor embedding

Tyro-3	tyrosine protein kinase
UMAP	uniform manifold approximation and projection for dimension reduction
UMI	unique molecular identifier
VCAN	versican
VEGF	vascular endothelial growth factor
WT	wildtype

CHAPTER 1

Title of Chapter: Background and Research Objectives

1.1 The Tumor Microenvironment

The tumor microenvironment (TME) is a complex matrix made up of many cell types including tumor cells, stromal cells, blood vessels, immune cells, and extracellular matrix (ECM) to support tumor growth. This microenvironment is dynamic and changes as the tumor grows.[1] Early in tumor growth, the components of the TME are essential to support cancer cell survival and local invasion through promotion of angiogenesis, nutrient supply, and prevention of immune destruction.[2]

Growing knowledge of the complex interplay between the immune system and tumors has shown an increasing pro-tumorigenic role of the immune system. In fact, avoiding immune destruction and tumor promoting inflammation are now recognized as two hallmarks of cancer.[3] Both of these immune-related hallmarks help to underscore the complex relationship between immune cells and tumor cells within TME. The type of immune infiltrate to the tumor can greatly impact patient outcomes and responses to therapy.

Tumors can be categorized based on the type, density, and location of immune cell infiltration. The quality of immune infiltration is quantified by a standardized scoring system known as Immunoscore allowing for an immune based, rather than tumor based, classification of tumors.[4-6] Tumors given a high Immunoscore are considered highly infiltrated or "hot" tumors while tumors with a low Immunoscore are non-infiltrated or "cold".[4, 7] While the Immunoscore only takes into account adaptive immune cells, "hot" tumors are typically T cell high and myeloid cell low, producing an anti-tumor environment. Conversely, "cold" tumors can either be T cell low and

myeloid cell high generating an immune suppressive environment or immune deserts with little to no immune infiltration (Figure 1.1).

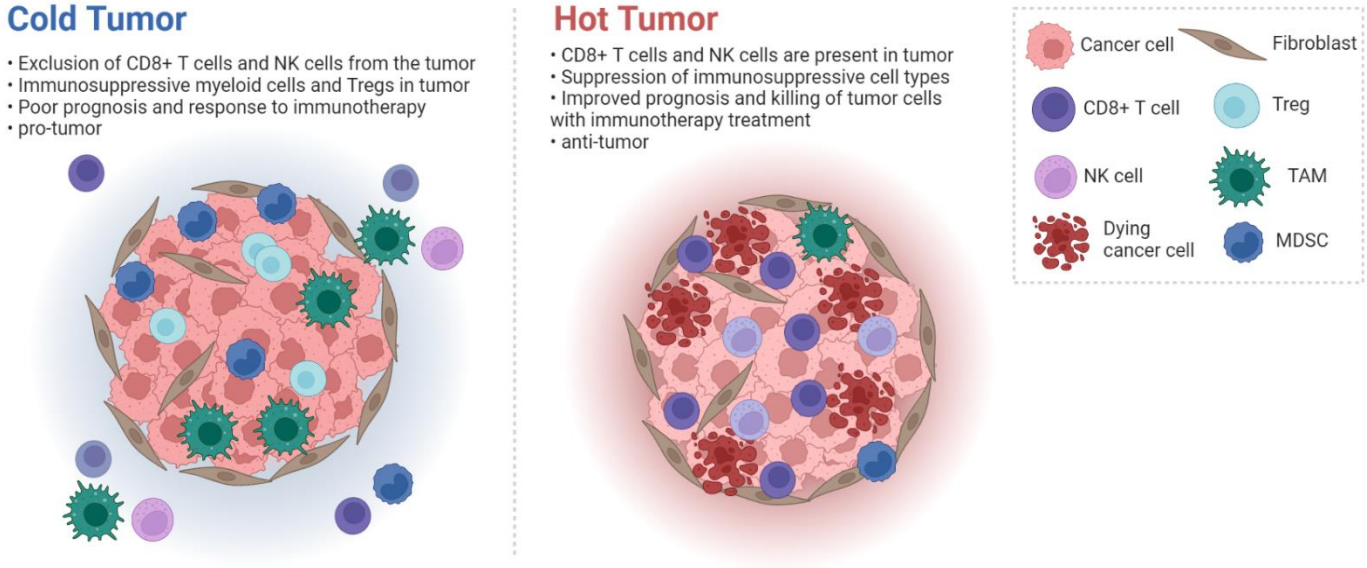

Figure 1.1 The TME can be classified as immune cold or immune hot depending on the immune composition. Immune cold tumors are classified by the exclusion of cytotoxic T cells and NK cells from the TME as well as immunosuppression mediated by myeloid cells and T regulatory cells leading to a pro-tumor environment (left). Conversely, immune hot tumors have high T and NK cell infiltration and less infiltration of immunosuppressive myeloid cells and Tregs. This leads to an anti-tumor immune response and improved response to immunotherapy (right). Figure made with BioRender.

1.2 T Cells in Cancer

Within the TME, cytotoxic T lymphocytes (CTL) and NK cells are the two major cell populations that can directly eliminate tumor cells. CTLs detect abnormal cancer antigens and target the tumor cells for destruction. Thus, an abundance of CTLs and NK cells in the TME typically corresponds to more positive outcomes in patients.[2] Two mechanisms by which CTLs induce cell death in tumor cells are perforin and granzyme-mediated cell lysis and ligation of cell death receptors resulting in apoptosis of the target cells. CTLs recognize target cells in an antigen dependent manner through the recognition of presented peptides in the context of MHC on antigen presenting cells (DCs, macrophages, B cells) by their T cell receptor. Full activation of these CTLs

also requires ligation of costimulatory molecules, such as CD28, CD80, and CD86. Once the target cell is recognized, the lytic molecule perforin is released resulting in pore formation in the membrane of the target cell which allows granzyme to enter the cell and induce apoptosis. Conversely, cell death can also be stimulated through interaction between Fas and FasL activating the apoptotic cascade.[8]

T cell cytotoxic activity is highly regulated to prevent out of control T cell activity and autoreactive T cell responses. One mechanism for preventing this is through the upregulation of inhibitory receptors on the surface of activated T cells which downregulates T cell function resulting in T cell exhaustion.[9] Due to consistently high stimulation in the TME, tumor infiltrating T cells typically show increased expression of inhibitory receptors.[10] CTLA-4 and PD-1 are two well studied inhibitory receptors that are utilized frequently in the clinic for cancer therapy.

Another mechanism in place to prevent out of control T cell activity are regulatory T cells (Tregs). Under typical immune responses, Tregs suppress inflammation and immune responses towards the resolution of infection to prevent out of control inflammation and autoimmune reactions. However, in the context of cancer, Tregs promote tumor survival through inhibition of the anti-tumor CTL response. Tregs can also directly interact with stromal cells in the TME to promote cancer cell survival through the production of growth factors.

In addition to Tregs, there are other subsets of $CD4^+$ T cells that play a key role in the TME. Th1 cells aid in the CTL and NK responses through the production of IFN-γ and thus play an anti-tumor role within the TME.[11] Conversely, Th2 cells produce many immune suppressive and anti-inflammatory cytokines such as IL-4, IL-5, and IL-10 which aid in tumor growth.[11] While the presence of these pro and anti-inflammatory cytokines exist in a balance within the TME, a skewing in either direction makes a big difference in generation of an immune permissive or

restrictive environment. The role of Th17 cells in the TME still remains controversial. These cells display both pro and anti-tumorigenic properties through promotion of both anti-tumor CTL and Th1 responses as well as tumor-promoting tumor associated macrophages (TAMs).[12, 13]

1.3 Myeloid Cells in Cancer

Myeloid cells are a critical component of the immune system with primary inflammatory and regenerative functions including phagocytosis, antigen presentation, and tissue repair. However, many of these functions become pro-tumorigenic within the TME resulting in a worse prognosis for patients with high macrophage and myeloid content tumors.[2]

During cancer progression, there is a high turnover of myeloid cells due to the induction of a chronic inflammatory response. Therefore, emergency myelopoiesis is initiated to allow for the continuous production and trafficking of myeloid cells to the tumor to fill this need.[14] Normal myelopoiesis is typically altered in cancer patients with a skewing away from the hematopoietic lineage resulting in the production of even more myeloid cells.[15] This causes an accumulation of immunosuppressive myeloid cells in the TME.

Tumor-associated macrophages (TAMs) are the most abundant myeloid subset within the TME and are generally associated with poor prognosis.[16] TAMs within the TME are highly heterogenous and the traditional M1/M2 nomenclature is unable to accurately define the spectrum of macrophage subtypes within the TME. Further, these macrophage subtypes are highly plastic and can evolve throughout tumor progression as well as after various treatments. During early phases of tumor development, TAMs display more M1-like characteristics and are more pro-inflammatory in nature. However, as a tumor progresses, TAMs will have a more M2-like phenotype with angiogenic and immunosuppressive functions.[17] Due to this plasticity and heterogeneity, TAMs are more commonly classified by their function in the TME rather than the

traditional M1/M2 subtypes (Figure 1.2).

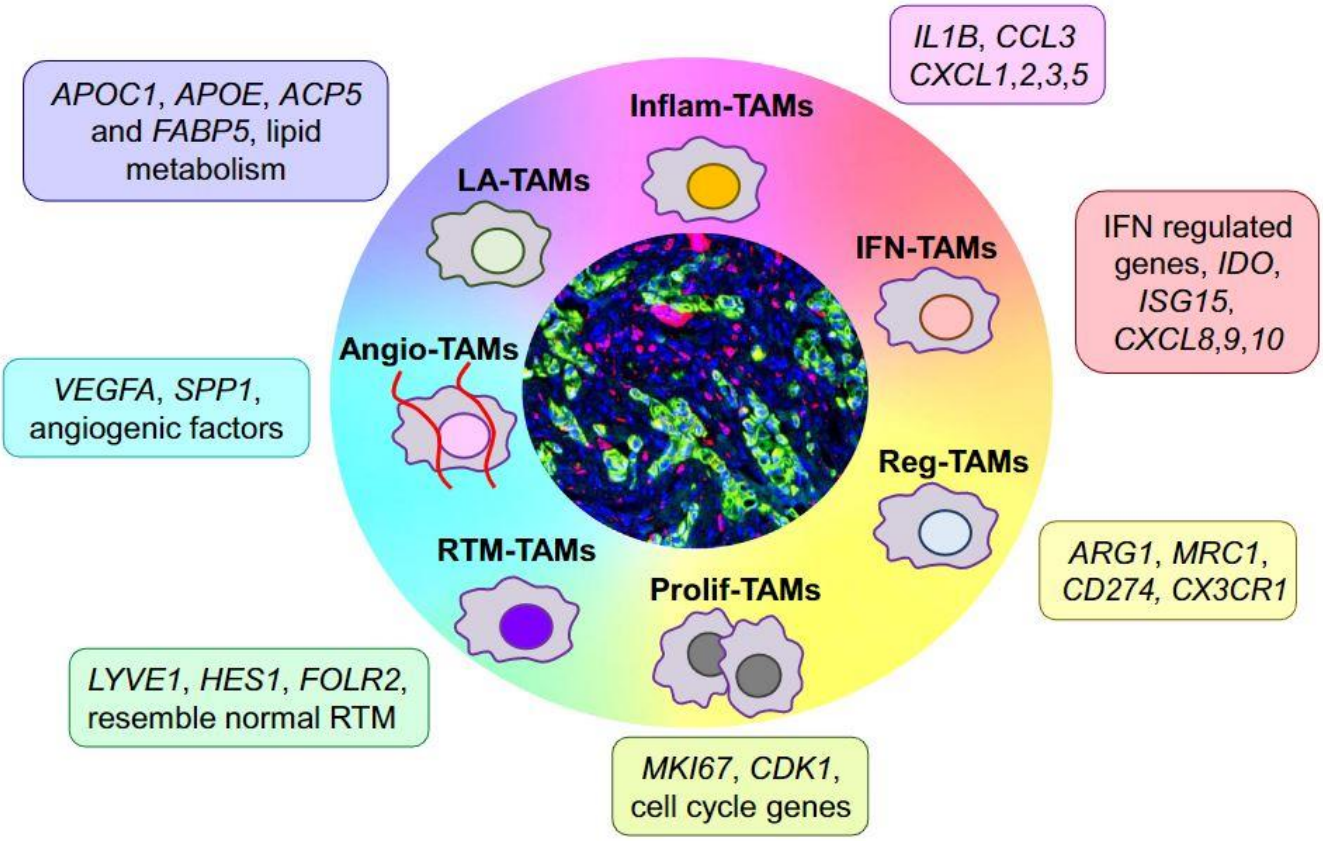

Figure 1.2 Heterogeneity of TAMs and their functions within the TME led to new classification of TAM subtypes. In depth sequencing analysis of the myeloid milieu in the TME revealed 7 new classifications of TAMs. IFN-TAMs have high expression of IFN-regulated genes and most closely align with the traditional M1 subset but still display T cell suppressive functions. Reg-TAMs encompasses macrophages with a wound healing gene signature that most closely resembles alternatively activated macrophages. Prolif-TAMs have high expression of Ki67 and cell cycle regulation genes and could act as a parent population giving rise to the other TAM subsets in the TME. RTM-TAMs most closely resemble tissue resident macrophages from tumor adjacent normal tissue and may regulate environmental cues. Angio-TAMs have a pro-angiogenic gene signature with high expression of angiogenic factors such as VEGF. These cells are typically enriched in hypoxic areas of the tumor. LA-TAMs have high expression of genes involved in lipid metabolism and oxidative phosphorylation pathways and are associated with immunosuppression and immune tolerance. Inflam-TAMs have high expression of inflammatory cytokines associated with the recruitment of pro-inflammatory immune cells to the TME. These TAM subsets are not exhaustive and can differ based on tumor type.[18]

Another important myeloid cell subset in the TME are myeloid derived suppressor cells (MDSCs). MDSCs are important mediators of immune evasion in cancer. Tumor infiltrating MDSCs are associated with worse overall survival and progression free survival in several types of solid tumors and are thought to establish an immunosuppressive TME through the inhibition of T cell effector function. MDSCs also have a direct pro-tumorigenic role within the TME by stimulating angiogenesis, proliferation, and motility.

Like TAMs, MDSCs are also heterogeneous with two major subtypes found in abundance in the TME. Granulocytic MDSCs (g-MDSCs) most closely phenotypically resemble neutrophils whereas monocytic MDSCs (m-MDSCs) more closely resemble immature monocytes. Since both of these subsets phenotypically and morphologically mimic other cell types, MDSCs can only truly be identified by their immunosuppressive function.[19] M-MDSCs are more highly enriched within the TME and have more potent immunosuppressive functionality than g-MDSCs. In addition, m-MDSCs are highly plastic with the ability to differentiate into TAMs as well as into g-MDSCs based off of environmental cues within the TME.[20]

The myeloid cell landscape is highly dependent on cues within the TME. Nutrient levels, cytokine production, metabolite presence, and soluble factors released from the tumor cells can all dictate the composition and function of myeloid cells in the TME. Further, the myeloid milieu is highly plastic and constantly changes throughout the duration of tumor development. However, the interaction goes both ways as the presence of myeloid cells critically shapes the TME to foster tumor growth. Both MDSCs and TAMs support immunosuppression and establish peripheral tolerance to inhibit the initiation of anti-tumor adaptive responses. These cells deplete CTLs of key nutrients preventing their function and expansion within the TME. MDSCs and TAMs support tumor growth directly through sustaining the metabolic needs of the tumor cells for continued

growth, promotion of angiogenesis to allow key nutrient delivery to tumor cells, and remodeling of the extracellular matrix to support tumor proliferation and invasion. [21]

1.4 The Hallmarks of Cancer

The hallmarks of cancer are a set of functional characteristics acquired by cells which allow them to transition from healthy cells to form malignant tumors (Figure 1.3). This framework was introduced to outline the common features among different tumors to better understand the multistep process of neoplastic transformation. Two of the more recently added hallmarks of cancer, avoiding immune destruction and tumor-promoting inflammation, highlight the importance of a pro-tumorigenic immune microenvironment for tumor growth.[3]

1.4.1 Evading immune destruction

A controversial topic surrounding tumor formation is the exact role that the immune system plays in tumor progression. As discussed previously, the immune composition of the TME plays a huge role in generating a pro or anti-tumorigenic environment. One acquired characteristic of tumors is the ability to skew this environment toward an immunosuppressive and tumor promoting phenotype which allows the growing tumor to evade immune destruction.[3] According to the theory of immune surveillance in which cells are constantly monitored by the immune system for abnormalities, very early neoplasms are constantly being recognized and eliminated within the human body.[22] However, in order for a tumor to grow, it must escape this immune surveillance which can be accomplished through an immunosuppressive TME. This is mediated primarily through the immunosuppressive TAMs, MDSCs, and Tregs.

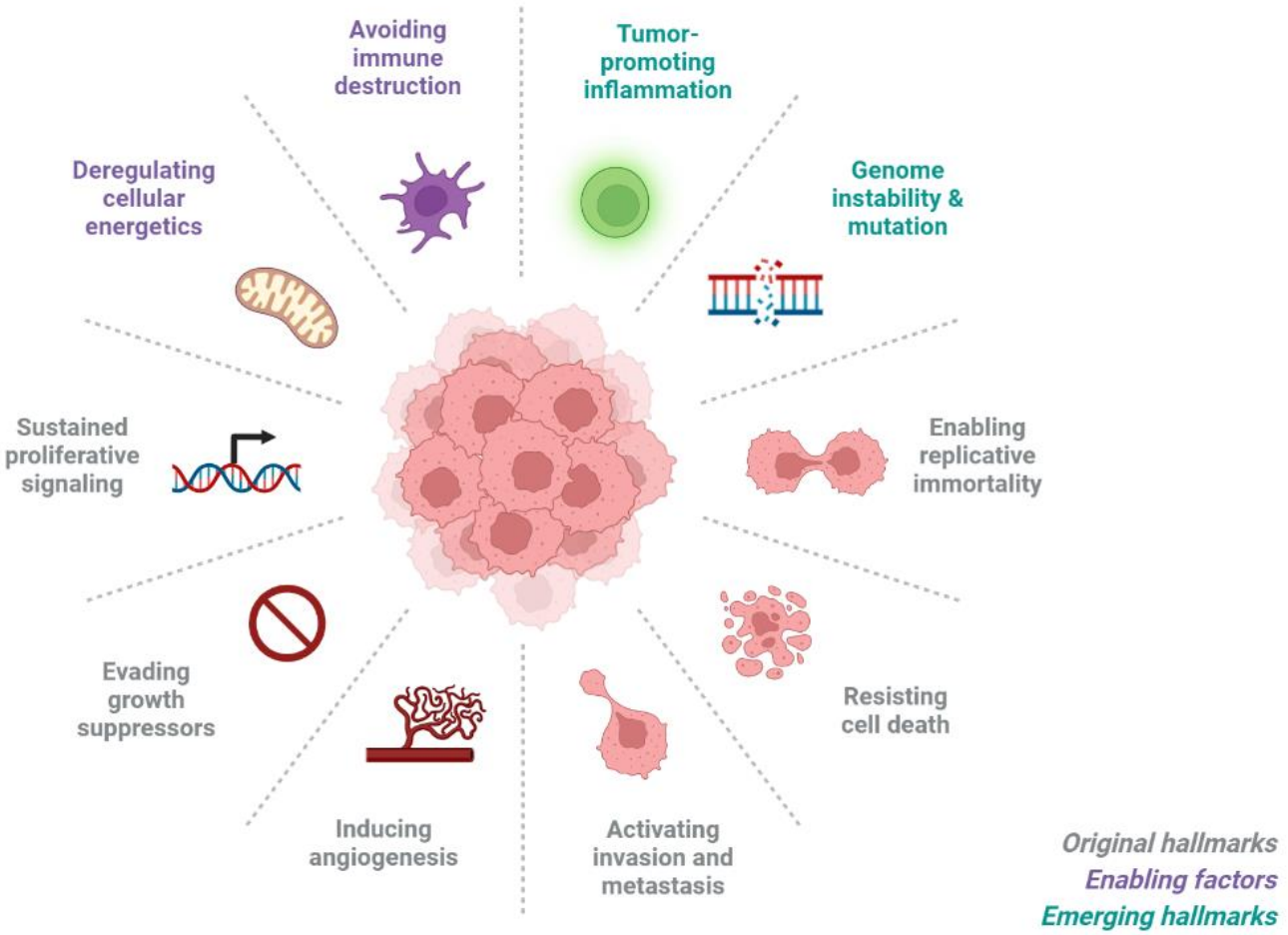

Figure 1.3 The hallmarks of cancer describe 10 acquired characteristics that enable tumor formation and growth. The hallmarks of cancer were generated to provide a framework for understanding pro-tumorigenic characteristics that a tumor gains to promote its survival. These characteristics can be broadly applied across all tumors. Characteristics such as genome instability, enabling replicative immortality, evading growth suppressors, and sustaining proliferative signaling describe the malignant transformation that occurs within a tumor cell to promote neoplasm formation. Characteristics like tumor-promoting inflammation, avoiding immune destruction, and resisting cell death are most important to foster the growth and survival of the new tumor. Induction of vasculature and activating invasion and metastasis become important once the tumor is established to promote dissemination of the tumor cells throughout the body. [23] Figure made with Biorender.com.

Within the TME, many mediators are produced by both the tumor cells and immunosuppressive immune cells to help evade immune recognition of the tumor. These mediators include cytokines such as TGF-β, IL-6, IL-10, and TNF-α. Cytokine production, as well as the production of VEGF, can inhibit dendritic cell maturation thus downregulating the presentation of tumor antigens to CTLs.[24, 25]

Another mechanism of evading immune destruction is through sustained T cell exhaustion within the TME. Exhausted T cells are in a terminally differentiated state and have high expression of exhaustion markers, such as PD-1 and LAG3. Expression of exhaustion markers is increased on T cells within the TME and further increases throughout the duration of tumor growth indicating that more effector T cells are transitioning to an exhausted state which is disadvantageous for a sustained anti-tumor T cell response.[26]

1.4.2 Cancer-promoting inflammation

Another important hallmark of cancer is the enabling characteristic of tumor-promoting inflammation. Cancer-associated inflammation is characterized by cytokine production, immune infiltration, angiogenesis, and tissue remodeling which plays an important role in promoting cancer formation, proliferation, invasion, and metastasis.[3] Acute inflammation is important for the wound healing process, however cancer acts as a wound that does not heal resulting in chronic inflammation-induced tissue remodeling and T cell dysfunction.[27, 28] Further, inflammation can foster a pro-tumor niche allowing early neoplasms to develop into large cancerous lesions.[29, 30] It is now becoming evident that an inflammatory TME is essential for tumorigenesis.

Tumor-promoting inflammation is mostly mediated through activation of innate immune cells. Activation of the innate immune system contributes directly to tumor growth through addition of

bioactive molecules in the TME, such as growth factors for sustained proliferative signaling, proangiogenic factors, survival factors, and ECM modifying factors to promote vascularization and metastasis of the tumor cells.[29, 31-33] In addition, chronic inflammation can also induce oncogenic mutations and genomic instability in cells causing neoplastic transformation. Further, chronic inflammation in the TME results in the secretion of immune regulatory cytokines allowing the potentiation of immune regulatory cells such as MDSCs and TAMs.[34, 35] Due to this, cancer-promoting inflammation is considered an enabling characteristic because it allows for the acquisition of hallmark capabilities by the tumor cells.[3]

Several types of inflammation, including environmental-induced, therapy-induced, chronic, autoimmunity, and infection, can all play a role in promoting cancer development and progression. Tumorigenic pathogens such as H. pylori or hepatitis B, promote tumorigenesis through evading normal immune defenses and instead inducing a chronic inflammatory environment.[36] In addition to inflammation during tumor induction, many solid tumors trigger an intrinsic inflammatory immune response that helps to induce a pro-tumorigenic TME.[37] Tumor-associated inflammation can also be induced by various cancer treatments. Many treatments, such as radiation and chemotherapy, are cytotoxic in nature resulting in substantial amounts of necrotic cell death in the tumor and surrounding tissues. This potentiates inflammatory responses and initiates the wound healing response in the TME.[38]

Inflammation also plays a critical role in tumor metastasis. Inflammation results in increased vascular permeability which can promote cancer cell intravasation into blood vessels. Chronic inflammation is critical for the generation of a pro-tumor pre-metastatic niche that cancer cells in circulation can colonize to create a metastasis.[39]

1.4.3 Dichotomy between cancer-promoting inflammation and immunosuppression

However, there is a balance between tumor promoting inflammation and an anti-tumor immune response that is often taken advantage of by the tumor to promote growth and metastasis. Many immune cells within the TME communicate with each other via various cytokines and chemokines. These immune mediators dictate whether the immune response will skew towards tumor-promoting inflammation or toward a CTL-mediated anti-tumor response.[40]

Even so, there is evidence that immunosurveillance and tumor-promoting inflammation can exist within the same tumor and tumor growth relies on the ability for tumor-promoting inflammation to outweigh any anti-tumor responses. It is important to note the multi-faceted roles of many immune cells and mediators that allow them to induce inflammation within the TME while also specifically suppressing any anti-tumor T cell responses. For example, many cytokines and chemokines that promote myeloid cell infiltration to the tumor are themselves immunosuppressive.

Given this complex interplay between tumor cells and the immune system, it is crucial to understand the mechanisms at play to generate a pro-tumorigenic TME so they can be targeted to reprogram the immune response toward an anti-tumor response.

1.5 Cancer Immunotherapy

Cancer immunotherapy, in particular checkpoint blockade, has revolutionized cancer treatment. These therapies drive activation of a more robust anti-tumor response by taking advantage of the immune system's natural mechanisms for regulation of T cell activity. Checkpoint inhibitors targeted against CTLA-4, PD-1, and PD-L1 are currently approved by the FDA for the treatment of many cancer types.[41] While patients who respond to checkpoint therapy

have long lasting anti-tumor responses, a large portion of patients don't respond to treatment. Because of this, research has shifted toward combination approaches that help to overcome this immune related resistance to checkpoint therapy.

While checkpoint blockade therapy can lead to long lasting anti-cancer responses, it can also cause many immune related toxicities for patients. Since checkpoint blockade removes the brakes from T cell activation, this results in a loss of the naïve T cell population and subsequent accumulation of overactive memory T cells that can invade peripheral organs causing inflammatory damage.[42] However, any toxicities associated with immunotherapy are still better tolerated than those associated with traditional chemotherapy and radiotherapy.

In addition to checkpoint blockade therapy, the use of cellular based therapies such as CAR-T cells has become important for the treatment of hematological malignancies. In CAR-T cell therapy, autologous T cells are harvested from the patient and transformed to express a CAR construct targeted towards a specific tumor antigen. These cells are then expanded *ex vivo* and infused back into the patient. There has been a lot of success for CD19 targeted CAR-T cells however success has been limited in solid tumors due to a lack of unique and universally expressed tumor antigens. Many studies have begun to explore the use of CAR-NK cells and CAR-macrophages for use in cancer therapy as well.

There are also a few cancer vaccine therapies that are FDA approved for use in patients. An autologous DC based vaccine containing autologous $CD54^+$ cells activated with prostatic acid phosphatase fused to GM-CSF is currently used for metastatic prostate cancer.[43] Additionally, an oncolytic virus based vaccine, T-VEC, using live attenuated HSV-1 virus that produces GM-CSF within the tumor is approved for use in advanced stage melanoma patients.[44] However, many additional clinical trials are currently in progress to evaluate the efficacy of personalized patient

specific cancer vaccine strategies.

In addition to these immunotherapy strategies, there are hundreds of clinical trials focusing on development of other immunomodulatory agents for cancer treatment. These treatment modalities include cytokine therapy to modulate the TME, angiogenesis inhibitors like anti-VEGF, STING and TLR agonists, as well as targeted therapies for specific cancer antigens such as HER2 and EGFR.[45] However, the field of cancer immunotherapy is constantly growing with hundreds of clinical trials in progress evaluating therapies for an ever emerging list of targets. These new classes of emerging immunotherapies aim to target the immunosuppressive TME and reprogram the immune response toward an anti-tumor response.

1.5.1 Targeting immunosuppressive myeloid cells in the TME

For checkpoint blockade therapy to be effective in a greater percentage of patients, the immunosuppressive TME also needs to be modulated. One mechanism for this is to alter the myeloid cell milieu in the TME by altering myeloid cell differentiation, proliferation, and recruitment through myeloid chemokine blockade or depletion of myeloid growth factors. For example, inhibition of either CCL2/CCR2, CSF-1R, or CXCR1/2 can reduce the chemoattraction of myeloid cells and thus reduce the numbers of myeloid cells within the tumor.[46-48] Another interesting route of myeloid cell inhibition is through blockade of their immunosuppressive functions. This includes strategies such as blocking the CD47-SIRPα interaction that is taken advantage of by tumor cells to evade phagocytosis and incite further immunosuppression.[49] Other therapeutic strategies have investigated myeloid cell reprograming to promote a more pro-inflammatory and anti-tumor phenotype in TAMs. Some strategies under investigation include TLR agonists, CD40 agonists, PI3 kinase inhibitors, and HDAC inhibitors.[50-54] As mentioned

previously, cytokine therapy to skew the immune response toward an anti-tumor response has shown some promise. Some methods for directly modulating myeloid cells in the TME via cytokines include type I interferons to upregulate DNA sensing pathways and IFN-γ, TNF-α, and IL-12 to promote anti-tumor inflammation.[55-57] Additionally, blockade of pro-tumor or pro-TAM cytokines such as IL-1β, IL-6, IL-10, and TGFβ are being explored. While most of these agents have not yet made it out of the early clinical phase of development, as our understanding of the myeloid cell populations and suppressive functions within the TME evolves, it will reveal new therapeutic targets.

1.6 The Inflammasome Signaling Pathway

The inflammasome is a multimeric cytosolic protein complex that assembles in response to different PAMPs (Pathogen Associated Molecular Patterns) and DAMPs (Damage Associated Molecular Patterns). This signaling pathway can be activated from invading pathogens or molecules associated with cellular damage through various sensor proteins (such as NLRP3, AIM2, NLRC4, etc.) and acts as an important innate first line of defense against infection. Upon

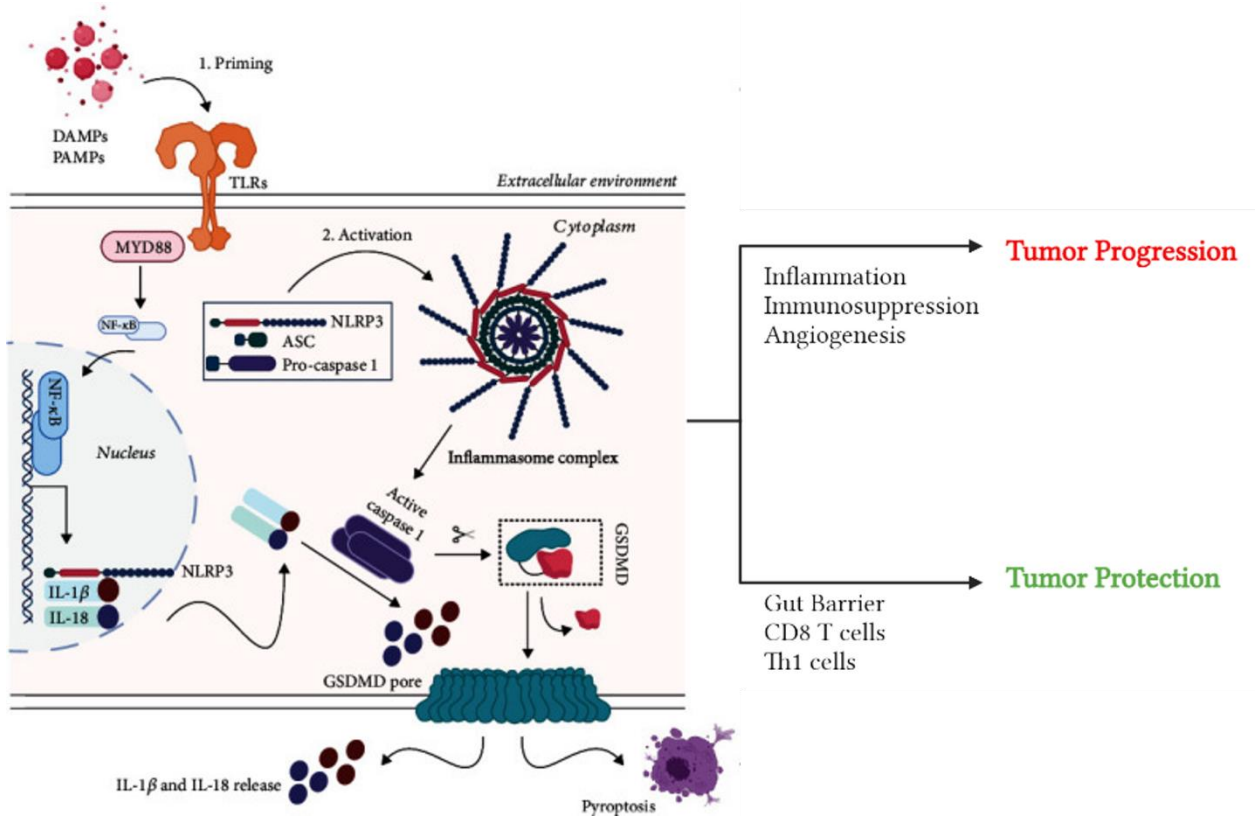

Figure 1.4 The role inflammasome signaling plays in cancer is controversial. Figure adapted from Balahura et al. *Journal of Immunology Research.* 2020.[58] The inflammasome pathway occurs with two distinct signals. The priming signal is mediated by recognition of PAMPs and DAMPs by TLRs to stimulate the transcription of NLRP3 and pro-IL-1β/18. The activation signal is the activation of the inflammasome sensor by PAMPs or DAMPs resulting in the assembly of the inflammasome complex and activation of caspase-1 resulting in IL-1β/18 release and pyroptosis. The role that this pathway plays in cancer is not clear. In some tumors, the inflammasome plays an anti-tumor role through the maintenance of epithelial barriers and CTL function. In other tumors, the inflammasome can be pro-tumorigenic through tumor-promoting inflammation, angiogenesis, and maintenance of immunosuppressive myeloid cells.

recognition of its specific stimuli, the sensor recruits an adapter molecule Apoptosis-associated Speck-like protein containing a Caspase-activation and recruitment domain (ASC) which is important for the recruitment of pro-caspase-1 to the inflammasome complex. Once recruited, pro-caspase-1 is activated through proximity-induced self-cleavage.[59] Activated

caspase-1 cleaves pro-IL-1β and pro-IL-18 into their active forms, as well as gasdermin D (GSDMD) and its N terminal cleavage product inserts into the cell membrane to induce pyroptosis, an inflammatory cell death pathway (Figure 1.4).[60]

There are five pathogen recognition receptors (PRRs) that form inflammasomes. These include NLRP1, NLRP3, NLRC4, AIM2, and pyrin.[61] However, despite the diversity of PRR and stimuli that activate the inflammasome, they all converge on a shared signaling cascade with the activation of caspase-1. The non-canonical inflammasome pathway can be activated directly by intracellular LPS resulting in the activation of caspase-4/5/11 but with functional redundancy in the downstream effector functions.

NLRP3 is the most studied inflammasome sensor molecule and has been shown to recognize a wide array of PAMPs and DAMPs. The NLRP3 inflammasome requires two distinct steps for activation: priming (signal 1) and inflammasome assembly (signal 2). The priming step occurs through the activation of the MyD88, NF-κB, or AP-1 pathways resulting in the upregulated transcription of *NLRP3*, pro-*IL1B*, and pro-*IL18*.[62, 63] Additionally, non-transcriptionally regulated methods of priming the NLRP3 inflammasome have been identified, such as direct LPS triggered MyD88 signaling resulting in deubiquitylation and subsequent priming of NLRP3.[64] Signal 2 can be provided by any PAMPs or DAMPs recognized by the NLRP3 sensor, including ATP, LPS, RNA, reactive oxygen species, and alterations in ion flux. The role of NLRP3 in infection and disease depends on whether the sensor recognizes self or microbial stimuli. During infection, NLRP3 inflammasome activation is protective and plays an important role in clearing the microbe. However, activation of this inflammasome has also been associated with inflammatory diseases, diabetes, obesity, and cancer.[65-67]

Regulation of this pathway is key for conducting a proper immune response without also

eliciting uncontrolled inflammation or autoimmune reactions. The NLRP3 inflammasome can be regulated post-transcriptionally through epigenetic changes such as DNA methylation and histone acetylation.[68] Further, various microRNAs and long noncoding RNAs can regulate NLRP3 priming to orchestrate inflammasome activation. Post-translational modifications of NLRP3 by phosphorylation and deubiquitylation are key mechanisms of non-transcriptional priming and activation of NLRP3 and thus are also highly regulated.[69] Additionally, various molecules can interact directly with components of the NLRP3 inflammasome to regulate its activation. Mediators that target ion efflux, mitochondrial function, and ROS production can also play a role in regulation.[69]

1.6.1 Downstream signaling from the inflammasome

The innate immune system is an important first line of defense against invading pathogens and the inflammasome pathway is a critical component of this. Under the context of infection, the inflammasome is activated within tissue resident myeloid cells or cells of the breached epithelial barrier at the site of infection. Activation of the inflammasome induces the production of anti-microbial peptides and restoration of any damaged epithelial barriers.[70] Production of IL-1β by the inflammasome results in the induction of fever, vasodilation, and hypotension. Further, IL-1β acts as a chemoattractant resulting in the infiltration of immune cells to the site of infection or tissue damage.[71] Production of IL-18 is important for IFN-γ production and skewing toward a CTL adaptive immune response. GSDMD cleavage and subsequent pyroptosis causes the release of DAMPs further propagating immune cell infiltration and activation.[72]

1.6.2 Inflammasome Signaling in Cancer

As discussed earlier, cancer-associated inflammation is one of the hallmarks of cancer and leads to a tumor permissive environment and tumor growth. The inflammasome signaling pathway can play a role in this pro-cancer associated inflammation. To date, the role of the inflammasome pathway in cancer has been contradictory and context-dependent.[73,74] Our group and others demonstrated that myeloid intrinsic inflammasome activation is an important mechanism to promote proinflammatory tumor growth *in vivo*.[75] However, NLRP3 has known tumor suppressive functions in colorectal cancer.[76, 77] The direct mechanisms through which NLRP3 can be tumor permissive in some tumor models while also being tumor suppressive in others are still unknown.

IL-1β has been shown to play a global cellular trafficking role for both cancer cells and immune cells and thus promotes cancer progression.[78, 79] Specifically, IL-1β generates a favorable environment for tumor metastasis by recruiting suppressive myeloid cells to the premetastatic niche.[80, 81] Further IL-1β skews $CD4^+$ T cell polarization to the Th17 subset.[82] In the TME, IL-1β promotes a chronic inflammatory microenvironment through downstream induction of other pro-inflammatory cytokines and chemokines.[83]

The role of IL-1β has been investigated with the Canakinumab Anti-inflammatory Thrombosis Outcomes Study (CANTOS) clinical trial. This trial aimed to study the effect of canakinumab, an IL-1β blocking antibody, on prevention of recurrent vascular events in heart attack patients. In a retrospective analysis of this trial, it was found that patients receiving the highest doses of canakinumab had significantly decreased lung cancer incidence.[84] This prompted canakinumab to move forward into clinical trials for the treatment of non-small cell lung cancer. However, these trials have failed to meet their primary endpoints of overall survival and progression-free survival.[85]

NLRP3 activation is also suspected to alter response to checkpoint blockade in patients.

Specifically, NLRP3 activation through PD-L1 ligation in tumor cells drove recruitment of granulocytic MDSCs to the TME resulting in resistance to anti-PD-1 checkpoint therapy.[86] While NLRP3 inhibitors have not yet been approved for use in cancer patients, a small molecule inhibitor of NLRP3, MCC950, has been deemed safe for use in patients with auto-inflammatory diseases. Additionally, pre-clinical data for use of MCC950 is promising showing both reduced tumor growth, reduced IL-1β levels, and reduced MDSCs, TAMs, and Tregs in the tumor.[87] There are also multiple caspase-1 inhibitors that have shown promising results in pre-clinical data but have not yet been evaluated in clinical trials for cancer treatment.

1.6.3 Inflammasome Signaling in T Cells

While the inflammasome pathway is traditionally thought to be mostly present in myeloid cells and epithelial cells, there has been emerging evidence of inflammasome gene expression in T cells. However, these studies focus on T cell-intrinsic inflammasome expression in the context of infection or autoimmunity with no published work to date in the context of cancer. Both conventional and unconventional inflammasome functions, such as cell fate decisions and T helper cell function, have been described.

T cell-intrinsic inflammasome expression was first described in HIV infection, where it was shown that $CD4^+$ T cells express caspase-1 as a defense mechanism against HIV infection. T cell-intrinsic inflammasome expression also plays an important role in T helper cell differentiation. T cell-derived IL-1β production promotes the maintenance of Th17 cells when it is driven by caspase-8 but the differentiation of Th1 cells when driven by caspase-1. AIM2 has been shown to promote Treg maintenance, whereas ASC inhibits Tregs through the inhibition of IL-10 production.[88]

1.7 Efferocytosis

An under-characterized dynamic process in the TME is efferocytosis,[89-92] a well-orchestrated and immunologically quiescent process of phagocytic clearance of apoptotic cells (AC).[93-95] In adults, an estimated 10^6 cells undergo efferocytic clearance as part of the daily turnover process,[96, 97] and this homeostatic process induces the expression of an immune suppressive and wound healing gene signature (high *Il10, Il4, Tgfb* and low *Il12)* in macrophages to regulate tolerance and aberrant activation of autoimmune responses.[98-101]

Efferocytosis occurs in three distinct phases: "find me," "eat me," and engulfment/digestion (Figure 1.5). During early apoptosis, cells will secrete "find me" signals to recruit phagocytes to the area allowing for easy recognition of apoptotic cells by recruited phagocytes. These "find me" signals include ATP, CX_3CL1, lysophosphotidylcholine, and sphingosine 1-phosphate.[102-105] Conversely, lactoferrin can act as a "keep out" signal when released by apoptotic cells by inhibiting the migration of phagocytes.[106] While "find me" signals serve to recruit phagocytes, "eat me" signals are important for identification of the AC by the phagocytes. The most well studied "eat me" signal is phosphatidyl serine, which flips to the outer leaflet of the cell membrane during apoptosis.[107] There are multiple receptors that can recognize the presence of phosphatidyl serine on an apoptotic cell. Receptors such as BAI-1, TIM-4, and Stabilin-2 can all bind directly to phosphatidyl serine, whereas MerTK uses various bridging ligands (Gas6, Protein S, Gal3, and TULP1) to bind.[108-114] After recognition of the apoptotic cell via "find me" and "eat me" signals, cytoskeletal rearrangement within the phagocyte occurs to

form the phagocytic cup allowing for engulfment of the apoptotic cell into the phagosome.[106]

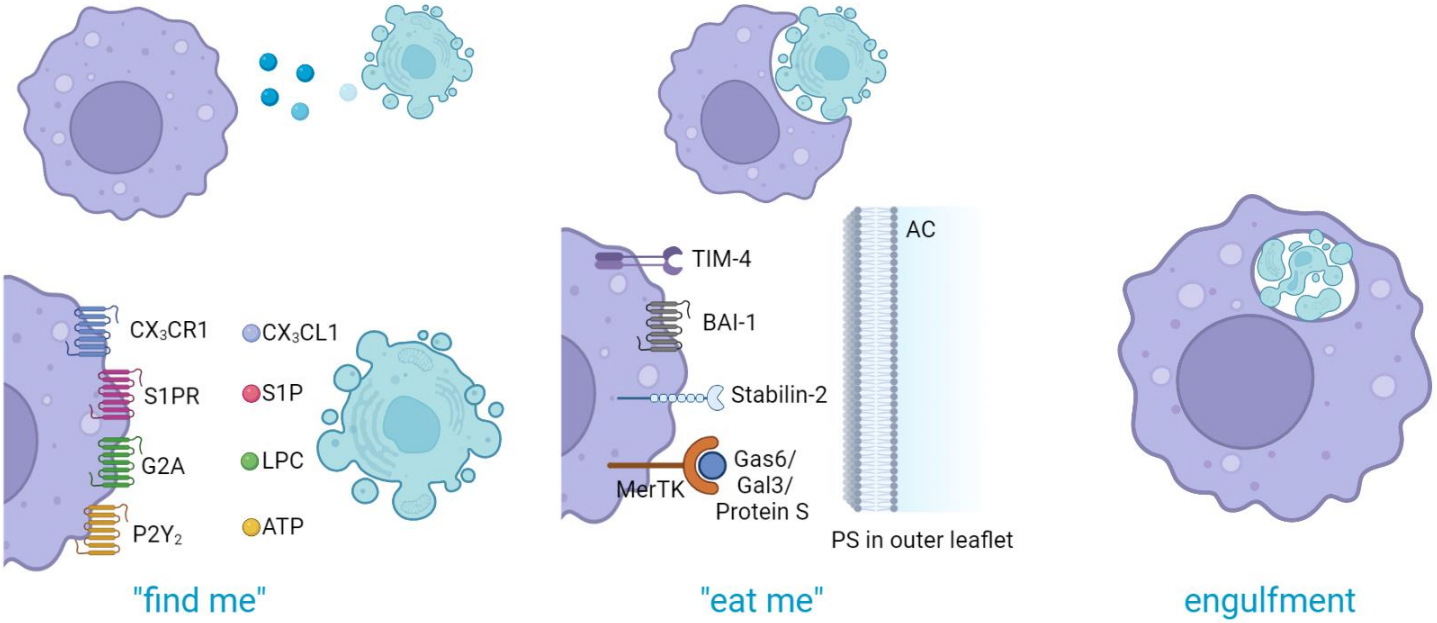

Figure 1.5 Efferocytosis consists of three distinctly orchestrated phases. In the "find me" phase, receptors on the phagocyte recognize signals released by the AC. This allows the phagocyte to recognize and traffic to the AC. In the "eat me" phase, receptors on the phagocyte recognize phosphatidylserine on the outer leaflet of the AC allowing the AC to be ingested. The AC is fully ingested and degradation of cellular material begins in the engulfment phase. Figure made with Biorender.com.

Conversely, ACs can display "don't eat me" signals to avoid efferocytosis by phagocytes. Some well-known "don't eat me" signals include CD47 and CD31 on ACs and SIRPα on phagocytes which inhibit the phagocytosis of healthy cells that may express phosphatidyl serine on their surface, such as platelets and endothelial cells.[115, 116]

Efferocytosis is a critical pathway orchestrated by myeloid cells to ensure tissue homeostasis. If efferocytosis is inhibited, the AC will undergo secondary necrosis resulting in cytoplasmic swelling, rupture of the plasma membrane, and release of cellular components.[117] The process of secondary necrosis is highly inflammatory. Post engulfment, multiple signaling events

are upregulated in the phagocyte causing skewing toward an M2 wound healing phenotype. Efferocytosis is typically associated with the termination of inflammatory responses, induction of self-tolerance, and activation of resolving pathways. [101, 118]

1.7.1 Efferocytosis in cancer

In tumors, mitogenic activity of the tumor cells and tumor aggressiveness is characterized by apoptotic indices (apoptotic nuclei per 100 intact neoplastic cells) as high as 5-10%.[119-121] Apoptosis is a routine process within the TME. Tumors with high apoptosis rates typically also display high cell growth rates resulting in high cell turnover which is key to driving tumor growth forward. However, in established tumors, the frequency of AC within the TME is typically low but rates of cell loss remain high indicating that these AC are being rapidly cleared.[122] It is thought that AC can contribute directly and indirectly to tumor growth through the recruitment and activation of TAMs, contributing to immunosuppression through the induction of immune tolerance, and providing nutrients for growing tumor cells.[123]

Several efferocytosis associated molecules have also been shown to play a role in cancer progression. Efferocytosis results in the production of wound healing and inflammation resolution cytokines such as IL-4, IL-10, and TGF-β. However, in the context of cancer, these cytokines play a key role in establishing an immunosuppressive TME.[124] Further, many molecules that help with recognition of AC by the phagocytes, such as MertK, Axl, and Tyro-3, have all been shown to be overexpressed in certain cancer types.[125]

There is now a growing appreciation that macrophage mediated efferocytosis in the TME acts as an innate immune checkpoint that polarizes myeloid cells towards a tumorigenic and metastasis-promoting M2 subtype.[89, 90, 126] M2 macrophages are important for enhancement of

angiogenesis, tissue remodeling, and immunosuppression, all features that facilitate tumor growth. "Find me" signals released by the AC, like S1P and TGF-β, further stimulate macrophage survival and polarization toward an M2 subtype.[127]

While many traditional chemotherapy and radiotherapy treatments for cancer focus on direct cell death of tumor cells, this massive increase of apoptotic indices can actually result in the immune-mediated promotion of the tumor.[128] Even though tumor size is initially decreased by these treatments, the continued generation of AC can actually promote tumor growth through tumor promoting cytokines from macrophages in the TME. As a result, advanced and aggressive tumors typically resist chemotherapy and radiotherapy treatments after a window of response.[129]

It is thought that if efferocytosis is blocked in the TME, this could force secondary necrosis and a subsequent pro-inflammatory anti-tumor response to occur. A tumor supporting role of efferocytosis was recently observed when pharmacological blockade of the efferocytic receptor MerTK on macrophages increased tumor immunogenicity to sensitize the preclinical tumors to anti-PD-1 or anti-PD-L1 therapy.[92] Although previous studies have reported that clearance of dying cells can induce inflammasome activation,[130, 131] the mechanistic relationship between efferocytosis of apoptotic tumor cells and inflammasome activation is unclear.

1.7.2 Efferocytosis in cancer treatment

Apoptosis and subsequent efferocytosis of AC within the TME is increasingly recognized for its role in promoting tumor growth and immunosuppressive myeloid cell maintenance. Therefore, targeting efferocytosis could provide a novel mechanism for reprogramming the myeloid cells in the TME to promote an anti-tumor immune response.

Since "find-me" signals are released by any AC and are not specific to tumor AC, more

research has been dedicated to blocking the "eat-me" signals involved in efferocytosis. One such pathway is targeting phosphatidylserine (PS) externalization as well as blockade of ligands for PS. In addition, PS is also expressed on vascular endothelial cells allowing PS targeted antibodies to block both PS expressing tumor cells and tumor blood vessels.[132, 133]

Other therapeutic strategies have sought to directly target TAMs through inhibition of certain efferocytosis associated molecules, such as Axl and MerTK. Axl inhibitors have been shown to reduce tumor cell migration and invasion while also suppressing efferocytosis and subsequent immunosuppressive TAM differentiation.[134] Currently Axl inhibitors in clinical trials consist mostly of small molecule inhibitors with significant off-target toxicity while less toxic monoclonal antibodies are still in the pre-clinical stages of development.[135, 136] MerTK can induce resistance mechanisms to Axl-targeting agents therefore necessitating possible Axl and MerTK combination therapy. However, dual targeting both Axl and MerTK can lead to significant toxicity and needs further pre-clinical exploration.[137]

In addition, blockade of the "don't eat me" signal CD47 has become of high interest. CD47 is overexpressed on virtually all cancers which enables cancer cells to evade destruction by phagocytosis and expression levels negatively correlated with survival of cancer patients.[138] Monoclonal antibodies against CD47 have been shown to facilitate phagocytosis of cancer cells and inhibit the ability of tumor cells to evade immune recognition. In clinical studies, combination of anti-CD47 antibodies with targeted therapies such as anti-HER2, anti-CD20, and anti-EGFR have demonstrated a synergistic effect.[139, 140]

As mentioned previously, it may be of benefit to explore combination of efferocytosis blockade with chemotherapy and radiotherapy. As these traditional treatment methods generate an abundance of apoptotic tumor cells, efferocytosis of these cells in the TME can potentiate tumor

immunosuppression which can contradictorily result in tumor progression. However, if efferocytosis is inhibited alongside chemotherapy and radiotherapy, it could result in more durable treatment efficacy and improved patient outcomes.

While much is known about the induction of efferocytosis of tumor AC in the TME, the mechanism by which efferocytosis contributes to tumor growth is still unclear. In addition, the NLRP3 inflammasome has been linked to the promotion of tumor growth in certain tumor models. However, NLRP3 can recognize a wide variety of stimuli and it is not yet known what activates this pathway in the TME. We hypothesize that efferocytosis of apoptotic tumor cells by myeloid cells in the TME provides the stimuli necessary to activate the NLRP3 inflammasome in these cells thus contributing to a pro-tumorigenic TME.

1.8 Research objectives

Our lab has previously demonstrated that overexpression of *CASP1* in HNSCC patients is associated with worse prognosis and progression free survival (Figure 1.6a). Further, we found that *CASP1* expression was increased in basal subtypes of HNSCC which is typically associated with worse clinical outcomes and absence of T cell infiltration (Figure 1.6b). [75, 141] This led us to investigate the role of the inflammasome and caspase-1 in promoting tumor growth. In doing so, we demonstrated *in vivo* that caspase-1 specifically in the MDSC compartment promotes tumor growth in a T cell independent manner (Figure 1.6c-d).[75] While we and others have previously demonstrated a pro-tumorigenic role for the inflammasome, there is still controversy that remains surrounding the inflammasome in cancer. Taken together, these data led us to question the specific tumorigenic role of the inflammasome pathway and the mechanism by which the inflammasome is activated within the TME.

Here, we aimed to examine the tumor intrinsic factor that regulates myeloid inflammasome signaling and its specific role in tumorigenesis in both human and murine tumors. To do so, we sought to phenotype the myeloid milieu within the TME. We revealed a wide array of tumor myeloid cell subsets that are more complex than the traditional M1/M2 nomenclature. Within these myeloid subsets, we identified 2 macrophage and 1 monocyte subset that is highly enriched in inflammasome pathway genes, most notably *NLRP3* and *IL1B*. We also identified a distinct pro-tumorigenic role for the NLRP3/caspase-1/IL-1β signaling axis which promotes tumor growth through the alteration of myeloid composition in the TME.

We also aimed to identify the molecular mechanism by which the NLRP3 inflammasome is activated in the TME. We hypothesized that efferocytosis of apoptotic tumor cells provides the stimuli to activate the NLRP3 inflammasome in tumor infiltrating myeloid cells. We confirmed that efferocytosis of tumor AC activates the NLRP3 inflammasome resulting in increased IL-1β production and tumor promotion. We also identified two macrophage subsets in the TME that express an efferocytosis gene signature and can give rise to the myeloid subsets enriched for inflammasome pathway genes.

Lastly, we aimed to identify the impact of tumor-intrinsic caspase-1 expression on T cell function. As discussed previously, T cell-intrinsic inflammasome gene expression has been shown to play important roles in the pathogenesis of HIV-1 infection and various autoimmune diseases. However, the role of the T-cell intrinsic inflammasome in cancer has not been explored. Here we show distinct phenotypic differences between WT and caspase-1 KO T cells. We show that caspase-1 KO T cells have greater cytotoxic capacity which translates to a greater anti-tumor T cell response *in vivo*. We hypothesize that T-cell intrinsic caspase-1 expression acts as a checkpoint mechanism for tumor infiltrating T cells to prevent anti-tumor T cell responses.

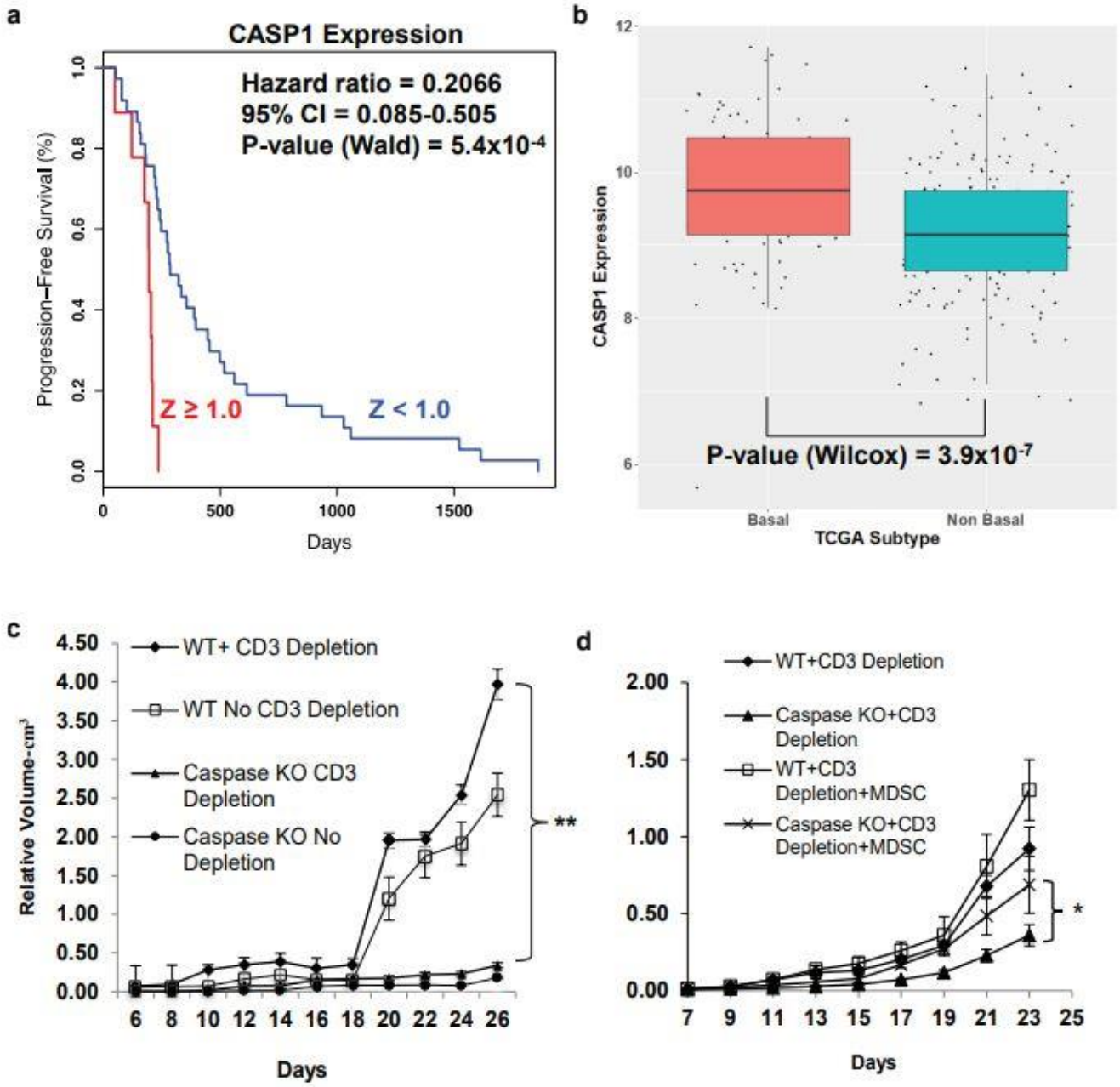
a
CASP1 Expression
Hazard ratio = 0.2066
95% CI = 0.085-0.505
P-value (Wald) = 5.4x10-4
Progression-Free Survival (%)
Z ≥ 1.0
Z < 1.0
Days
b
CASP1 Expression
P-value (Wilcox) = 3.9x10-7
Basal
Non Basal
TCGA Subtype
c
WT+ CD3 Depletion
WT No CD3 Depletion
Caspase KO CD3 Depletion
Caspase KO No Depletion
Relative Volume-cm3
**
Days
d
WT+CD3 Depletion
Caspase KO+CD3 Depletion
WT+CD3 Depletion+MDSC
Caspase KO+CD3 Depletion+MDSC
*
Days

Figure 1.6 Role of caspase-1 expression in both human and murine tumors.[75]

Analysis of TCGA data for caspase-1 gene expression in HNSCC patients. a) Kaplan-Meier showing progression-free survival. Of 46 patients for whom CASP1 gene expression and progression-free survival data were available, nine were defined as overexpressing CASP1 (Z-score ≥ 1.0; red line) and 36 were defined as wild-type expression (Z-score < 1.0; blue line). b). Box plot of caspase-1 expression in basal and non-basal subtypes. Boxplots: interquartile range (IQR; box height) with the upper horizontal line showing the 75% quantile, lower showing the 25% quantile, and center line representing the median. c-d) Tumor growth experiments in vivo were performed with chimeric C57BL/6 mice adoptively transferred with bone marrow cells from caspase-$1^{-/-}$ KO or wildtype (WT) mice. $CD3^{+}$ T cells were depleted via antibody depletion i.p. twice a week. Wildtype Gr-$1^{+}CD11b^{+}$ MDSCs (enriched from splenocytes of tumor-bearing wildtype mice) were transferred into tumor-bearing chimeric mice (left lower panel).

CHAPTER 2

Title of Chapter: Enrichment of inflammasome signaling in tumor infiltrating myeloid cells promotes tumor growth and myeloid persistence

2.1 Introduction

Inflammasome-associated genes are highly expressed in myeloid lineage cells and epithelial cells. As a result, studies on the inflammasome in cancer have been mostly centered around tumor cell-intrinsic inflammasome activation without also considering the importance of the immune system. These studies have shown that tumor-intrinsic inflammasome signaling is often used by the tumors to skew towards an immunosuppressive myeloid landscape. Further, looking exclusively at tumor inflammasome signaling has produced contradictory results that are dependent on the cancer type studied.[142-144] However, the expression patterns and functional implications of the inflammasome in tumor infiltrating myeloid cells are not well understood. Here we sought to understand the mechanisms driving myeloid-intrinsic inflammasome-driven tumor progression. Our objective was to determine inflammasome gene expression patterns in tumor infiltrating myeloid cell populations. Here, we used a dual pronged approach involving both bulk and single cell RNA sequencing to profile the myeloid landscape in HNSCC patients. Further, we aimed to characterize how this pathway contributes to the myeloid milieu and functionality to promote tumor progression.

2.2 Methods

2.2.1 Human Samples

This study was performed in compliance with approved Vanderbilt University Medical Center Institutional Review Board protocols in accordance with the Belmont Report and US

Common Rule. All subjects provided written informed consent prior to participation, and the specimens were de-identified prior to analysis. Included were HNSCC patients undergoing surgery for curative intent. Excluded were those with autoimmune diseases and chronic steroid use. Fresh tumor specimens (typically 1 cm^3) were harvested from non-margin areas and processed in DMEM base media within 2 hours of resection.

Human PBMC Processing

Peripheral blood mononuclear cells (PBMC) were collected from blood using Ficoll-Paque Plus, following manufacturer's instruction. In brief, fresh blood samples were collected in heparinized blood collection tubes and mixed with equal parts PBS. 10 ml of the blood/PBS mixture was layered over 5 ml of Ficoll-Paque Plus in a conical tube and centrifuged at 400g for 30 minutes, 18˚C, and no brake. The PBMC layer was isolated and washed with PBS prior to lysis of red blood cells with ACK lysis buffer.

Human Tumor Processing

Fresh tumor samples were processed using Miltenyi Biotec human tumor dissociation kit and the Miltenyi GentleMACS Octo dissociator tough tumor dissociation program following manufacturer's instructions. The dissociated tumor was filtered with a 100 µM filter prior to red blood cell lysis with ACK lysis buffer. All tumor samples were used fresh the same day for experiments and analysis by flow cytometry.

2.2.2 Mouse studies

Mouse lines

6-week-old female C57BL/6J wildtype were purchased from The Jackson Laboratory. *Casp1*$^{-/-}$, *Aim2*$^{-/-}$, and *Nlrp3*$^{-/-}$ male and female mice were purchased from The Jackson

Laboratory and bread for colony maintenance. *Gsdmd*$^{-/-}$ mice were a gift from T.D. Kanneganti (St. Jude Children's Research Hospital).

Il1b$^{-/-}$ mice were generated with the help of Leesa Sampson at the Vanderbilt Genome Editing Resource. In brief, CRISPR guide RNAs were placed directly flanking the *Il1b* coding sequence to generate a complete deletion of the gene. Three founder pups were identified to contain a complete *Il1b* deletion and were backcrossed two generations to wildtype C57BL/6 mice. Confirmation of *Il1b* deletion was confirmed utilizing the Transnetyx genotyping service for all subsequent generations.

All experiments involving animals were reviewed and approved by the Institutional Animal Care and Use Committee at Vanderbilt University Medical Center. All experiments were performed according to NIH guidelines, the Animal Welfare Act, and US Federal law.

In vivo tumor model

To look at tumor growth in wildtype C57Bl/6 mice or knockout mice, $1x10^5$ B16-mOVA or MOC2 cells were injected subcutaneously into the flanks of the mice. Tumors were measured 3x/week with calipers and tumor volumes were estimated using the formula $V\ (cm^3) = 3.14 \times [\text{largest diameter} \times (\text{perpendicular diameter})^2]/6$. Mice were sacrificed when the tumors measured 2 cm in the largest diameter. Depleting anti-PD-1 (100 μg/mouse), anti-IL-1β (100 μg/mouse), recombinant IL-1β (1 μg/mouse), or control PBS (100 μl/mouse) was injected intraperitoneally twice a week in some cohorts.

Mouse tumor and splenocyte processing

Mice were sacrificed at study endpoint and tumors were excised. Tumors were incubated with 1 mg/ml Collagenase II and 0.25 mg/ml DNase for 1 hour at 37˚C. Tumors were filtered with a 100 μM filter prior to red blood cell lysis with ACK lysis buffer. All tumor samples

were used fresh the same day for experiments and analysis by flow cytometry.

Spleens were isolated from euthanized WT and inflammasome KO C57Bl/6 mice. Spleens were placed on 100 µM filters and pulverized with a syringe plunger. Splenocytes were washed with PBS prior to red blood cell lysis with ACK lysis buffer.

Generation of mouse bone marrow derived MDSCs

Wildtype C57Bl/6 or knockout bone marrow cells were obtained from the femur and tibia, cultured in RPMI-1640 supplemented with 10% FBS, 1% penicillin/streptomycin, 1% HEPES, 1% Glutamax, and 0.1% beta-mercaptoethanol. 10 ng/ml GM-CSF was added to induce suppressive myeloid cells. After 4 days, non-adherent cells were collected and $CD11b^+$ cells were positively selected by magnetic-activated cell sorting (described in detail below).

2.2.3 Cells

Cell line maintenance

Cell lines used included murine melanoma cell line B16-mOVA, Cal27, and murine head and neck cell line MOC2. All cell line aliquots were obtained from ATCC and stored in liquid nitrogen when not in use. Cells were cultured with RPMI-1640 medium, with 10% FBS, 1% penicillin/streptomycin, 1% HEPES, 1% Glutamax, and 0.1% beta-mercaptoethanol. All reagents were obtained from Gibco®.

Bead Enrichment of Immune Cells

$CD11b^+$ cells were enriched via positive selection, according to manufacturer protocol, using CD11b MicroBeads from Miltenyi Biotec. In brief, cells were resuspended 9:1 in sort buffer (PBS containing 0.5% FBS and 2 mM EDTA) and CD11b microbeads and incubated

at 4˚C for 15 minutes prior to washing with sort buffer. Cells were then positively selected using magnetic separation.

$CD3^+$, $CD4^+$, and $CD8^+$ T cells were enriched according to manufacturer protocol using MojoSort isolation kits from Biolegend. In brief, cells were resuspended in sort buffer at a concentration of 10^8 cells/ml and treated with 10 µl biotinylated antibody cocktail per 10^7 cells. After incubation on ice for 15 minutes, 10 µl streptavidin nanobeads per 10^7 cells were added and incubated as above. Cells were then negatively selected using magnetic separation.

2.2.4 Single cell RNA sequencing

Head and neck cancer patient samples were weighed and cut into pieces prior to digestion using human tumor digestion mix for 1hr on the tumor dissociator. Cells were then passed through a 70uM cell strainer to remove debris and centrifuged at 300g for 5 minutes. RBC were lysed with RBC lysis buffer. Cells were then centrifuged again and resuspended at 600cells/µl PBS and dropped off for Chromium Single Cell 3' Library construction (10X Genomics) and sequencing at VANTAGE sequencing facility at VU following the manufacturer's instructions. Libraries were sequenced on an Illumina HiSeq4000 and mapped to the human genome (build GRCh38) by CellRanger (Version 3.0).[145]

Single cell RNA sequencing data processing

The raw FASTQ files were demultiplexed and aligned with STAR[146] algorithm imbedded in CellRanger package. The raw unique molecular identifier (UMI) count matrix with the cell barcodes and the feature list for each sample was extracted and imported into R environment with Seurat 4.0 for downstream analysis.[147] For quality control, cells with UMI less than 1500 or greater than 15000 or mitochondrial-derived UMI counts over than 10% were excluded.

Potential doublets were further checked and removed with Scrublet.[148] To factor out the technical factors including sequencing depth, normalization and variance stabilization of UMI matrix was performed with SCTransform function, by considering the total UMI counts and percentage of mitochondrial-derived UMIs as confounders, fitting in Gamma-Poisson Generalized Linear Model, with considering the top 5000 variable features after ranking by residual variance. Data from each sample was then integrated in Seurat as described in Stuart et al, 2019.[149] During this process, we first got top 5000 variable genes as potential anchors with FindIntegrationAnchors function of Seurat and then use IntegrateData function to integrate data. The technical batch effect between samples was regressed out during this step. Principal component analysis (PCA) was performed on the 5000 genes integrated matrix to reduce the dimensionality of the scRNA-Seq dataset, and top 50 PCs were chosen to keep more features of the dataset. The main cell clusters were identified with the FindClusters function in Seurat. Two-dimensional representation of the clusters was shown with tSNE or UMAP plots.

Major cell type annotation

We used reference dataset-based annotation strategy to annotate the major cell types at single cell resolution. A fine annotated single cell RNAseq dataset[150] was downloaded at the NCBI GEO depository under the accession number GEO: GSE127465. Raw matrices of all human samples were imported into R environment and prepared as Seurat object by following the standard procedure (https://satijalab.org/seurat/articles/get_started.html). Meta data with the annotated cell types information was used as guideline of the reference. FindTransferAnchors and TransferData functions were performed sequentially to annotate our dataset with the reference.

Since the reference dataset was generated from human non-small-cell lung cancer samples and used different single cell generating platform (InDrop), to validate the robustness of the annotation approach, canonical cell markers of different major cell types were manually checked. The cell types with small cell numbers (RBCs, n = 5) were excluded from the downstream analysis.

Myeloid cell subtypes annotation

To further annotate the myeloid population, subset of myeloid cells, including MoMacDC supercluster, pDCs, and Mast cells were extracted from the total dataset (due to small number, n = 12, Neutrophils were not included for further investigation). PCA and clusters were reanalyzed on the subsets of myeloid cells.

Pan-cancer level single myeloid cells were investigated across multiple cancer types and showed systematic view of the composition of tumor-infiltrating myeloid cells.[151] We downloaded the expression data of the pan-cancer myeloid cells from Gene Expression Omnibus (GEO: GSE154763) as the reference dataset. Following the same workflow as described above, we prepared the integrated dataset as a Seurat object and added in the meta data, including the myeloid cell annotation information.

Instead of the label transferring methods in Seurat, we used a multiple correspondence analysis (MCA) based technique, called Cell-ID to annotate the myeloid cells in our dataset.[152] Cell-ID can project the cells and genes in the same low-dimensional space and therefore, can annotate single cell transcriptomes and report the gene signatures. Cell-ID was proven to be robust even when there were batch effects, different donors, model organisms, tissues of-origin, and single-cell omics protocols, which is ideal to be used as the tool for our myeloid cell annotation with pan-cancer myeloid cell reference data.

MCA dimensionality reduction was performed for both reference dataset and our myeloid cells. First, gene signatures of each myeloid cell type from the reference pan-cancer myeloid cells were extracted with GetGroupGeneSet function from Cell-ID using the first 50 dimensions. Then group-to-cell matching and label transferring across datasets strategy were adopted for annotation with RunCellHGT function in Cell-ID. If no significant hits are found, a cell will label as "Other." Marker genes related to each sub-types of myeloid cells were manually reviewed and compared with the reference datasets. Similarity matrix defined based on the proportion of the shared marker genes between reference and our dataset in total number of marker genes showed each sub-types in our dataset have highest similarity with the same subtypes in reference dataset (data not shown). Per-cell functional enrichment analysis were performed by checking custom defined gene signatures (e.g., inflammasome and efferocytosis pathways) or gene sets from MsigDB.[153-155]

Marker gene identification

The cell type specific marker genes were identified using preferentially expressed genes in certain cell types or differentially expressed genes between tumor- and blood-derived cells using the FindAllMarkers or FindMarkers function in Seurat with "MAST" method by setting min.pct = 0.25, logfc.threshold = 0.25.[156]

RNA velocity analysis

Spliced, unspliced, and ambiguous matrices were extracted from the bam file generated by CellRanger for each sample and saved into loom file by velocyto.[157] Guided with the expression matrix in seurat object as described above, these three matrices were integrated, and filtered for the low quality cells. RNA velocity analysis was carried out for the myeloid cells with scVelo using the dynamical model for more consistent velocity estimates and better

identification of transcriptional states compared with the stochastic model.[158] The embedding information was inherited from the expression analysis to have the consistent dimension reduction plot. To portray the cell transitions between subclusters of myeloid cells, Partition-based graph abstraction (PAGA) was used for trajectory inference based on velocity-inferred directionality.[159] Cluster-specific top-likelihood genes in the dynamic model were identified for each cluster to find the potential drivers that showed evident dynamic behavior.

2.2.5 Bulk RNA sequencing

$CD11b^+$ myeloid cells were flow sorted from previously untreated HNSCC tumors and matched blood (n=7). Briefly, tumors were digested using human tumor digestion buffer following manufacturer's instructions to obtain single cells. Following this, cells were stained with live dead dye, CD45, CD11b, CD3, and NK1.1. RNA was isolated from sorted $CD11b^+$ cells using Trizol and used for sequencing at VANTAGE next generation sequencing facility at VU.

Bulk RNA sequencing data analysis

Raw fastq files were mapped to reference genomes (GRCh38 or GRCm38) with STAR software. Gene reads count were calculated with FeatureCounts in R.[160] Gene by sample matrix were integrated and performed the differential gene expression analysis workflow as described at https://bioconductor.org/packages/release/bioc/vignettes/DESeq2/inst/doc/DESeq2.html mainly using DESeq2 package.[161]

Pathway analysis

GO and KEGG enrichment analysis was performed on DE genes with clusterProfiler.[162]

Pre-ranked GSEA was performed based on the ranking of gene list from the DE analysis using fgsea package.[163] Single-sample-GSEA was conducted with the GSVA package.[164] Differences of the ssGSEA enrichment scores of the gene sets between different sample or cell groups or clusters were calculated with a linear model offered by the Limma package.[165] Functional enrichment analysis was also performed using IPA (QIAGEN Inc).

2.2.6 Flow Cytometry

For analysis of tumor-infiltrating populations, mice were sacrificed at indicated time points and tumors were harvested, minced in small pieces, and incubated with collagenase and DNase for 1 hour at 37°C. Single-cell suspensions were prepared by transferring the tumors through a 70-μm cell strainer (BD Biosciences). Cells were first incubated with live/dead fixable dead cell stain (Thermo Fisher Scientific, L34959) in PBS for 15 minutes at 4˚C. Subsequently, cells were incubated with monoclonal antibodies for 15 minutes at 4˚C. Samples were acquired on a BD FACSCelsta flow cytometer, and results were analyzed using the FlowJo software. For intracellular staining, the cells were surface stained and then fixed and permeabilized for 30 minutes with Fix/Perm buffer at 4˚C. Following fix/perm, cells were intracellularly stained for 30 minutes in perm buffer at 4˚C. For IFN-γ, perforin, and granzyme, cells were incubated with PMA/ionomycin (Cell stimulation cocktail, Invitrogen) and monensin (BioLegend) for 4 hours at 37°C prior to antibody staining.

2.2.7 *in vitro* myeloid cell assays

ELISA

BMDM or human macrophages were cultured and efferocytosis performed as described

earlier. 200 µl of supernatant from each well of cultured efferocytic mouse macrophages of different treatment conditions were collected at different time points for measurement of IL-1β and IL-18 using ELISA kits without dilutions. Each assay had duplicated wells for the standard curve and triplicated wells for the samples. Concentration was calculated from the standard curve using the recombinant cytokines, per the manufacturer's instructions.

T cell suppression assay

$CD3^+$ T cells were isolated from the spleens of wildtype C57Bl/6 or knockout mice by magnetic activated cell sorting and stained with 5 µM CFSE for 5 minutes in PBS + 5% FBS. Cells were washed twice with PBS + 10% FBS prior to plating. Isolated $CD3^+$ T cells were co-cultured with bone marrow derived MDSCs at indicated ratios on 96 well plates with anti-CD3/CD28 stimulation beads. The percentages of proliferating $CD3^+$ T cells were determined by CFSE dilution and PD-1 expression was assessed by flow cytometry analysis.

Viability assay

Wildtype and knockout MDSCs were generated as stated above. MDSCs were plated at a concentration of 100,000 cells/well in 100 µl in a 96 well plate. Certain groups were also treated with LPS or tumor conditioned media. Cells were treated with 5 µm green caspase 3/7 dye and red annexin V dye. Fluorescing cells were counted using the Incucyte FLR live imager and software.

Caspase-Glo assay

B16-mOVA tumors were grown in wildtype and caspase-1 knockout C57Bl/6 mice. Tumors and spleens were harvested on day 16 post injection. $CD11b^+$ cells were positively selected using magnetic activated cell sorting. Cells were plated at a concentration of 100,000 cells/well in 100 µl in a 96 well plate. Caspase-1 activity was determined using the Caspase-1

glo kit (Promega) according to manufacturer protocol.

2.2.8 Statistics

All the graphical illustrations statistical tests were performed using Prism-6 software (GraphPad software, Inc., La Jolla, CA). All data reported in graphs are expressed as mean ± standard error of mean (SEM) unless otherwise mentioned and were compared using unpaired student T-test or ANOVA where mentioned. p values were considered statistically significant when less than 0.05. All experiments were repeated at least 3 times unless specified. *P < .05; **P < .005; ***P < .0005. ns=not significant.

2.3 Results

2.3.1 Multipronged sequencing analysis reveals inflammasome enrichment in tumor infiltrating myeloid cells

To obtain a high-resolution view of the HNSCC TME, we adopted a dual sequencing approach in which both bulk RNA sequencing and sc-RNAseq of both tumor and peripheral blood mononuclear cells (PBMC) was performed. This approach allowed us to improve the resolution of heterogeneity between individual cells, one of the most complex aspects of the TME, that cannot be done with bulk sequencing alone. We first performed bulk RNA sequencing of $CD11b^{+}$ myeloid cells sorted from human head & neck squamous cell carcinoma (HNSCC) tumors with their matched PBMC. To do so, cells were positively sorted for CD11b and lack of other lineage specific markers such as CD3 and Nkp46.

We noted increased inflammasome transcripts, including *NLRP3* and *IL1B* genes in the tumor infiltrating myeloid cells compared to those in circulation (Figure 2.1a-b). However, not all

the transcripts associated with the inflammasome were enriched in the tumor, such as *IL18*, *AIM2*, *PYCARD*, and *GSDMD*, indicating a skewing toward a specific IL1B driven inflammasome signaling axis in tumor myeloid cells (Figure 2.1a-b). GSEA using both IPA and GO algorithms identified IL-1 signaling and IL-1 production were among the most significantly altered pathways in tumor associated myeloid cells over those in peripheral blood (Figure 2.1c). As expected, both IPA and gene analyses revealed pathways associated with tumor microenvironment (Hif-1α signaling, IL-10 signaling), T cell exhaustion and checkpoint signaling, and several immunosuppressive signaling pathways (TGF-β signaling, IL-10 signaling) to be highly altered in the tumor derived myeloid cells (Figure 2.1c). This identified a distinct immunosuppressive and tumorigenic expression profile in tumor infiltrating $CD11b^{+}$ cells that is not present in circulating myeloid cells, including increased expression of the inflammasome genes *NLRP3* and *IL1B.*

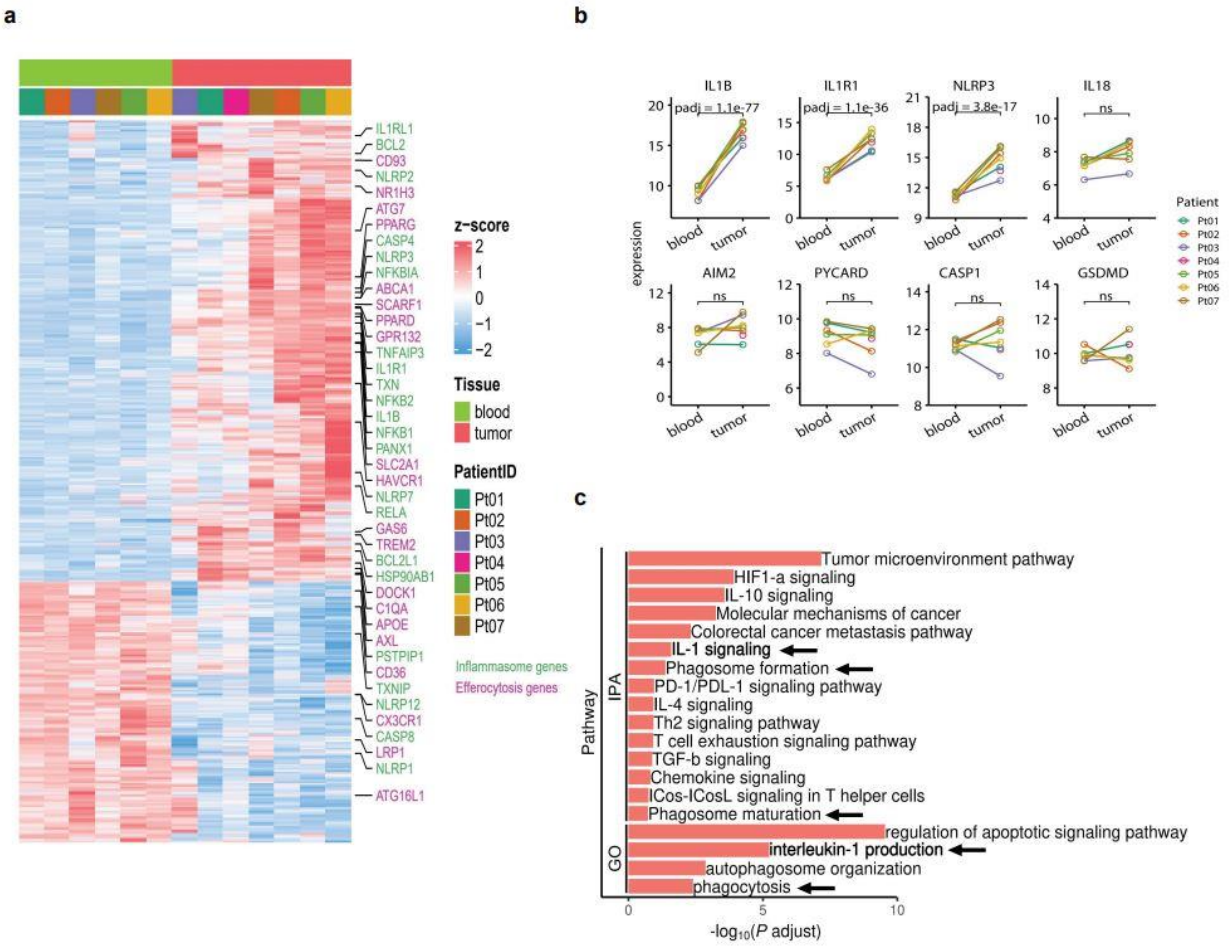

Figure 2.1. IL-1β signaling pathways are enriched in tumor infiltrating myeloid cells in human HNSCC

a) Heatmap showing differential gene expression profile between CD11b^{+} myeloid cells from matched blood or tumor from 7 HNSCC patients as measured by bulk RNA-seq. CD45^{+}CD11b^{+}Lin^{-} cells were isolated using florescence activated cell sorting (FACS) from matched blood and tumor from HNSCC patients. RNA was isolated from the sorted population and submitted for sequencing at VANTAGE. FACs and RNA sequencing were performed on the same day the sample was received. Sequencing data was processed as outlined in methods section 2.2.5. b) Differential inflammasome signature in tumor and blood myeloid cells (n=7). Differential expression analysis was performed as outlined by Love et al. which generates p values using the Wald test.[161] c) Ingenuity pathway (IPA) and gene ontology (GO) analyses showing enrichment of IL-1 signaling in tumor infiltrating myeloid cells over those from blood. The workflow for generation of IPA and GO is outlined in methods section 2.2.5.

2.3.2 Single cell transcriptomic sequencing shows enrichment of inflammasome pathway signaling among 13 distinct clusters of human tumor-infiltrating myeloid cells

To account for the heterogeneity of tumor infiltrating myeloid cells, we performed single cell RNA sequencing of HNSCC tumors with matched PBMC. Unsupervised Seurat and cell type annotation clustering analyses revealed 13 different cell subsets within the TME (see methods). We identified 8 tumor infiltrating $CD45^+$ major immune cell subsets (Figure 2.2a-b) including *LILRA4*$^+$ plasmacytoid DC (pDC), *C1QC*$^+$ and *LYZ*$^+$ myeloid cells encompassing monocytes, macrophages and conventional dendritic cells (MoMacDC; mononuclear phagocytes), *CD3*$^+$ T cells, *KLRC1*$^+$ NK cells, *MS4A1*$^+$ (CD20) B cells, *IGHA1*$^+$ plasma cells, *KIT*$^+$ mast cells, and *OSM*$^+$ neutrophils, largely consistent with recent sc-RNA seq studies from multiple cancer types.[150, 151, 166-174] Within the blood, we identified the same B cell, NK cell, monocyte, pDC, plasma cell, and T cell populations (Figure 2.3a-b).

Using a previously published pan-cancer Cell ID algorithm to increase the resolution of the mononuclear phagocytes from the scRNA sequencing dataset outlined above,[151] we identified 13 and 6 different myeloid subsets in tumor and blood respectively (Figure 2.2c-d and 2.3c-d). Within the tumor, out of the 13 different myeloid populations, we characterized 5 major cell lineages- monocytes, macrophages, conventional DC (cDC), pDC, and mast cells. Our analysis revealed 5 tumor infiltrating macrophage subsets - Macro_C1QC (*FCGR3A/C1QC/C1QA*), Macro_INHBA (*INHBA/CXCL8/CCL4*), Macro_ISG15 (*TYMP/ISG15/IFITM3*), Macro_NLRP3 (*NLRP3/IL1B/BCL2A1*), and Macro_SPP1 (*SPP1/APOC1/CSTB*) - and 3 monocyte subsets (Mono_CD14, Mono_CD16, and Mono_CD14CD16) along with 4 tumor-infiltrating DC subsets (cDC1_CLEC9A, cDC2_CD1c, cDC3_LAMP3, and pDC_LILRA4) and mast cells (Figure 2.2c-d). The three monocyte subsets were characterized by the expression of either *CD14* or *CD16*.

Classical *CD14*$^{+}$ monocytes expressed high levels of the MDSC-associated markers *S100A9, S100A8,* and *FCN1*, whereas the non-classical *CD16*$^{+}$ subset was enriched for *LST1*, *CFP*, and *AIF1*. We also identified an intermediate *CD14*$^{+}$*CD16*$^{+}$ monocyte subset which was present in low abundance in the tumor (Table 2.1). Matched peripheral blood myeloid cells were mainly enriched in classical *CD14*$^{+}$ monocytes (*LYZ, S100A9, S100A8*), non-classical *CD16*$^{+}$ monocytes (*LST1, C1QC, IFITM2*), cDC2_CD1c (*CFP, HLA-DPA1, FCER1A*), and pDC_LILRA4 (IRF7, GZMB, LILRA4) (Figure 2.3 c-d). The relative abundance of each of these cell types in both the tumor and blood is outlined in Table 2.1-2.2.

Within the tumor, only 3 mononuclear phagocytes - *CD16*$^{+}$ monocytes, *NLRP3*$^{+}$ macrophages, and *INHBA*$^{+}$ macrophages (Figure 2.2e-f and 2.3e) – had elevated levels of *NLRP3* and *IL1B* expression. In these populations, we found a much stronger enrichment of *NLRP3* expression over other sensors in the tumor myeloid cells (Figure 2.2f). The *NLRP3*$^{+}$ subset also expressed high level of genes with known tumor supportive roles like *IL10, VEGFA, TIMP1, CD300E, FPR1, SERPINA1, CCL20,* and *VCAN* compared to other mononuclear phagocytes. Similarly, *INHBA*$^{+}$ macrophage subset co-expressed pro-tumorigenic molecules such as *IL6, TGFb, TIMP1, CCL20, CXCL1,* and *IL10,* highlighting the highly plastic and complex nature of tumor infiltrating myeloid cells *in vivo,* consistent with recent similar studies in other solid tumors.[150, 151, 167-176] From this clustering, single sample Gene Set Enrichment Analysis (ssGSEA) primarily revealed enriched IL-1 and inflammasome related pathways in *NLRP3*$^{+}$ and *INHBA*$^{+}$ macrophage populations in the tumor. ssGSEA analysis also associated both these macrophage subsets with alterations in several pathways related to carcinoma progression, T cell exhaustion, cell migration, angiogenesis, and wound healing, in agreement with tumor supportive roles reported for *NLRP3* and *INHBA.*[177-180] When we determine relative cell type abundance within

these samples, we find highest numbers of macro_C1QC macrophages in the TME whereas the other macrophage populations identified have similar abundance (Table 2.1). Of note, none of these macrophage populations were identified in the peripheral blood (Table 2.2). This cellular level phenotyping of the myeloid milieu in the TME outlines the complex heterogeneity of tumor myeloid cells with none of the subsets identified aligning with traditional M1 or M2 subtypes.

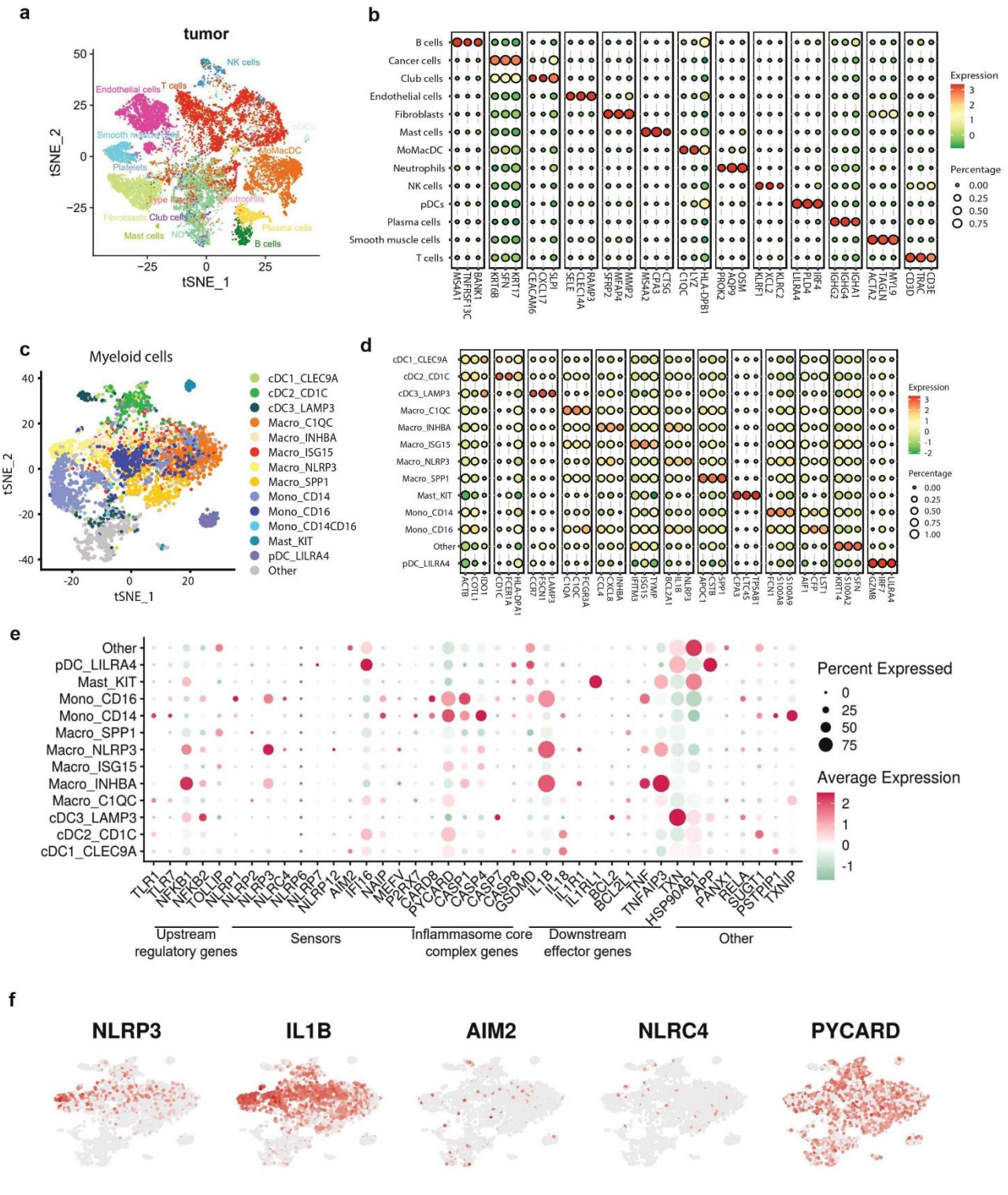
a
tumor
NK cells
Endothelial cells
T cells
pDCs
MoMacDC
Platelets
Neutrophils
Fibroblasts
Club cells
Plasma cells
Mast cells
B cells
tSNE_1
tSNE_2
b
B cells
Cancer cells
Club cells
Endothelial cells
Fibroblasts
Mast cells
MoMacDC
Neutrophils
NK cells
pDCs
Plasma cells
Smooth muscle cells
T cells
Expression
Percentage
c
Myeloid cells
cDC1_CLEC9A
cDC2_CD1C
cDC3_LAMP3
Macro_C1QC
Macro_INHBA
Macro_ISG15
Macro_NLRP3
Macro_SPP1
Mono_CD14
Mono_CD16
Mono_CD14CD16
Mast_KIT
pDC_LILRA4
Other
d
e
Percent Expressed
Average Expression
Upstream regulatory genes
Sensors
Inflammasome core complex genes
Downstream effector genes
Other
f
NLRP3
IL1B
AIM2
NLRC4
PYCARD

Figure 2.2. Single cell transcriptomic atlas reveals a heterogenous tumor infiltrating myeloid cell landscape with differential inflammasome signature in each subtype.

a) tSNE plot showing the transcriptome landscape of 19,193 major cell populations in the TME from n=6 patients with HNSCC. Colors indicate cell types. For single cell RNA sequencing, HNSCC tumors were dissociated into a single cell suspension and viability was confirmed using trypan blue. Samples with >75% viability were submitted to VANTAGE for Chromium Single Cell 3ʾ Library construction and sequencing. Samples were sequenced the same day they were received. Single cell sequencing analysis and cell type annotation workflow is outlined in methods section 2.2.4. b) Bubble heat map showing relative expression levels of typical signature genes for all cell types shown in panel A. c) tSNE showing the phenotypic heterogeneity of 3072 myeloid cells in the tumor from the same n=6 patients in figure a, divided into 13 different subclusters. The "other" subset could not be characterized. d) Bubble heat map showing expression levels of selected signature genes for the tumor infiltrating myeloid cell populations shown in panel C. e) Bubble heat map showing relative expression of inflammasome pathway genes in the tumor infiltrating myeloid cell subclusters. f) Feature plots showing gene expression of selective inflammasome genes in the identified tumor infiltrating myeloid cell populations. Red and gray mean high and low expression, respectively.

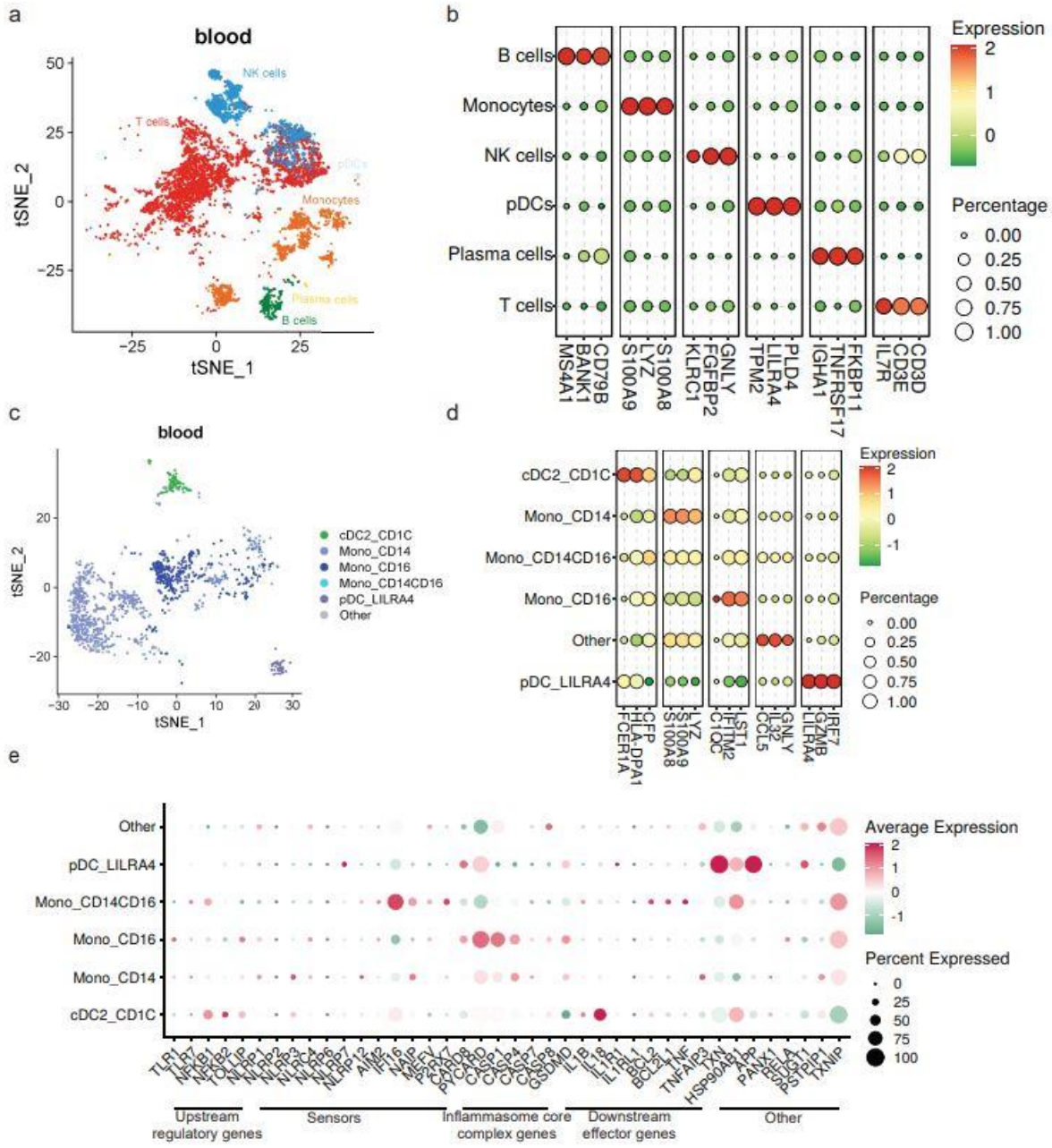
a
blood
NK cells
T cells
pDCs
Monocytes
Plasma cells
B cells
tSNE_2
tSNE_1
b
B cells
Monocytes
NK cells
pDCs
Plasma cells
T cells
MS4A1
BANK1
CD79B
S100A9
LYZ
S100A8
KLRC1
FGFBP2
GNLY
TPM2
LILRA4
PLD4
IGHA1
TNFRSF17
FKBP11
IL7R
CD3E
CD3D
Expression
Percentage
0.00
0.25
0.50
0.75
1.00
c
blood
cDC2_CD1C
Mono_CD14
Mono_CD16
Mono_CD14CD16
pDC_LILRA4
Other
d
cDC2_CD1C
Mono_CD14
Mono_CD14CD16
Mono_CD16
Other
pDC_LILRA4
FCER1A
HLA-DPA1
CFP
S100A8
S100A9
LYZ
C1QC
IFITM2
IST1
CCL5
IL32
GNLY
LILRA4
G2MB
IRF7
e
Other
pDC_LILRA4
Mono_CD14CD16
Mono_CD16
Mono_CD14
cDC2_CD1C
Average Expression
Percent Expressed
Upstream regulatory genes
Sensors
Inflammasome core complex genes
Downstream effector genes
Other

Figure 2.3 ScRNA seq reveals enrichment for NLRP3 inflammasome pathway in tumor derived CD11b^{+} cells over matched peripheral myeloid cells

a) tSNE plot showing transcriptomic atlas of 8506 different cell types identified in blood of HNSCC patients (n=6). For single cell RNA sequencing, matched PBMCs for the HNSCC tumors in Figure 2.2 were obtained using ficoll density centrifugation and viability was confirmed using trypan blue. Samples with >75% viability were submitted to VANTAGE for Chromium Single Cell 3' Library construction and sequencing. Samples were sequenced the same day they were received. Single cell sequencing analysis and cell type annotation workflow is outlined in methods section 2.2.4. b) Top three markers for each cell type identified in blood of HNSCC patients identifying T cell subsets, NK cells, B cells, and myeloid cells. c) 3489 Different myeloid subsets identified in blood of HNSCC patients (n=6) excluding neutrophils shown with (d) their top three markers. The "other" subset could not be characterized. e) Bubble plot showing inflammasome signature across different myeloid sub clusters in the blood of HNSCC patients.

Abundance of tumor infiltrating myeloid cell populations	
Cell type	**Number of cells**
cDC1_CLEC9A	99
cDC2_CD1c	205
cDC3_LAMP3	182
Macro_C1QC	671
Macro_INHBA	210
Macro_ISG15	189
Macro_NLRP3	297
Macro_SPP1	369
Mono_CD14	15
Mono_CD16	15
Mast_KIT	81
pDC_LILRA4	102
Other	762

Table 2.1 Abundance of tumor infiltrating myeloid cell populations

Absolute cell numbers for the cell types identified in the tumor single cell sequencing using the pan cancer cell ID algorithm from n=6 HNSCC tumors.

Abundance of blood myeloid cell populations	
Cell type	**Number of cells**
cDC2_CD1c	84
Mono_CD14CD16	14
Mono_CD14	661
Mono_CD16	347
pDC_LILRA4	38
Other	29

Table 2.2 Abundance of blood myeloid cell populations

Absolute cell numbers for the cell types identified in the blood single cell sequencing using the pan cancer cell ID algorithm from n=6 PBMC samples matched to the tumors in Table 2.1.

2.3.3 Inflammasome signaling is functionally upregulated in human tumor infiltrating myeloid cells

We next wanted to assess how inflammasome signaling is associated with tumor growth in HNSCC patients. Using The Cancer Genome Atlas (TCGA), we probed for HNSCC patients with alterations in *IL1B* copy number and found that increased *IL1B* copy number negatively correlated with overall survival (Figure 2.4a). We investigated if this increased IL1B expression coincided with increased IL-1β production by the tumor infiltrating myeloid cells and found that $CD11b^+$ isolated from HNSCC tumors had much higher basal IL-1β production than those from PBMC (Figure 2.4b). IL-1β production was abrogated upon stimulation with LPS indicating that the tumor infiltrating myeloid cells are already primed to the threshold of IL-1β production within the tumor and additional LPS stimulation likely promotes cell death. Together this confirms that increased expression of inflammasome genes in tumor infiltrating myeloid cells translates to an increase in inflammasome functional activity.

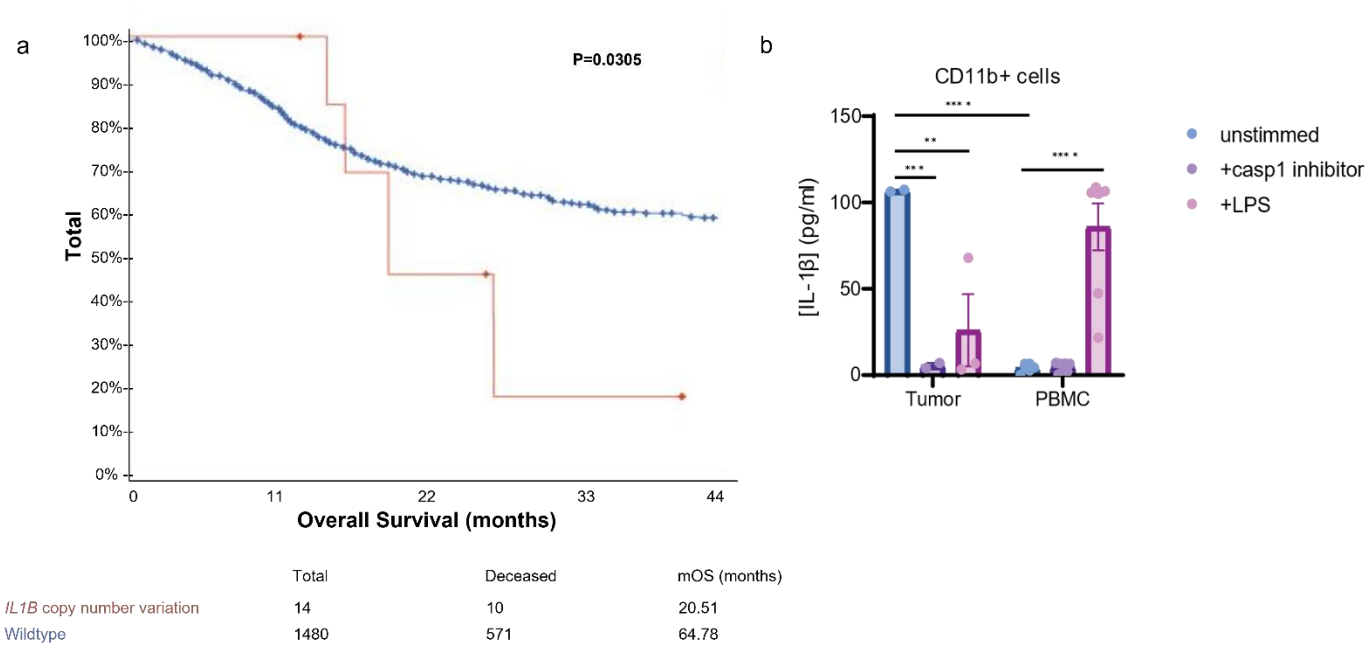

Figure 2.4 Inflammasome mediated IL-1β production is highest in tumor infiltrating CD11b$^+$ cells and reduces overall survival in HNSCC patients

a) TCGA dataset showing HNSCC patients with an increased IL1B copy number have a threefold reduction in overall survival. b) IL-1β production is much higher in CD11b$^+$ cells isolated from fresh HNSCC tumors and cultured in cRPMI overnight than those isolated from PBMCs. LPS (1 μg/ml) stimulation resulted in robust IL-1β production from blood CD11b$^+$ cells but not those isolated from the tumor (n=3 for tumor and 5 for PBMC). Treatment with caspase-1 inhibitor (10 μM Ac-YVAD-cmk) diminished IL-1β production. Statistics represent logrank test (a) and one-way ANOVA with multiple comparisons between tumor and blood CD11b$^+$ cells and among LPS and caspase-1 inhibitor treatment conditions (b). Error bars represent SD. (*=p<0.05, **=p<0.01, ***=p<0.001, ****=p<0.0001, ns=not significant)

2.3.4 NLRP3/Caspase-1/IL-1β signaling axis promotes tumor growth *in vivo*

Since the scRNA-seq dataset noted increased human caspase-1 expression in the tumor, we hypothesized that a distinct tumor intrinsic factor regulates specific myeloid cells towards a tumor supportive phenotype. Our single cell analysis of human TME phagocytes showed a strong association among the expression of *NLRP3* over other inflammasome sensors (Figure 2.2e-f), therefore, we focused on *in vivo* tumor growth studies in NLRP3 null mice. Here we found that tumor growth was blunted in NLRP3 null mice, which phenocopied the previously demonstrated protective effect found in caspase-1 null mice but was unaltered in AIM2 null mice (Figure 2.5a-b) further supporting the role of NLRP3 in human tumors suggested in our gene expression analysis. GSDMD is activated by caspase-1 to execute pyroptosis, and others suggested that GSDMD is associated with tumor growth.[181-183] However, we did not find a tumor supportive role for GSDMD in our models (Figure 2.5a-b). Together this indicates that the NLRP3/caspase-1 axis is important for promoting tumor growth without requiring the pyroptotic functions of GSDMD.

As previously described,[84, 184, 185] we confirmed that the downstream mediator responsible for tumorigenesis was IL-1β as its depletion resulted in significant reduction of tumor growth (Figure 2.5c-d) which phenocopied both the caspase-1 and NLRP3 null mice. Conversely, when we treated wildtype mice with recombinant IL-1β, we saw a modest increase in tumor volume (Figure 2.5e). In accordance with the single cell transcriptomic profile in the human TME, we found that myeloid intrinsic NLRP3-mediated activation of caspase-1 and subsequent GSDMD independent IL-1β release is permissive towards tumor growth among specific clusters of mononuclear phagocytes.

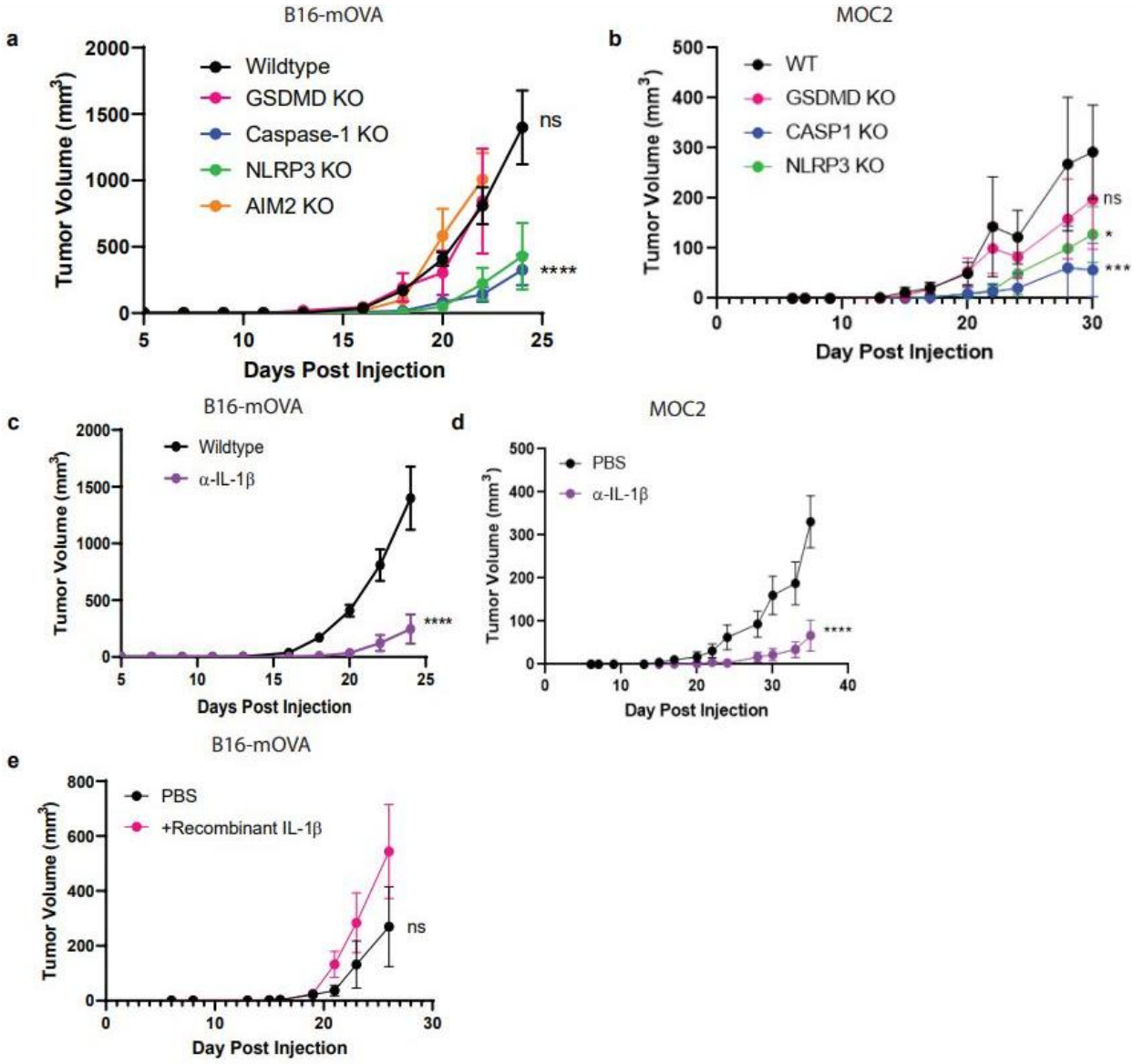

Figure 2.5 NLRP3/Casp-1/IL-1β axis drives tumor growth

a-b) The inflammasome sensor, NLRP3, and caspase-1 are required for tumor growth. B16-mOVA (a) and MOC2 (b) tumor growth shown in GSDMD, caspase-1, AIM2, and NLRP3 global knockout mice as compared to tumor volume in WT mice. (n=10 mice/group). c-d) IL-1β is required for B16-mOVA (c) and MOC2 (d) tumor growth as shown by a reduction in tumor volume upon IL-1β depletion compared to control PBS treated mice. Mice treated with 100 µg of IL-1β depleting monoclonal antibody or control 100 µl PBS 2x/week (n= 10 mice/group). e) Increased IL-1β drives B16-mOVA tumor growth indicating a pro-tumorigenic role of chronic elevated IL-1β. Mice treated with 5 ng recombinant IL-1β or control 100 µl PBS 2x/week (n=5 mice/group). All statistics represent two-way ANOVA and all error bars represent SEM. (*=p<0.05, **=p<0.01, ***=p<0.001, ****=p<0.0001, ns=not significant)

2.3.5 Caspase-1 deletion negatively regulates myeloid cell landscape in TME

We next sought to identify how the inflammasome pathway shapes the TME toward a tumor permissive phenotype. When we examined the tumor microenvironment in caspase-1 null mice, we surprisingly found that tumor infiltrating $CD45^+$ cells were significantly reduced in tumors grown in caspase-1 null mice, which was attributed to granulocytes ($MHCII^-Ly6G^+$), macrophages ($MHCII^+CD68^+$), and monocytic MDSCs ($MHCII^-Ly6C^+Ly6G^-$) in both B16 and MOC2 tumors (Figure 2.6a-c,f). When we specifically looked at the live $CD11b^+$ immune infiltrate into the tumor, we found that TME in tumors grown in caspase-1 null mice was significantly lacking live myeloid cells (Figure 2.6e). It is currently thought that suppressive myeloid cells have a short half-life within the TME and are constantly replaced by emergency myelopoiesis and the generation of new myeloid cells.[186, 187] Our data suggests that inflammasome signaling plays a role in this regulation of emergency myelopoiesis thus resulting in a lack of new myeloid cell recruitment to the TME in its absence.

No alterations were found in the tumor infiltrating T and NK cells (Figure 2.6d,g) which was consistent with our previous findings that the protective anti-tumor effects of myeloid caspase-1 deficiency were not T cell dependent.[75] Interestingly, tumors grown in gasdermin D null mice, that should lack the ability to undergo pyroptosis, did not phenocopy the TME profile of tumors from caspase-1 null mice (Figure 2.6).

We next wanted to assess the functional implications of inflammasome signaling on suppressive myeloid cells in the tumor microenvironment. We first generated murine bone marrow derived MDSCs and investigated the role of inflammasome signaling on myelopoiesis *in vitro* (Figure 2.7a). We found that skewing of bone marrow towards suppressive MDSC subsets was not significantly altered in either caspase-1 or GSDMD null bone marrow (Figure 2.7b). The main

functional role of MDSCs within the TME is to inhibit T cell function and prevent an anti-tumor immune response.[188] Inflammasome knockout MDSCs, including caspase-1, GSDMD, NLRP3, and IL1B knockouts, all retained suppressive capacity and were able to directly inhibit T cell proliferation *in vitro* similar to wildtype MDSCs (Figure 2.7c).

To probe if inflammasome signaling is activated by stimuli specific to the TME, we utilized an enzymatic caspase-1 specific activity assay in which a luciferin-tagged substrate for caspase-1 is incubated with cells and cleaved resulting in bioluminescence upon caspase-1 activity. This showed that $CD11b^+$ myeloid cells isolated from tumors in wildtype mice have high levels of caspase-1 activity which is not present in splenic myeloid cells from tumor bearing mice. This indicates the stimuli for this pathway is specifically within the TME and is not a PAMP that can be found in circulation (Figure 2.7d).

Since caspase-1 had a paradoxical effect on the TME $CD45^+$ mononuclear phagocytes, we directly evaluated LPS-induced myeloid apoptosis in bone marrow derived myeloid suppressor cells from caspase-1 null mice and noted that LPS-induced apoptosis was distinct from GSDMD-dependent pyroptosis. As expected, caspase-1 null cells had lower apoptosis rates, as identified by annexin V positivity and absence of caspase-3/7 staining, compared to LPS treated myeloid suppressor cells from wildtype mice, but they showed consistently higher rates of apoptosis than both untreated wildtype and GSDMD null myeloid suppressor cells (Figure 2.7e). Since we showed that $CD11b^+$ caspase-1 activity was significantly upregulated only in the tumor, there are likely tumor intrinsic factors that can regulate their non-pyroptotic NLRP3/caspase-1 signaling axis and promote tumor growth (Figures 2.6-2.7). Taken together, these data suggest that myeloid intrinsic NLRP3-mediated activation of caspase-1 and subsequent GSDMD independent IL-1β release is permissive towards tumor growth, and that caspase-1 regulates the survival but not

trafficking or function of the myeloid cells to the TME.

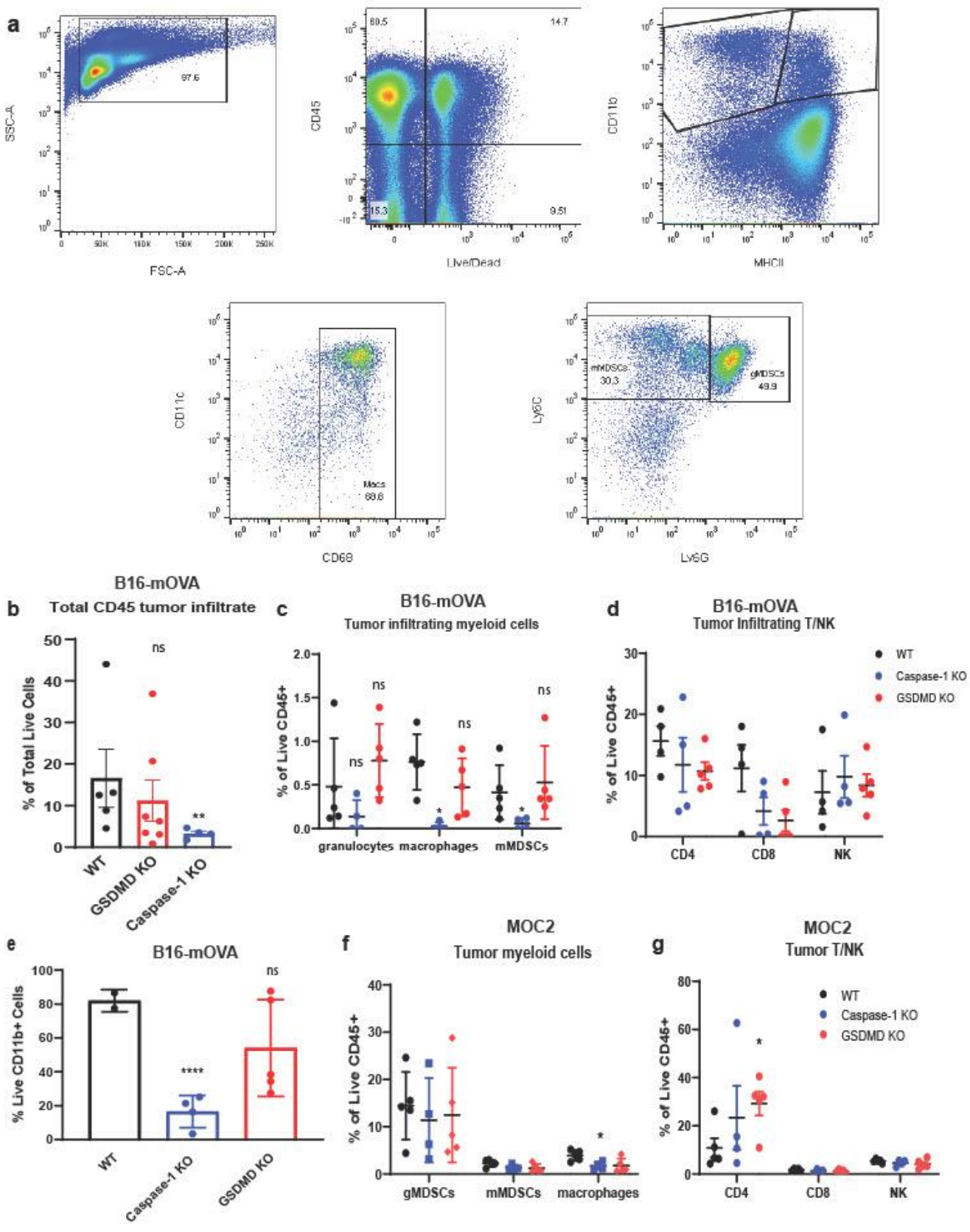
a
SSC-A
FSC-A
97.6
CD45
Live/Dead
80.5
14.7
15.3
9.51
CD11b
MHCII
CD11c
CD68
Macs
68.6
Ly6C
Ly6G
mMDSCs
30.3
gMDSCs
49.9
B16-mOVA
b
Total CD45 tumor infiltrate
% of Total Live Cells
ns
**
WT
GSDMD KO
Caspase-1 KO
B16-mOVA
c
Tumor infiltrating myeloid cells
% of Live CD45+
granulocytes
macrophages
mMDSCs
B16-mOVA
d
Tumor Infiltrating T/NK
% of Live CD45+
WT
Caspase-1 KO
GSDMD KO
CD4
CD8
NK
B16-mOVA
e
% Live CD11b+ Cells
****
MOC2
f
Tumor myeloid cells
% of Live CD45+
gMDSCs
mMDSCs
macrophages
MOC2
g
Tumor T/NK
% of Live CD45+

Figure 2.6 Caspase-1 deletion affects intratumoral immune landscape and myeloid cell survival *in vivo*

a) B16 tumors isolated from WT, caspase-1 KO, and gasdermin D KO mice 2 weeks post injection. Tumors were processed into single cell suspensions for analysis by flow cytometry. After gating on the Live, $CD45^+$, $CD11b^+$ population, macrophages were defined as $MHCII^+$, $CD68^+$, mMDSCs were defined as $MHCII^-$, $Ly6C^+$, $Ly6G^-$, and gMDSCs were defined as $MHCII^-$, $Ly6C^+$, $Ly6G^+$. b) Caspase-1 deletion reduces global $CD45^+$ cells in the TME as noted by flow cytometry (n=5 mice/group, GSDMD= gasdermin D KO). B16-mOVA tumors were harvested from WT or caspase-1/GSDMD global KO mice 2 weeks post tumor inoculation (subcutaneous injection of 100,000 B16-mOVA cells). Data shown as the total live $CD45^+$ cells in the total tumor. c) Caspase-1 reduces the percentage of macrophages and monocytic MDSCs in the tumor as noted by flow cytometry of B16-mOVA tumors (n=5 mice/group). d) Flow cytometry identification of tumor infiltrating T and NK cells. B16 mOVA tumors were harvested from WT or caspase-1/GSDMD null mice 2 weeks post tumor inoculation (subcutaneous injection of 100,000 B16-mOVA cells) (n=5 mice/group). e) Caspase-1 reduces the percentage of total live $CD11b^+$ cells in the TME as noted by flow cytometry of B16-mOVA tumors. Data shown as a percentage of the total live $CD11b^+$ cells in the tumor. (n=5 mice/group, GSDMD=gasdermin D KO) f-g) Flow cytometry analysis of wildtype MOC2 tumor infiltrating myeloid and T cells grown in wildtype C57Bl/6, caspase 1 and gasdermin D knockout mice 2 weeks post tumor inoculation (subcutaneous injection of 100,000 MOC2 cells). (n= 5 mice/group) Statistics represent one-way ANOVA with multiple comparisons of WT compared to both caspase-1 KO and GSDMD KO and error bars represent SD. (*=$p<0.05$, **=$p<0.01$, ***=$p<0.001$, ****=$p<0.0001$, ns=not significant)

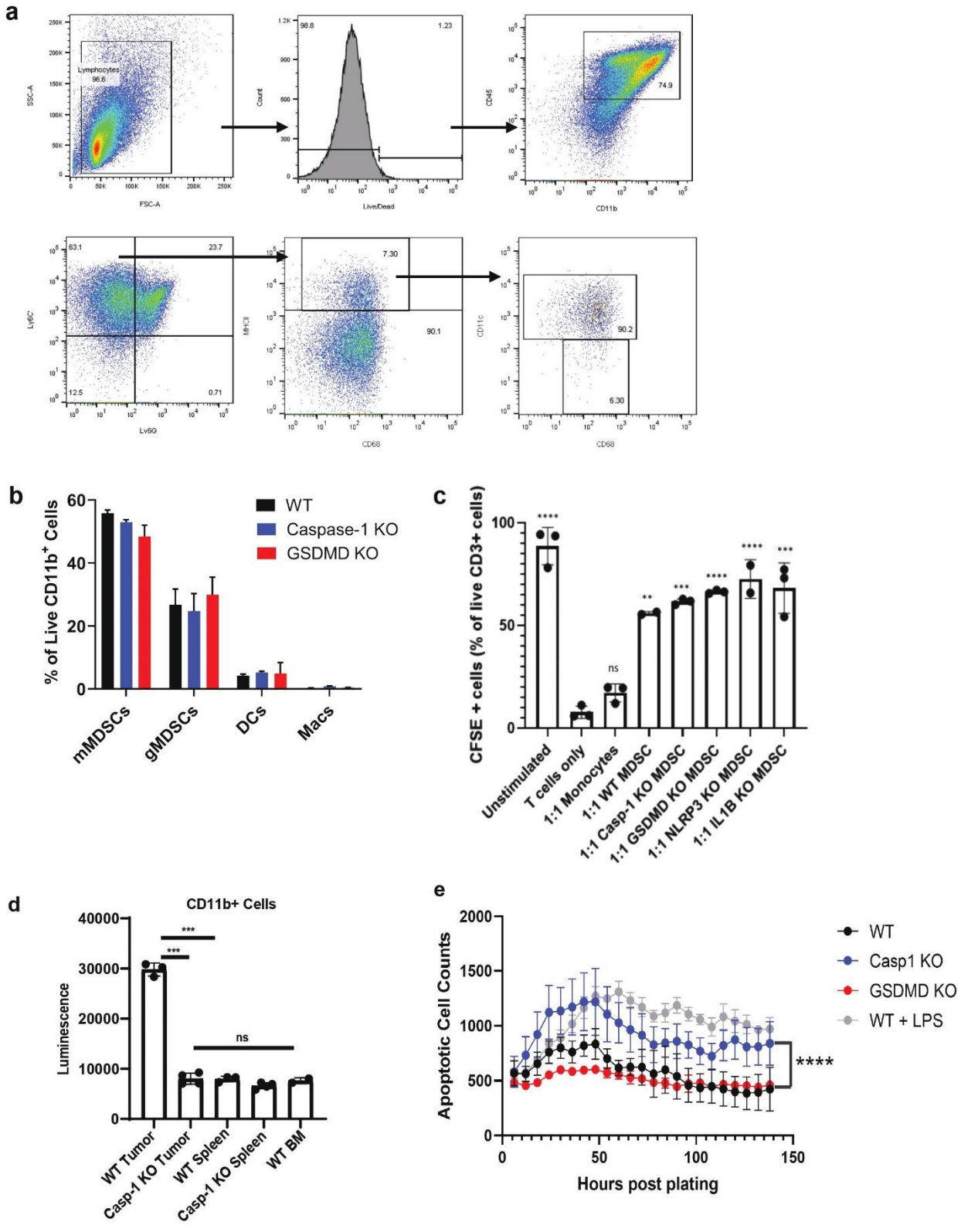
a
Lymphocytes
96.6
SSC-A
FSC-A
98.8
1.23
Count
Live/Dead
74.9
CD45
CD11b
63.1
23.7
12.5
0.71
Ly6C
Ly6G
7.30
90.1
MHCII
CD68
90.2
6.30
CD11c
CD68
b
% of Live CD11b+ Cells
WT
Caspase-1 KO
GSDMD KO
mMDSCs
gMDSCs
DCs
Macs
c
CFSE + cells (% of live CD3+ cells)
Unstimulated
T cells only
1:1 Monocytes
1:1 WT MDSC
1:1 Casp-1 KO MDSC
1:1 GSDMD KO MDSC
1:1 NLRP3 KO MDSC
1:1 IL1B KO MDSC
ns
d
CD11b+ Cells
Luminescence
WT Tumor
Casp-1 KO Tumor
WT Spleen
Casp-1 KO Spleen
WT BM
ns
e
Apoptotic Cell Counts
Hours post plating
WT
Casp1 KO
GSDMD KO
WT + LPS

Figure 2.7. Inflammasome signaling does not alter myeloid cell skewing or suppressive function

a) Flow cytometry analysis of wildtype bone marrow derived MDSCs gating strategy. Monocytic MDSCs were defined as $CD11b^+$, $Ly6C^+$, $Ly6G^-$, $MHCII^-$, granulocytic MDSCs were defined as $CD11b^+$, $Ly6G^+$, $MHCII^-$, dendritic cells were defined as $CD11b^+$, $CD11c^+$, $MHCII^+$, and macrophages were defined as $CD11b^+$, $MHCII^+$, and $CD68^+$. b) Wildtype, caspase-1, gasdermin D, IL-1β, and NLRP3 knockout bone marrow skewing to mMDSCs, PMN-MDSCs, DCs, and macrophages. Bone marrow cells were isolated and cultured for 4 days in 10 ng/ml GM-CSF and bead enriched for the $CD11b^+$ population. c) Proliferation of 100,000 wildtype $CD3^+$ T cells isolated from the spleens of C57Bl/6 mice co-cultured with equal number wildtype, caspase 1, gasdermin D, IL-1β, or NLRP3 knockout bone marrow derived myeloid cells. $CD3^+$ cells were stained with 5μM CFSE prior to plating. Proliferation was analyzed as a reduction in $CFSE^+$ T cells via flow cytometry. (N=3 per group). d) Caspase-1 activity is prominent in $CD11b^+$ beads enriched from B16-mOVA tumors 2 weeks post tumor inoculation (n=3). $CD11b^+$ cells were immediately utilized for caspase assay after sorting. Unstimulated mouse bone marrow derived myeloid suppressor cells were utilized as a negative control. Equal numbers (100,000) cells were plated for each condition. e) Caspase-1 KO bone marrow derived MDSCs display higher rates of apoptosis over a 7-day time course analyzed with the IncuCyte using Annexin V as a marker of apoptotic cells and caspase 3/7 as a marker of cell death. LPS (1μg/ml) treated WT myeloid cells were used as a positive control for both markers. GSDMD KO myeloid cells were a negative control for inflammasome-mediated pyroptotic cell death. Stimulation of WT MDSCs with LPS (1μg/ml) increases apoptosis rates. (n=3). Statistics represent one-way ANOVA with multiple comparisons comparing WT to each individual genotype (b-c), paired t test (d), and two-way ANOVA (e), and error bars represent SD. (*=$p<0.05$, **=$p<0.01$, ***=$p<0.001$, ****=$p<0.0001$, ns=not significant)

2.7 Discussion

Despite increasing number of studies focusing on inflammasome signaling in tumors, the understanding of the role of each inflammasome component and the enrichment pattern in the tumor myeloid compartment was lacking. Our analyses revealed that specific myeloid subpopulations isolated from the tumors were enriched for several inflammasome related genes including *NLRP3*, *IL1B*, and *IL1R1*. In addition, our single cell sequencing dataset identified a previously uncharacterized and highly complex myeloid landscape in HNSCC. Consistent with the current knowledge that questions the dichotomic M1/M2 nomenclature of macrophages,[189] we could not confirm or identify distinctly polarized macrophage clusters in the tumor milieu. For instance, the *NLRP3*$^{+}$ and *INHBA*$^{+}$ myeloid clusters that expressed high levels of proinflammatory molecules like *IL1B* and *IL6* were also enriched for several molecules with well characterized tumor-supportive functions (*VEGFA, IL10*). These findings concur with recent reports in other cancer models and highlight the greater heterogeneity and plasticity of tumor associated myeloid cells *in vivo*. [190-194] Further, we show that tumor progression was driven by NLRP3/Caspase-1/IL-1β axis independent of AIM2 or GSDMD. Contrary to pyroptosis onset, our studies show a pro-survival role of NLRP3/Caspase-1 dependent inflammasome signaling in myeloid cells.

Our previous reports demonstrated a role for caspase-1 in monocytic MDSCs as a tumor growth mediator in a T cell-independent manner to warrant IL-1β blockade in cancer therapeutics.[75] Interestingly, the CANTOS trial, which enrolled over 10,000 cancer-free patients, showed that those treated with canakinumab (IL-1β blocking agent) had reduced lung cancer incidence and cancer-associated mortality.[84, 195] This paved the way for multiple clinical trials (CANOPY) with canakinumab as a single agent or in combination with PD-1 blockade or chemotherapy. However, the CANOPY trial failed to meet the primary endpoints of overall survival and progression-free

survival.[196, 197] These clinical studies suggest that IL-1β plays an important role in early carcinogenesis in humans. Thus, therapeutic targeting of inflammasome signaling may be more effective in patients with early-stage disease or as adjuvant therapy in patients with a high risk of recurrences.

Together, our data has demonstrated the dichotomy between the traditional myeloid cell delineation and what occurs in the TME as evidenced by our human sc-RNAseq dataset. Further, we have shown a distinct pro-tumorigenic role for the NLRP3-driven inflammasome signaling axis which ultimately requires the production of IL-1β to drive tumor growth.

CHAPTER 3

Title of Chapter: Efferocytosis of apoptotic cancer cells activates NLRP3 inflammasome-dependent secretion of IL-1β

3.1 Introduction

NLRP3 is the most well studied sensor protein of the inflammasome. Therefore, a wide variety of unrelated stimuli, including microbial and viral PAMPs, endogenous DAMPs, and environmental irritants, have been identified to activate NLRP3. Generally, factors that induce cellular stress can lead to the activation of NLRP3, however, the exact mechanism by which this occurs is still unknown. Many studies have shown that NLRP3 activation is caused by cellular homeostatic disruptions such as K^+ or Cl^- efflux, Ca^{2+} influx, lysosomal disruption, and mitochondrial dysfunction.[198-202] Further, phagocytosis of either self or foreign-derived particles can cause lysosomal destabilization resulting in rupture and release of particles into the cytoplasm of the cell. Prior to this, the lysosome will undergo acidification which can activate NLRP3 upon rupture.[203] Therefore, we hypothesized that efferocytosis of apoptotic cancer cells within the TME could activate this pathway as well through a similar mechanism.

A role for efferocytic clearance of AC in infection has been well established, however, the role of efferocytosis in the TME is unclear. Our objective was to demonstrate a direct link between the efferocytosis of apoptotic cancer cells by macrophages and the stimulation of the NLRP3 inflammasome within those macrophages. We aimed to study this by utilizing the ASC-citrine mouse model to visualize inflammasome complex assembly both *in vitro* and *in vivo*.[204]

3.2 Methods

3.2.1 Mouse Lines

R26-CAG-LSL-ASC-citrine mice were purchased from the Jackson Laboratory. These mice are a Cre recombinase-dependent fluorescent reporter of inflammasome complex activation. The R26-CAG-LSL-ASC-citrine floxed allele has a CAG promoter and *loxP*-flanked STOP cassette upstream of the ASC-citrine fusion protein, all inserted into the *Gt(ROSA)26Sor* locus. These were bred with LysMcre mice obtained from the Jackson Laboratory. Following removal of the floxed-STOP cassette, the mice express a fluorescent adaptor fusion protein (ASC-citrine) in the myeloid cells that retains the function of endogenous ASC, forming assembled inflammasome complexes (specks) upon exposure to inflammasome activator(s) both *in vitro* and *in vivo*.[204] All other mouse lines were obtained as outlined above in the chapter 2 methods section.

3.2.2 Generation of human peripheral blood derived macrophages

Peripheral blood was obtained from healthy volunteers. Buffy coat was isolated using Ficoll Plaque gradient. $CD11b^+$ cells were isolated from the buffy coat using CD11b microbeads from Miltenyi Biotech following manufacturer's instructions. Monocytes were then cultured at 37°C with 5% CO_2 in RPMI 1640 containing 10% fetal bovine serum, 2 mmol/L glutamine, 1% HEPES, 1% Glutamax, 0.1% beta-mercaptoethanol, 100 μg/mL streptomycin, and 100 U/mL penicillin for 7 days, with either 100 ng/mL GM-CSF or M-CSF. Fresh media supplemented with appropriate concentrations of GM-CSF or M-CSF was added every alternate day. To generate M1 macrophages, on day 7, cells were treated with a cocktail of 1 μg/ml LPS and 20 ng/ml IFN-γ for 24 hours. For M2 macrophages, on day 7, cells were treated with 20 ng/ml IL-4 for 24 hours.

3.2.3 Generation of mouse bone marrow derived macrophages

For generation of mouse macrophages, bone marrow from the femur and tibia of mice was flushed out with ice-cold PBS using a 25-gauge 30cc needle. Red blood cells (RBC) were removed using RBC lysis buffer. Cells were resuspended in complete media and differentiated using either 50 ng/ml GM-CSF or 100 ng/ml M-CSF for 7 days. Fresh media supplemented with appropriate concentration of GM-CSF or M-CSF was added every alternate day. Where mentioned, to generate M2 macrophages, on day 7, cells were treated with 20 ng/ml IL-4 for 24 hours. For M1 macrophages, on day 7, cells were treated with 1 μg/ml LPS and 20 ng/ml IFN-γ for 24 hours.

3.2.4 Efferocytosis Assays

Induction of apoptosis

Apoptosis was induced in Cal27 cells by treating cells with 2 μM Staurosporine for 15 hours. To induce apoptosis in MOC2 cells, they were incubated with 75 μM AZD5582 for 20 hours. Cells were harvested and washed in PBS and resuspended in 100 μl 1x Annexin V staining buffer. Cells were stained with 5 μl Annexin V (APC) for 15mins in the dark at RT. Cells were washed once in Annexin V buffer, stained with PI, and analyzed by flow cytometry. This process regularly yielded 70-80% early apoptotic cells (Annexin V^+PI^-). Efferocytosis experiments were strictly conducted with cells that were early apoptotic.

Efferocytosis assay

For efferocytosis assays, macrophages were plated in either cell culture petri dishes or two-well chambers (for confocal imaging). Either Annexin V^+/PI^- Cal27 or MOC2 cells were added to the macrophages for the indicated time points. Where mentioned, apoptotic cells

were stained with PKH26 cell membrane labeling kit following manufacturer's instructions. For RNA sequencing experiments, efferocytosis was stopped after 1 hour (pulse) using ice cold PBS. Macrophages were vigorously washed with PBS to remove non-phagocytosed cancer cells. Fresh media was added for another 6 hours (chase) following which cells were harvested, stained with antibodies against CD11b and F4/80. Macrophages that had efferocytosed apoptotic cancer cells were isolated by flow sorting as $CD11b^{+}F4/80^{+}PKH26^{+}$ cells and processed for bulk RNA sequencing. Where mentioned, macrophages were treated with small molecule inhibitors to target inflammasome pathway or block the uptake of apoptotic tumor cells. For confocal assays, macrophages were washed with 1x PBS and stained with WGA cell labeling dyes and Hoechst.

3.2.5 Detection of inflammasome speck formation by confocal microscopy

Macrophages were grown in two-well chambers as described previously. Where mentioned, cells were treated with 1 μg/ml LPS and/or 5 μg/ml Nigericin as inflammasome agonists. Following efferocytosis, macrophages were washed with 1x PBS and stained with WGA594 for 5 minutes in 4°C. Cells were washed with 1x PBS and nuclei were stained using Hoechst dye in PBS for 5 minutes and analyzed by Zeiss LSM 800 with Airyscan at the VU CISR imaging facility. Data were analyzed and processed with the Zeiss Zen 2010 software. All confocal data were quantified using ImageJ software, and graphical illustrations were made using GraphPad Prism software as mentioned later.

Detection of inflammasome "speck" formation in myeloid cells from murine tumors

MOC2 cells (200,000) were subcutaneously injected into the flank of ASC Citrine/LysmCre mice. Where mentioned, mice were treated with MCC950 I.P. (15 mg/kg

body weight) daily for first three days and then every alternate day for rest of the study. Tumors were harvested after 15 days and digested to get single cells. F4/80^{+} cells were isolated using magnetic bead separation and immediately processed for analysis by confocal microscopy. Hoechst was used to stain the nucleus.

3.2.6 Murine bulk RNA sequencing

BMDM were incubated with Annexin V^{+}/PI^{-} Cal27 cells stained with PKH26^{+} dye following manufacturer's instructions. After 1 hour, macrophages were washed with ice cold DPBS to remove excess apoptotic cells that were not engulfed. Flow cytometry was then used to sort out efferocytic macrophages that had engulfed apoptotic Cal27 cells. RNA was isolated from sorted CD11b^{+} cells using Trizol and used for sequencing at VANTAGE next generation sequencing facility at VU. Raw fastq files were mapped to reference genomes (GRCh38 or GRCm38) with STAR software. Gene reads count were calculated with FeatureCounts in R.[160] Gene by sample matrix were integrated and performed the differential gene expression analysis workflow as described at https://bioconductor.org/packages/release/bioc/vignettes/DESeq2/inst/doc/DESeq2.html mainly using DESeq2 package.[161]

3.3 Results

3.3.1 Efferocytosis induces *Il1b* signature in macrophages

We sought to investigate the tumor intrinsic factors that can potentially activate the NLRP3-mediated inflammasome in tumor infiltrating mononuclear phagocytes. An under characterized dynamic process in the TME is efferocytosis, which is an immunologically silent

phagocytic clearance of apoptotic tumor cells.[90, 93, 94, 98, 101] While there have been several preclinical reports that this is associated with tumor progression and response to checkpoint blockade[92, 205-207], the mechanistic link between efferocytosis of tumor apoptotic cells (AC) and inflammasome activation is currently unknown.

We reanalyzed the bulk and single cell sequencing dataset, and our data revealed that several genes associated with distinct stages of efferocytosis were upregulated in tumor derived $CD11b^+$ cells in comparison with their PBMC counterpart. Tumor associated myeloid cells exhibited higher transcriptional expression of molecules linked to the "find me" (*G2A*), "eat me" (*CD93, TIM1, SCARF1, SLC2A1, GAS6, TREM2, AXL, C1QA*) and downstream processing (*NR1H3, ATG7, PPARG, ABCA1, PPARD, DOCK180*) phases of efferocytosis. Furthermore, IPA and GO analyses revealed pathways related to phagocytosis, phagosome maturation, and autophagosome organization were also significantly altered in myeloid cells isolated from the tumor.

Single cell dataset revealed an enrichment of multiple efferocytosis related genes in distinct myeloid subsets within the tumor (Figure 3.1a-b), specifically, $SPP1^+$, $ISG15^+$, $C1QC^+$ macrophages, and $CD14^+$ monocytes in the tumors (Figure 3.1d), which were distinct from the scRNA-Seq from the peripheral blood. Our ssGSEA analyses revealed these macrophage subsets were associated with significant changes in pathways related to apoptotic cell clearance, late endosome and phagocytic vesicle and engulfment over other non-efferocytosis gene rich myeloid clusters. $ISG15^+$ and $C1QC^+$ macrophages also mobilized signaling cascades related to carcinoma and T cell exhaustion, respectively. We mentioned earlier that in addition to inflammasome signaling, ssGSEA analysis associated $NLRP3^+$ and $INHBA^+$ macrophage subsets with multiple pathways related to carcinoma, angiogenesis, wound healing, and T cell exhaustion, all classical

hallmarks of efferocytosis.[208] Based on this, we initially hypothesized that efferocytosis in myeloid cells in the TME activates NLRP3 dependent inflammasome signaling. Interestingly, we did not observe significant overlap of these two pathways in the 8 mononuclear phagocytic populations (Figure 3.1c). However, when we performed RNA velocity analysis that imputes cell fates,[157, 158, 167, 209-213] we identified a strong directional flow from the efferocytosis^{high} *C1QC*$^{+}$ macrophages towards the inflammasome^{rich} *NLRP3*$^{+}$ subset through an intermediate *ISG15*$^{+}$ macrophage state (Figure 3.1e). We observed that another efferocytosis rich cluster, *SPP1*$^{+}$, can also develop into the *NLRP3*$^{+}$ macrophage subset (Figure 3.1e). Additionally, our analysis showed that a fraction of the *NLRP3*$^{+}$ macrophages can arise from the *CD14*$^{+}$ and *CD16*$^{+}$ monocytes as well as from the *INHBA*$^{+}$ macrophage subset. *NLRP3*$^{+}$ macrophages also expressed high levels of *S100A6/8/9* which in part supports their monocytic origin. This trajectory analysis was further validated by the directional flow between dendritic cells and from monocyte subsets to macrophage subsets. As mentioned above, our scRNA seq dataset further showed that *NLRP3*$^{+}$ and *INHBA*$^{+}$ macrophages also expressed several well characterized immune suppressive tolerogenic molecules, suggesting efferocytosis can activate a unique heterogenous complex signature in the tumor infiltrating mononuclear phagocytes.

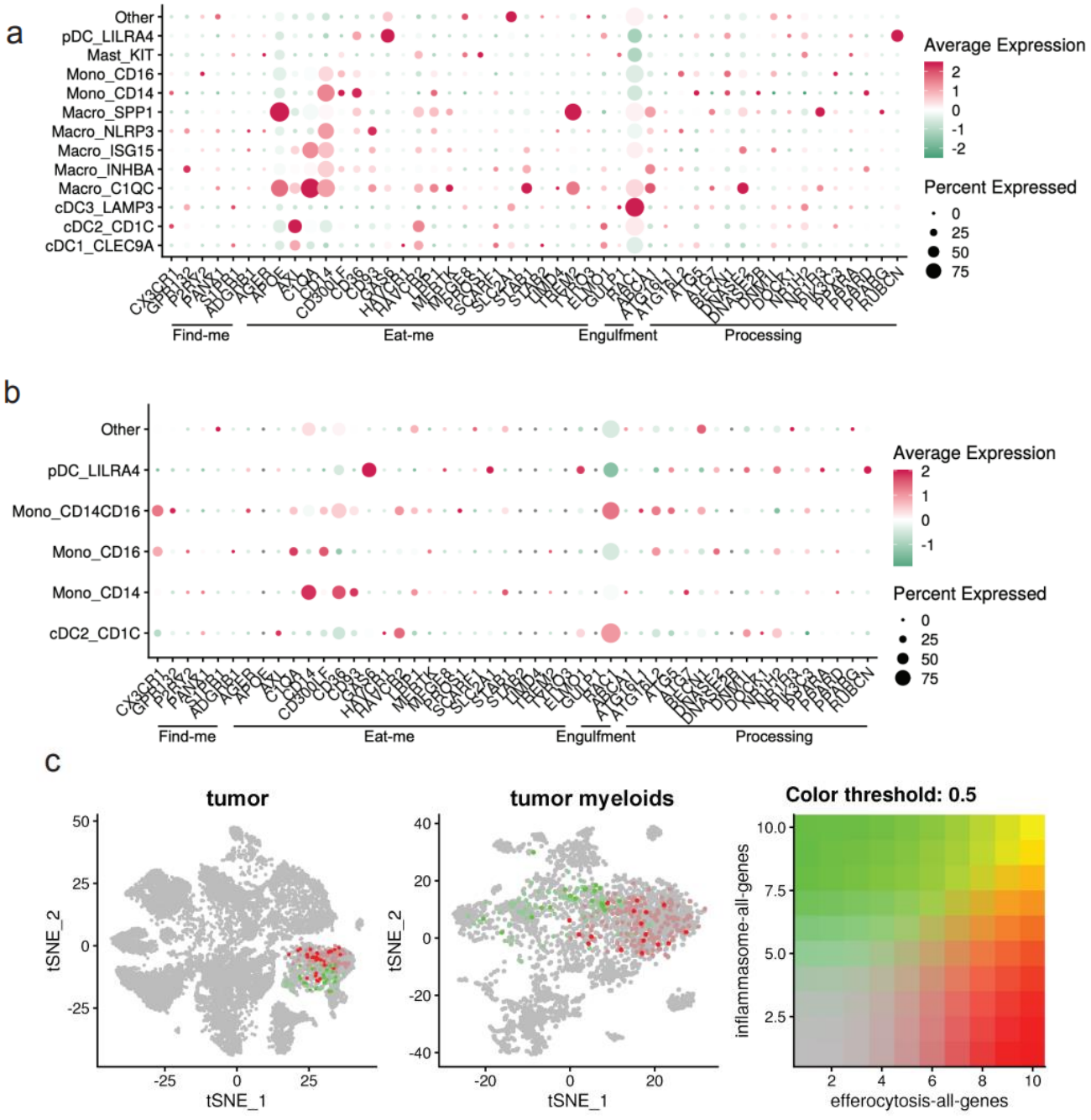
a
Other
pDC_LILRA4
Mast_KIT
Mono_CD16
Mono_CD14
Macro_SPP1
Macro_NLRP3
Macro_ISG15
Macro_INHBA
Macro_C1QC
cDC3_LAMP3
cDC2_CD1C
cDC1_CLEC9A
Find-me
Eat-me
Engulfment
Processing
Average Expression
2
1
0
-1
-2
Percent Expressed
0
25
50
75
b
Other
pDC_LILRA4
Mono_CD14CD16
Mono_CD16
Mono_CD14
cDC2_CD1C
Find-me
Eat-me
Engulfment
Processing
Average Expression
2
1
0
-1
Percent Expressed
0
25
50
75
c
tumor
tumor myeloids
Color threshold: 0.5
tSNE_1
tSNE_2
inflammasome-all-genes
efferocytosis-all-genes

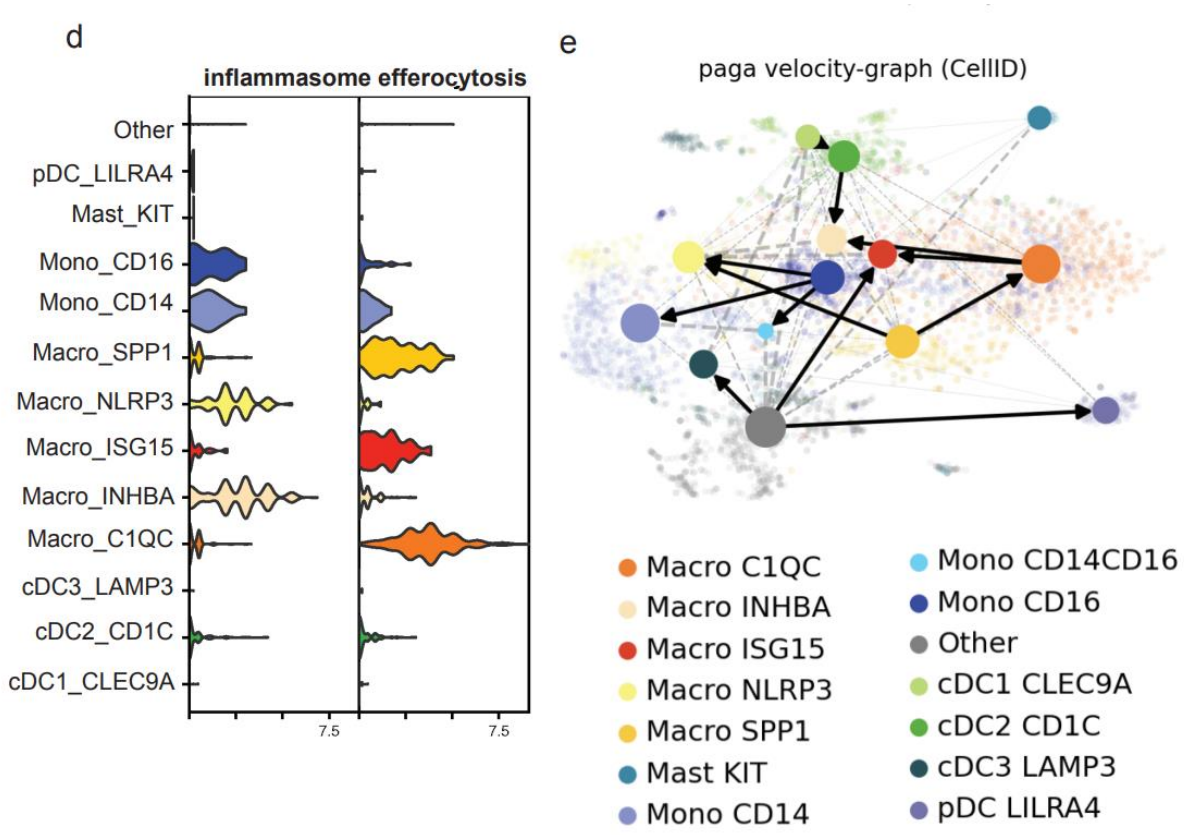

Figure 3.1. Efferocytosis gene atlas is enriched across single cell myeloid subsets in the tumor and can potentially develop into inflammasome rich macrophages in the TME

a-b) Single cell dataset from HNSCC patients was analyzed for genes associated with efferocytosis pathway in the myeloid subsets (n=6). Bubble heat map showing relative expression pattern of several efferocytosis genes across various myeloid subsets in the tumor (a) compared to matched blood (b). c) Feature plot shows inflammasome and efferocytosis pathway associated genes across different myeloid subsets within the tumor are not transcriptionally enriched in similar clusters. d) Representative violin plot highlighting efferocytosis and inflammasome genes are enriched differentially in distinct myeloid subsets within the tumor. e) Developmental trajectory of monocytes and macrophages enriched in the tumor indicate efferocytosis rich $C1QC^{+}$ and $SPP1^{+}$ macrophages can develop into inflammasome gene rich $INHBA^{+}$ and $NLRP3^{+}$ subsets respectively in the TME. Cells are colored according to their cluster origin. Single cell RNA sequencing analysis, cell type annotation, and RNA velocity workflow outlined in methods section 2.2.4.

To directly test whether efferocytosis induces NLRP3 dependent inflammasome signaling in macrophages, we first modeled this process *in vitro*. To induce apoptosis, tumor cells were incubated with staurosporine and the early apoptotic cell population, confirmed by Annexin V positivity and absence of propidium iodide staining, were fed to BMDM (Figure 3.2a and d). The use of a human HNSCC cell line in this experiment allowed us to clearly identify the gene expression pattern derived from the phagocytes and rule out cross-contamination from AC. BMDM were allowed to engulf tumor AC stained with PKH26 dye for 1 hour, washed to remove non-phagocytosed AC debris, and sorted for AC^+ macrophages that were then subjected to RNA sequencing (Figure 3.2b-c, 3.3a). ACs are cleared from phagocytes within 6 hours post ingestion,[214] therefore this allowed us to explore signaling pathways mobilized specifically during late stages of efferocytosis or post processing and clearance the apoptotic debris.

Efferocytosis of tumor AC downregulated several inflammatory genes like *Nos2*, *Il12rb1*, and increased several suppressive and tumor promoting genes like *Tgfb1* and *Vegfa*, among others (Figure 3.3a).[90, 215-217] Post efferocytosis, we observed a significant increase in the transcriptional activation of *Il1b* and *Il1r1* and a modest change in the mRNA levels of *Nlrp3* (Figure 3.3a and c), consistent with our bulk RNA-seq analysis from sorted human tumor derived $CD11b^+$ cells. Several genes associated with the "find me" (*S1pr1, Gpr132, P2ry2, Panx1*), "eat me" (*Cd36, Slc2a1*), and downstream processing phases of efferocytosis (*Atg7, Nr1h3, Ppard*) (Figure 3.3a) were also upregulated in the efferocytic BMDM. IPA and GO pathway analyses revealed IL-1 signaling and apoptotic cell clearance and phagosome formation was among the most significantly altered in efferocytic macrophages (Figure 3.3b). Additionally, IPA and GO analyses showed efferocytic macrophages altered several tumor supportive pathways including IL-10 signaling, T cell exhaustion pathway, and PD-1/PD-L1 signaling pathways to mimic the human tumor derived

myeloid transcriptomic profiles (Figure 3.3b). While this sequencing dataset provides an interesting link between efferocytosis and inflammasome activation, we next sought to functionally confirm this relationship.

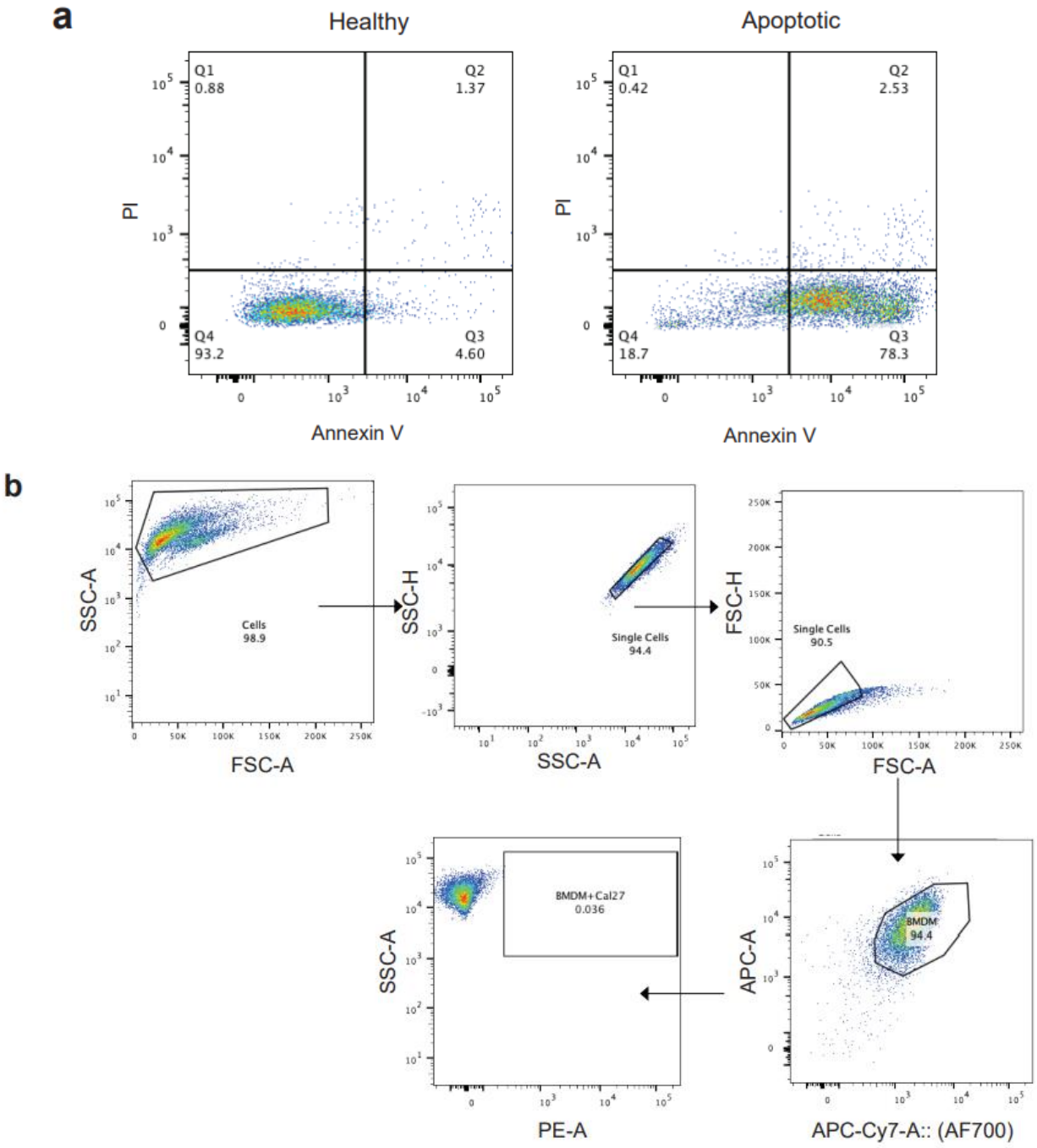
a
Healthy
Apoptotic
Q1
0.88
Q2
1.37
Q4
93.2
Q3
4.60
Q1
0.42
Q2
2.53
Q4
18.7
Q3
78.3
PI
Annexin V
b
SSC-A
FSC-A
Cells
98.9
SSC-H
SSC-A
Single Cells
94.4
FSC-H
FSC-A
Single Cells
90.5
SSC-A
PE-A
BMDM+Cal27
0.036
APC-A
APC-Cy7-A:: (AF700)
BMDM
94.4

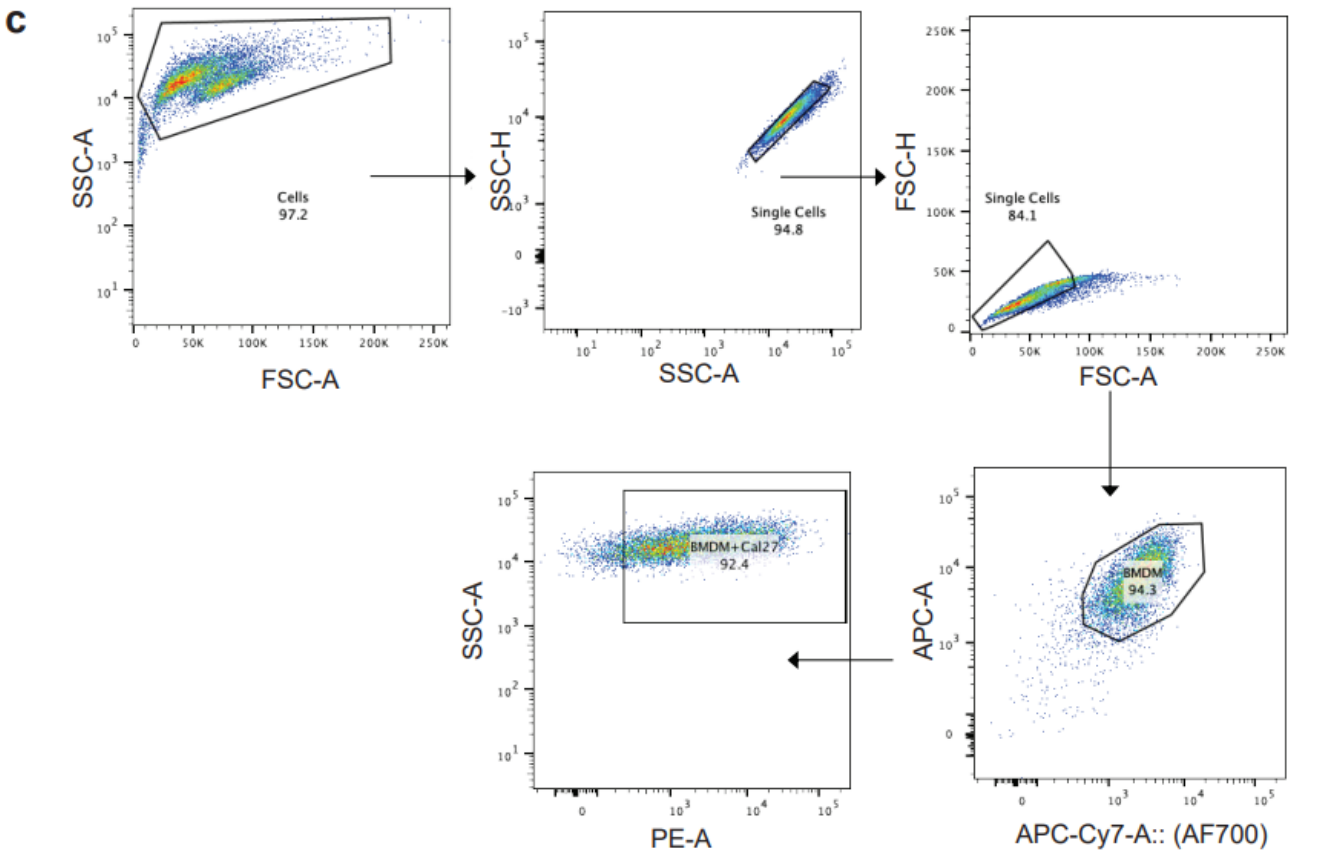
c
SSC-A
FSC-A
Cells
97.2
SSC-H
SSC-A
Single Cells
94.8
FSC-H
FSC-A
Single Cells
84.1
SSC-A
PE-A
BMDM+Cal27
92.4
APC-A
APC-Cy7-A:: (AF700)
BMDM
94.3

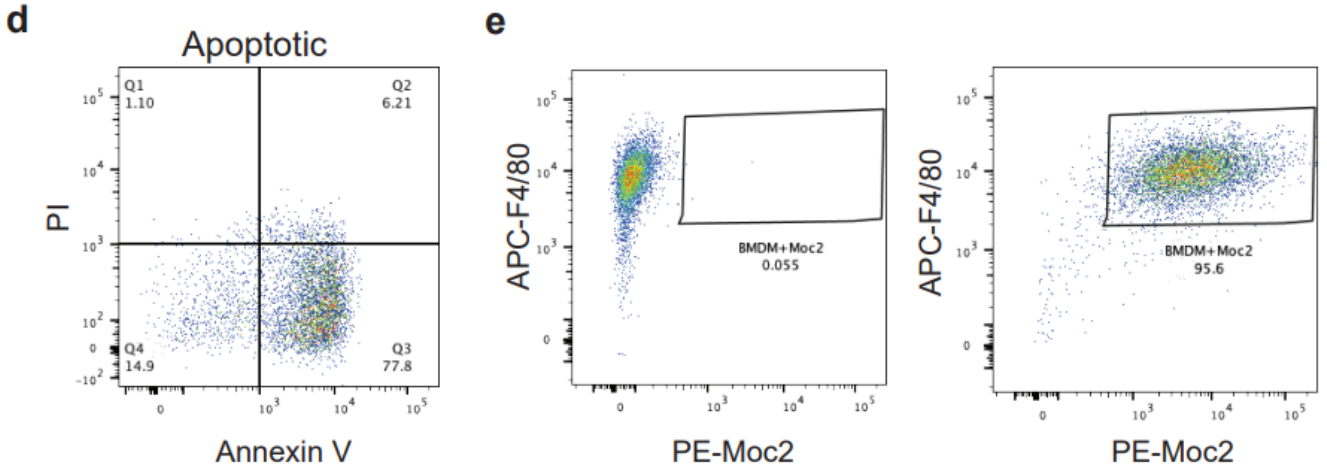
d
Apoptotic
PI
Annexin V
Q1
1.10
Q2
6.21
Q4
14.9
Q3
77.8
e
APC-F4/80
PE-Moc2
BMDM+Moc2
0.055
APC-F4/80
PE-Moc2
BMDM+Moc2
95.6

Figure 3.2. Induction of apoptosis in cancer cells and gating strategy for flow sorting PKH26$^+$ AC$^+$ BMDM

a) representative graph showing treatment of Cal27 with 2μM ST for 15 hours yields mostly 70-80% Annexin V$^+$ PI$^-$ early apoptotic cells. b-c) Gating strategy for flow sorting AC$^+$ BMDM post efferocytosis assay. BMDM cultured with M-CSF (100ng/ml) for 7 days were incubated with 70-80% Annexin V$^+$PI$^-$ early apoptotic Cal27 cells stained with PKH26 cell labeling dye for 1 hour following which non-engulfed cells were washed away with 1X PBS. After additional 6 hours post efferocytosis, BMDM were harvested and processed for flow cytometric sorting of PKH26 AC$^+$ BMDM and RNA isolation. d) Representative plot showing Annexin V and PI staining in MOC2 cells treated with 75μM AZD5582 for 20 hours. e) representative uptake efficiency of apoptotic MOC2 cells by BMDM.

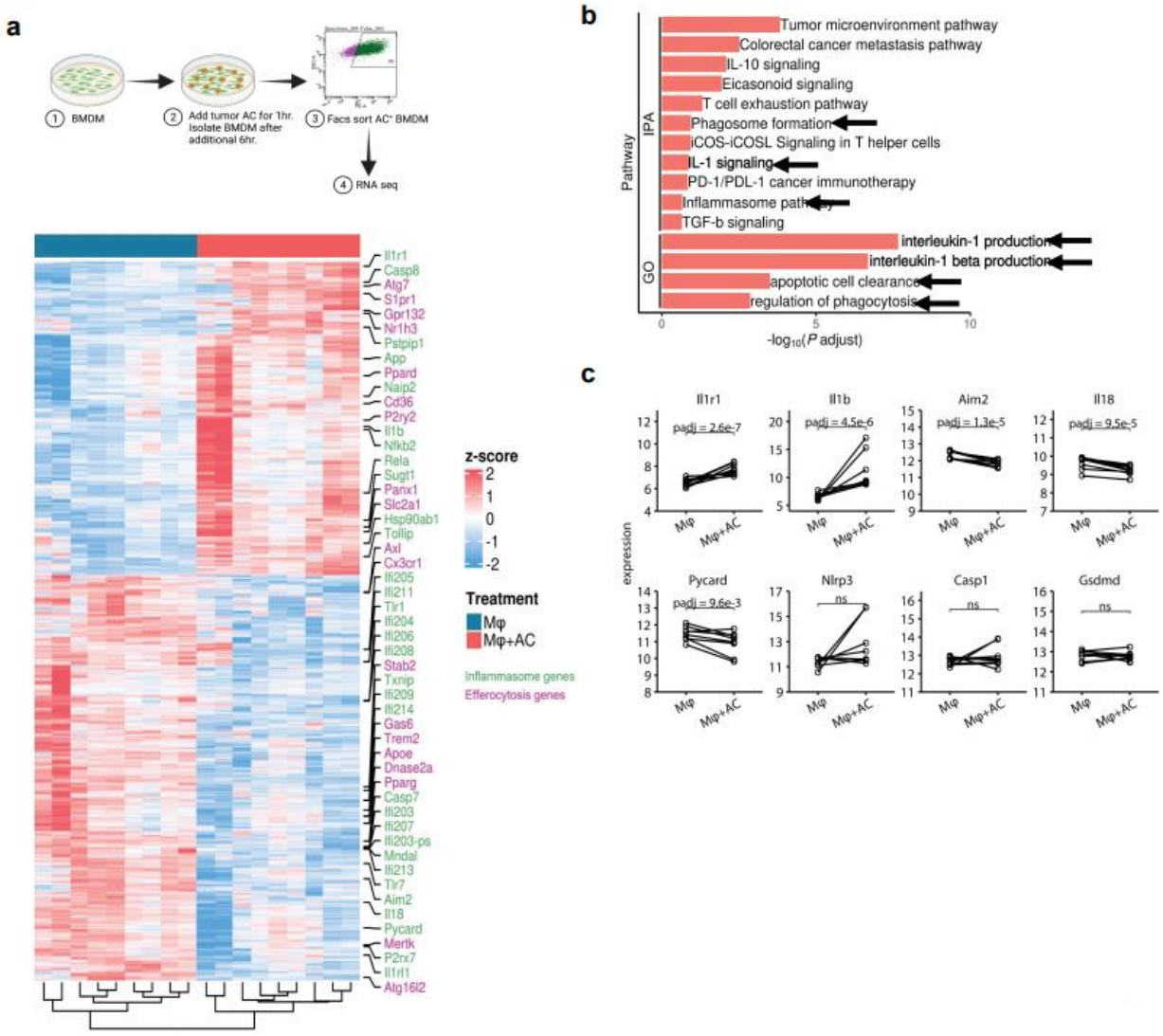

Figure 3.3. Efferocytosis in macrophages upregulates inflammasome gene expression

a) Experimental workflow and heatmap for induction of efferocytosis in mouse bone marrow derived macrophages and subsequent RNA-seq (n=5). BMDM were incubated with PKH26 labeled AC for 1hr. Non-engulfed AC were washed with 1X PBS and after an additional 6hr, $PKH26^{+}$ BMDM were sorted and processed for RNA seq. Heatmap showing differential gene expression profiles between macrophages pre and post induction of efferocytosis as measured by bulk RNA-seq. b) IPA and GO analyses show increased expression of IL-1 signaling pathways post efferocytosis. c) Graphical representation of selected inflammasome genes indicate enrichment of NLRP3/IL-1 pathway post efferocytosis. Differential expression analysis was performed as outlined by Love et al. which generates p values using the Wald test.[161] Workflow for RNA sequencing expression analysis and IPA and GO pathway analysis is outlined in methods section 3.2.6.

3.3.2 Efferocytosis of tumor AC activates NLRP3 dependent inflammasome activation and IL-1β secretion in macrophages *in vivo*

To study the efferocytosis driven NLRP3-dependent inflammasome activity *in vivo*, we exploited a commercially available transgenic mouse model which allowed us to observe "speck" formation, a hallmark for inflammasome activation, when the adaptor protein ASC oligomerizes to form a large aggregate.[204] We first incubated BMDM from the ASC-citrine/LysmCre compound mice with Annexin V^+PI^- early apoptotic MOC2 cells (Figure 3.4a) and observed inflammasome "speck" formation in BMDM at 8 and 12 hours post efferocytosis (Figure 3.4b-c). This was associated with significant levels of IL-1β production in response to efferocytosis with low detectable levels of IL-18 secretion (Figure 3.4d). IL-1β has been shown to have a strong tumor promoting role while conversely, IL-18 has anti-tumorigenic effects.[84, 185, 218, 219] Here the ratio of IL-1β/IL-18 shows that IL-1β was secreted at a higher concentration than IL-18 from efferocytic macrophages indicating skewing toward a more pro-tumorigenic phenotype (Figure 3.4d). When we treated BMDM with MCC950, a known small molecule inhibitor for NLRP3, we did not observe any ASC "speck" formation or IL-1β secretion in BMDM following efferocytosis (Figure 3.4b-d). Notably, MCC950 did not affect the uptake efficiency of tumor AC in macrophages (Figure 3.5a). Importantly, we did not find inflammasome activation with recombinant IL-4 or conditioned media from live and tumor AC (Figure 3.5c) indicating that the effect is not mediated by either immunosuppressive cytokines or soluble factors released from apoptotic cells alone.

We also did not observe "speck" formation following efferocytosis in cytochalasin D treated BMDM, which prevented the engulfment of tumor AC by the macrophages, further indicating that engulfment of tumor AC is required for inflammasome activation (Figure 3.4c and e, 3.5b). In alignment with this, we did not detect any IL-1β or IL-18 secretion in cytochalasin D

treated macrophages following efferocytosis (Figure 3.4d). To rule out the possibility that cytochalasin D alone affected "speck" formation, we incubated LPS and nigericin treated BMDM with the same dose of Cytochalasin D used for our efferocytosis assays and saw no significant change in the average number of "speck" positive cells in these macrophages (Figure 3.5d). Treatment of BMDM with Annexin V beads alone failed to induce inflammasome "specks" suggesting activation of the inflammasome pathway requires the presence of tumor AC (Figure 3.5e).

We finally examined efferocytosis induced NLRP3 dependent inflammasome activation *in situ* from MOC2 tumor bearing ASC-citrine mice. We detected speck formation in these F4/80^{+} tumor infiltrating macrophages, and these specks were abrogated following I.P. treatment of tumors with MCC950 (Figure 3.4f, Figure 3.6). Further, we were able to rescue the pro-tumor effect of NLRP3 signaling with the addition of recombinant IL-1β (Figure 3.4g). Human macrophages showed efferocytosis dependent IL-1β secretion in a time dependent manner without the production of IL-18 and we did not see production of either cytokine in efferocytic human macrophages treated with MCC950 or Cytochalasin D (Figure 3.4h).

These *in vitro* findings clearly link efferocytosis of tumor AC and inflammasome-mediated IL-1β release in macrophages to support our hypothesis. Taken together, our findings support the key oncogenic role of efferocytosis of tumor AC to activate NLRP3 dependent inflammasome signaling in the TME to induce non-pyroptotic IL-1β secretion to promote tumor growth (Figure 3.7).

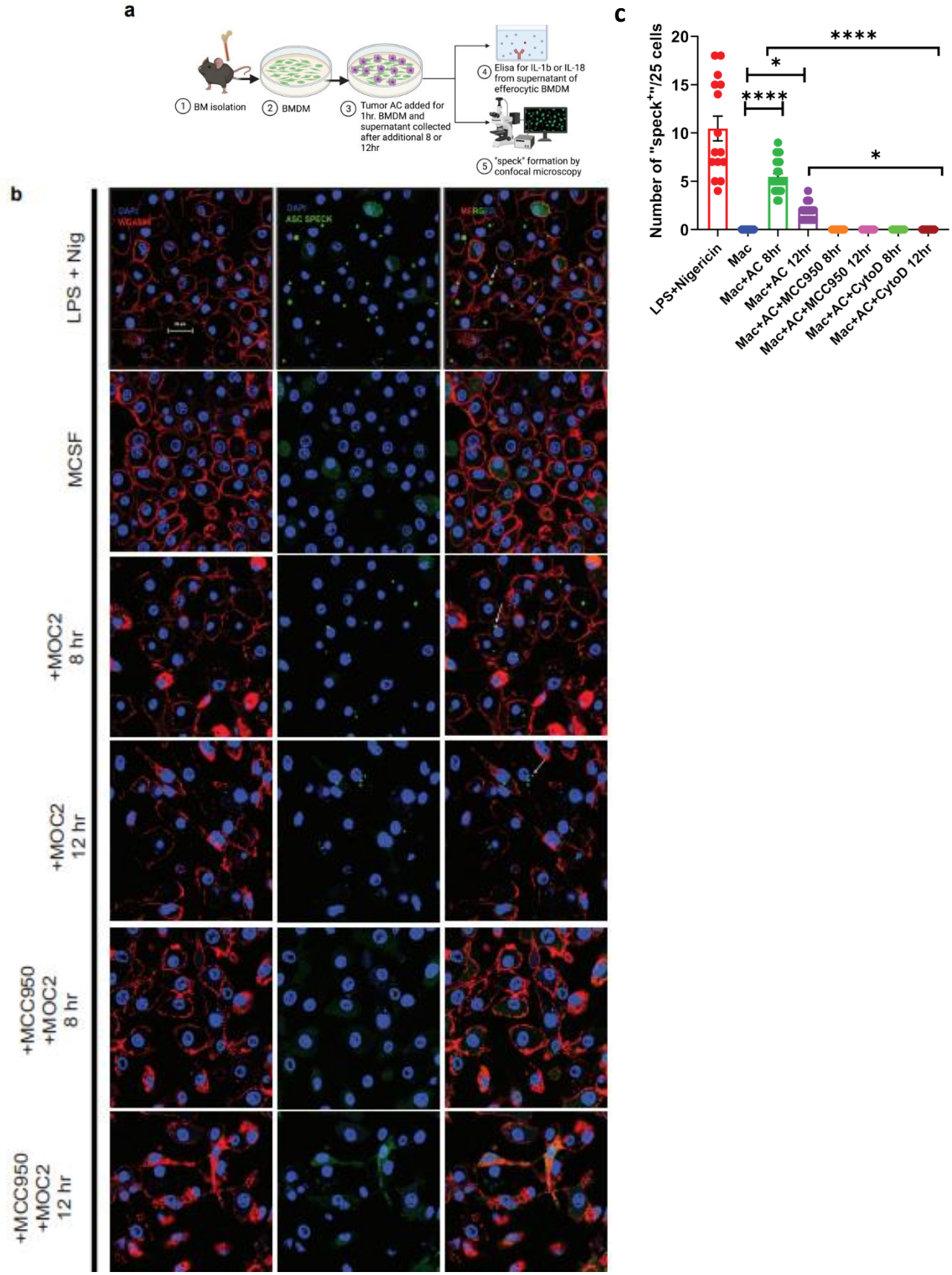
a
1 BM isolation
2 BMDM
3 Tumor AC added for 1hr. BMDM and supernatant collected after additional 8 or 12hr
4 Elisa for IL-1b or IL-18 from supernatant of efferocytic BMDM
5 "speck" formation by confocal microscopy
b
LPS + Nig
MCSF
+MOC2 8 hr
+MOC2 12 hr
+MCC950 +MOC2 8 hr
+MCC950 +MOC2 12 hr
c
Number of "speck+"/25 cells
0
5
10
15
20
****
*
****
*
LPS+Nigericin
Mac
Mac+AC 8hr
Mac+AC 12hr
Mac+AC+MCC950 8hr
Mac+AC+MCC950 12hr
Mac+AC+CytoD 8hr
Mac+AC+CytoD 12hr

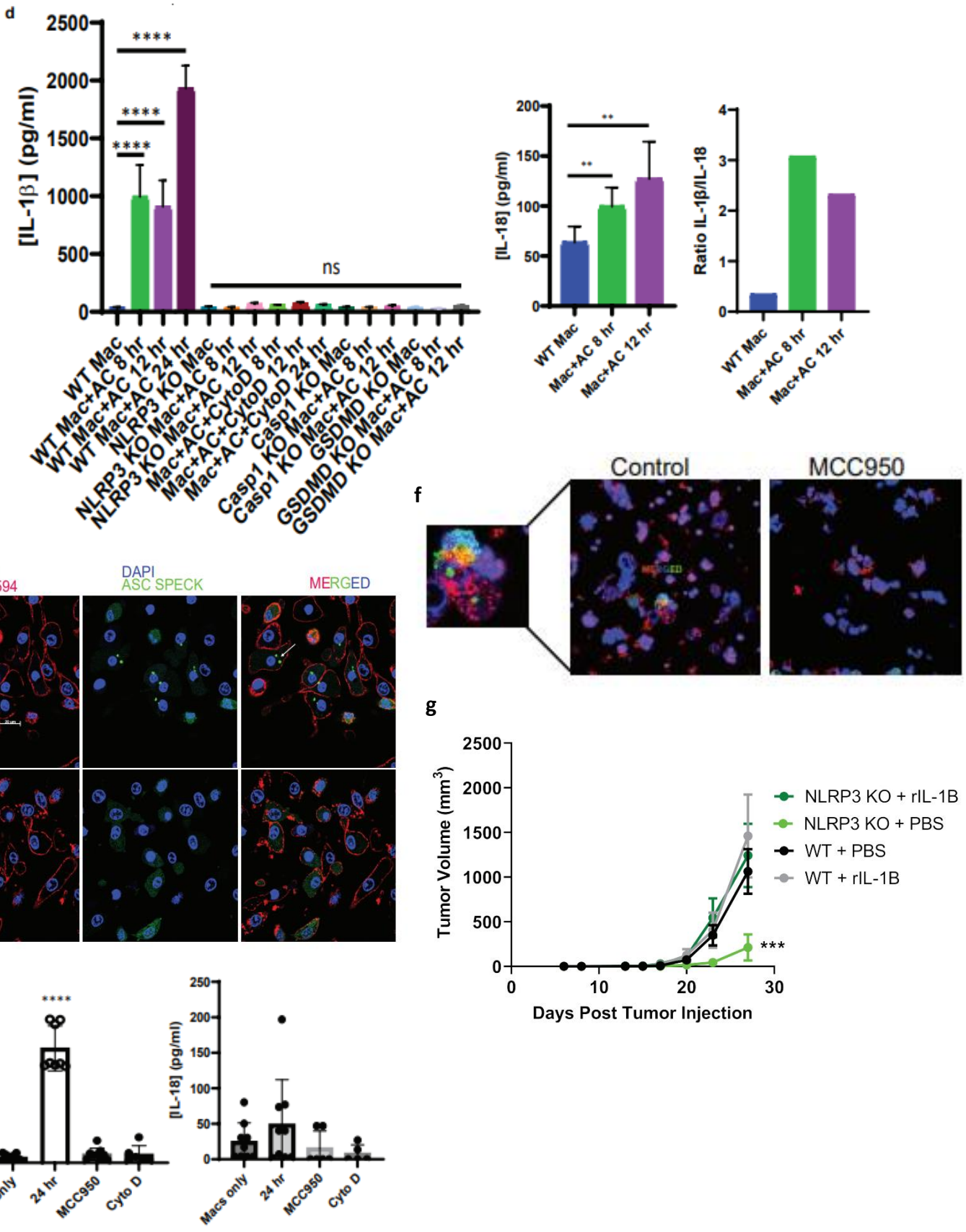
d
[IL-1β] (pg/ml)
2500
2000
1500
1000
500
0
****
****
****
ns
WT Mac
WT Mac+AC 8 hr
WT Mac+AC 12 hr
WT Mac+AC 24 hr
NLRP3 KO Mac
NLRP3 KO Mac+AC 8 hr
NLRP3 KO Mac+AC 12 hr
Mac+AC+CytoD 8 hr
Mac+AC+CytoD 12 hr
Mac+AC+CytoD 24 hr
Casp1 KO Mac
Casp1 KO Mac+AC 8 hr
Casp1 KO Mac+AC 12 hr
GSDMD KO Mac
GSDMD KO Mac+AC 8 hr
GSDMD KO Mac+AC 12 hr
[IL-18] (pg/ml)
200
150
100
50
0
**
**
WT Mac
Mac+AC 8 hr
Mac+AC 12 hr
Ratio IL-1β/IL-18
4
3
2
1
0
WT Mac
Mac+AC 8 hr
Mac+AC 12 hr
e
DAPI
WGA594
DAPI
ASC SPECK
MERGED
+MOC2
+MOC2
+ CytoD
f
Control
MCC950
g
Tumor Volume (mm3)
2500
2000
1500
1000
500
0
0
10
20
30
Days Post Tumor Injection
***
NLRP3 KO + rIL-1B
NLRP3 KO + PBS
WT + PBS
WT + rIL-1B
h
[IL-1β] (pg/ml)
250
200
150
100
50
0
****
Macs only
24 hr
MCC950
Cyto D
[IL-18] (pg/ml)
250
200
150
100
50
0
Macs only
24 hr
MCC950
Cyto D

Figure 3.4. Efferocytosis induces inflammasome assembly and IL-1β production in macrophages in an NLRP3-dependent manner

a) Schema of efferocytosis induced inflammasome activity using ASC Citrine/LysMCre BMDM. b) Efferocytosis of MOC2 AC induces inflammasome "speck" formation in BMDM in a time dependent manner. BMDM from ASC Citrine/LysMCre mice were incubated with AC for 1hr. Non-engulfed AC were then washed off and "speck" formation was assessed using confocal microscopy at mentioned time points. BMDM were treated with LPS (1μg/ml) +Nigericin (5μg/ml) for 1 hour (top) as a positive control. Treatment with the NLRP3 small molecule inhibitor MCC950 (1μM) for 1 hour prior to incubation with AC abolished the effect. The first panel shows macrophages (red). The second panel shows "specks" (green). The third panel shows merged images of macrophages with inflammasome "specks" formation. Scale bar, 20μm. c) Graphical representation showing quantification of "speck" positive cells under conditions shown in (b). d) Graphical representation of ELISA assay showing secretion of IL-1β and IL-18 from BMDM post treatment with AC at time points=8, 12 and 24hr. Ratio of IL-1β and IL-18 post efferocytosis is also shown. e) BMDM treated with Cytochalasin D abrogated "speck" formation following efferocytosis. The top row represents BMDM incubated with AC. The bottom row shows BMDM treated with 10uM Cytochalasin D for 1 hour prior to AC uptake. Scale bar, 20μm. f) $F4/80^+$ TAM (red) isolated from MOC2 tumors from ASC Citrine/LysmCre mice 2 weeks post tumor inoculation (100,000 MOC2 cells injected subcutaneously) show inflammasome activation (green) *in vivo*. DAPI was used to stain nuclei. Mice were treated with 15mg/kg MCC950 for one week prior to isolation of TAMs for this assay. g) Recombinant IL-1β treatment rescues B16-mOVA tumor growth in NLRP3 KO mice. Mice were treated with 5 ng recombinant IL-1β 2x/week (n=5 mice/group). h) PBMC were differentiated to macrophages using M-CSF (100 ng/ml) for 7days and then subjected to efferocytosis with tumor AC. IL-1β but not IL-18 is secreted from human macrophages post efferocytosis. MCC950 (1μM) and Cytochalasin D (10μM) blocked IL-1β secretion in efferocytic macrophages. Data for "speck" formation and ELISAs shown from independent experiments with n=3-5 mice. Statistics represent one-way ANOVA with multiple comparisons of control unstimulated macrophages to each treatment condition (c,d, and h) and two-way ANOVA (g). Graphs shown as mean ± SEM. (*=p<0.05, **=p<0.01, ***=p<0.001, ****=p<0.0001, ns=not significant)

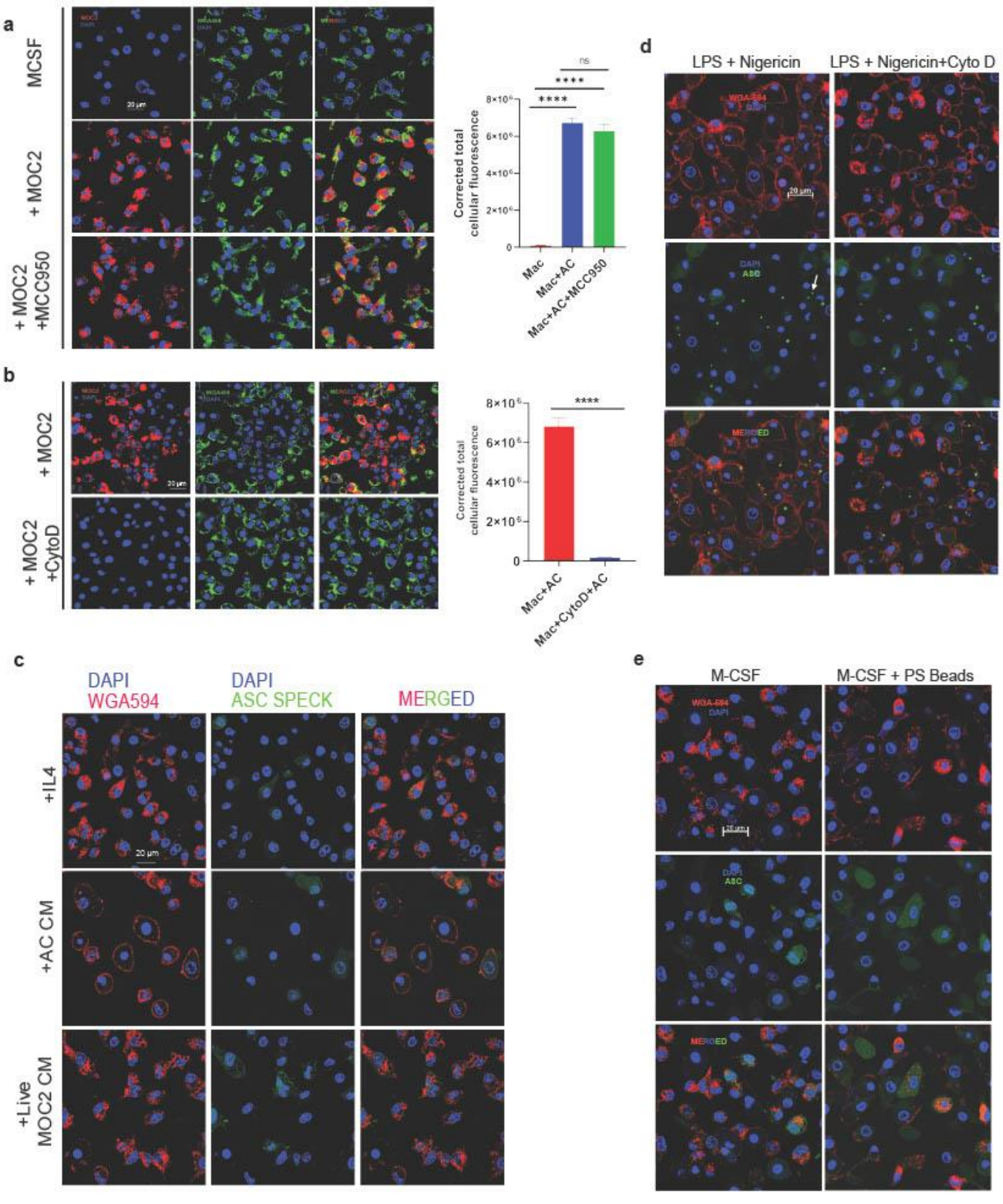
a
MCSF
+ MOC2
+ MOC2 +MCC950
Corrected total cellular fluorescence
ns
****
****
Mac
Mac+AC
Mac+AC+MCC950
b
+ MOC2
+ MOC2 +CytoD
****
Mac+AC
Mac+AC+CytoD
c
DAPI WGA594
DAPI ASC SPECK
MERGED
+IL4
+AC CM
+Live MOC2 CM
d
LPS + Nigericin
LPS + Nigericin+Cyto D
e
M-CSF
M-CSF + PS Beads

Figure 3.5. Effect of different conditions on uptake efficiency and inflammasome "speck" formation in BMDM

a) BMDM were cultured for 7days with M-CSF and then subjected to PKH26 stained MOC2 AC uptake (red) for 1 hour. Where mentioned, BMDM were treated with MCC950. Corrected total cellular fluorescence (red) was analyzed using Image J as a measure of uptake efficiency. Data shown from n=3 biological replicates. Scale bar 20μm. b) BMDM were treated with Cytochalasin D (10μM) for 1 hour to block the uptake of AC and then incubated with PKH26 labeled AC for 1 hour. Non-engulfed AC were washed away, and macrophages were stained with WGA488 (green) and DAPI (blue) used to visualize the nuclei. Corrected total cellular fluorescence (red) was analyzed using Image J as a measure of uptake efficiency. Data shown from n=3 biological replicates. Scale bar 20μm. c) BMDM grown for 7 days in the presence of M-CSF (100 ng/ml) were treated with either recombinant IL-4 (20 ng/ml) or conditioned media (1:1 ratio) from live or apoptotic MOC2 cells and stained with WGA594 (red) cell labeling dye. DAPI (blue) was used to visualize the nuclei. Inflammasome "speck" formation (green) under these conditions were evaluated using confocal microscopy. Data shown from independent assays with n=3 biological replicates. Scale bar 20μm. d) BMDM treated with LPS (1 μg/ml) and IFN-γ (20 ng/ml) were incubated with 10μM dose of Cytochalasin D for 1 hour (as used in efferocytosis assays). e) M-CSF (100 ng/ml) treated BMDM were incubated with Annexin V beads (1:1 ratio). Cells were then stained with WGA594 (red) and DAPI (blue) used for visualizing the nuclei. Inflammasome "speck" formation (green) was investigated using confocal microscopy. Top row shows BMDM (red). Middle row shows "speck" positive cells. Bottom row shows merged images of "speck" containing BMDM. Data shown from independent experiments with n=3 biological replicates. Scale bar 20μm. Statistics represent a two-way ANOVA and all error bars represent SEM. (*=$p<0.05$, **=$p<0.01$, ***=$p<0.001$, ****=$p<0.0001$, ns=not significant)

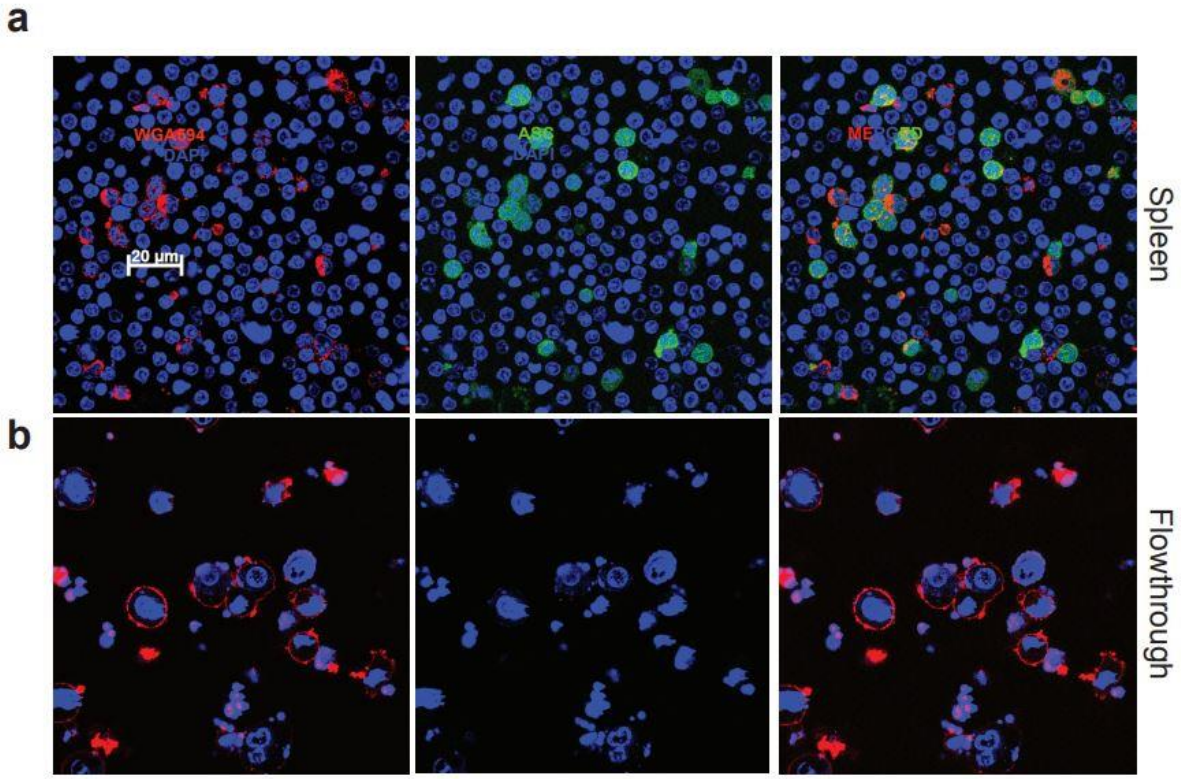

Figure 3.6. Splenocytes or F4/80$^-$ fraction from tumor do not exhibit "speck" positive myeloid cells

a) Splenocytes harvested from the spleen of MOC2 tumor bearing ASC-Citrine/LysM Cre mice 2 weeks post tumor inoculation (100,000 MOC2 cells injected subcutaneously) were stained with WGA594 (red) and DAPI (blue). b) F4/80$^-$ fraction from MOC2 tumor grown in ASC-Citrine/LysMCre mice was harvested 2 weeks post tumor inoculation (100,000 MOC2 cells injected subcutaneously). Cells were stained with WGA594 and DAPI and "speck" formation was interrogated using confocal microscopy. Representative data shown from n=5 mice/group. Scale bar 20µm.

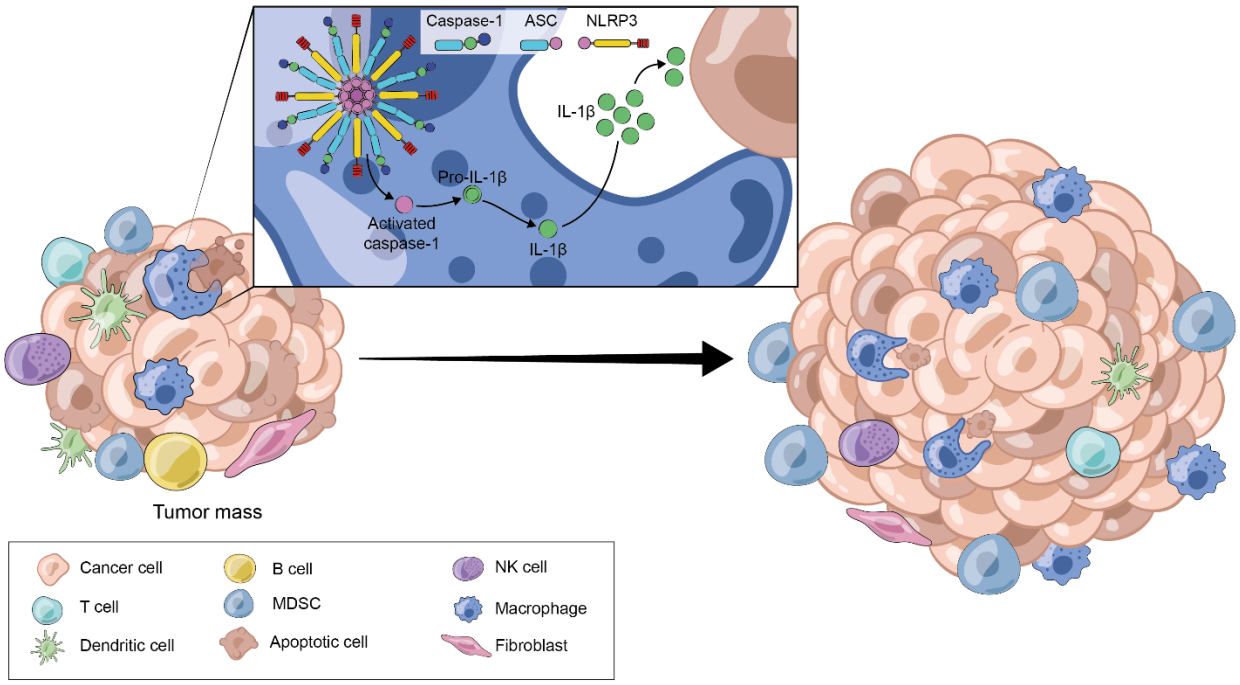

Figure 3.7. Efferocytosis of tumor AC activates NLRP3 dependent inflammasome signaling in the TME to induce non-pyroptotic IL-1β secretion and promote tumor growth.

3.4 Discussion

Our findings demonstrate for the first time that efferocytosis of apoptotic tumor cells activates myeloid-intrinsic NLRP3/caspase-1/IL-1β signaling in the tumor microenvironment to promote tumor growth. Others showed that apoptotic tumor cell clearance can be an immunologically quiescent process,[220-227] and we now offer a mechanistic link that efferocytosis can direct canonical inflammasome signaling to enrich for immunosuppressive tumor-infiltrating macrophages and MDSCs. Although earlier reports showed that cells undergoing apoptosis or autophagic death can activate NLRP3 dependent inflammasome signaling in macrophages,[131, 228] the relationship between efferocytosis of AC and inflammasome signaling was not known. While some GI and colon tumor models indicate that tumor-intrinsic inflammasome signaling may have anti-tumorigenic effects,[229, 230] we have complemented our *in vivo* studies with a single cell transcriptomic profile of human squamous carcinoma that corroborates a distinct pro-tumorigenic role for the myeloid-intrinsic NLRP3-dependent inflammasome. Our investigations clearly demonstrate the mechanistic role of efferocytosis driving NLRP3-dependent inflammasome activation in the TME that is pro-tumorigenic.

For the current study, we focused our attention on the interplay between efferocytosis and inflammasome pathways in macrophages. When we modeled this *ex vivo*, we found many efferocytosis associated genes were upregulated however some like, *Mertk, Axl,* and *Gas6* were downregulated post efferocytosis. One possible explanation could be at the time point chosen for performing the RNA sequencing, these genes were downregulated. Earlier reports have demonstrated a time point dependent variation in the gene expression pattern in efferocytic macrophages.[216]

Several phagocytosis targeting agents that are hypothesized to shift the

immunosuppressive TME towards an activated anti-tumor phenotype are being evaluated.[92, 127, 231] However, because efferocytosis involves many receptors, focusing on just one may be insufficient as illustrated by a compensatory increase in MerTK expression when Axl is targeted, highlighting the importance of simultaneously targeting multiple efferocytosis related genes or downstream effector pathways.[137, 232] Alternatively, our data suggests that instead of combining multiple efferocytosis blocking agents, targeting efferocytosis through inflammasome blockade may be more effective in reducing tumor burden.

Together, the findings from the first two data sections demonstrate that efferocytosis of tumor AC creates a tumor permissive microenvironment by activating NLRP3 dependent inflammasome signaling and IL-1β secretion. This work points to a targetable pathway for patients with myeloid cell-rich tumors that are refractory to T cell-based immunotherapy.

CHAPTER 4

Title of Chapter: T cell-intrinsic caspase-1 expression inhibits T cell activation and anti-tumor responses

4.1 Introduction

4.1.1 T cell intrinsic inflammasome expression

The inflammasome signaling complex is mostly studied in innate immune cells as a first line of defense against invading pathogens. However, recently inflammasome pathway gene expression and functional roles have been identified in T cells.

The most widely documented instance of inflammasome expression in T cells is during HIV-1 infection.[233-236] HIV is a virus with a tropism for T cells, thus T cells require an additional defense mechanism against infection. In addition, the massive T cell death associated with HIV infection has been attributed to pyroptosis induced by the activation of various inflammasome pathway sensors (NLRP3, IFI16, NLRP1, NLRC4, and AIM2) through the recognition of HIV-derived nucleic acids and subsequent caspase-1 activation and GSDMD cleavage.[237] Further, traditional ART treatment of HIV-1 infection results in the activation of the NLRP3 inflammasome which can contribute to T cell loss as well as drug hypersensitivity reactions.[238] However, upon treatment of HIV-1 patients with the caspase-1 inhibitor VX-765, there was notable suppression of $CD4^+$ T cell loss and subsequent chronic inflammation, suggesting a prominent role for T cell-intrinsic inflammasome activation during HIV-1 infection in addition to disease related complications.[234, 236]

Certain inflammasome components have also been shown to play a role in T helper cell differentiation. A recent study found that T cell intrinsic ASC expression is involved in the maintenance of pathogenic Th17 cells and upon activation of the inflammasome with LPS,

these Th17 cells released mature IL-1β. [239, 240] Further, NLRP3 was shown to be induced by IL-2 to promote Th2 differentiation by acting as a transcription factor for IL-4. [241]

While the role of T cell-intrinsic inflammasome signaling is becoming important in autoimmunity and infection, the role of the inflammasome in tumor-infiltrating T cells is still unknown. Therefore, we sought to investigate the phenotypic and functional implications of T cell-intrinsic inflammasome expression in a tumor model. Specifically, we studied T cell caspase-1 expression as a mechanism for T cell regulation in the TME.

4.2 Methods

4.2.1 Human Samples

Tumor and blood processing

Peripheral blood mononuclear cells (PBMC) were collected from blood using Ficoll-Paque Plus, following manufacturer's instruction. In brief, fresh blood samples were collected in heparinized blood collection tubes and mixed with equal parts PBS. 10 ml of the blood/PBS mixture was layered over 5 ml of Ficoll-Paque Plus in a conical tube and centrifuged at 400g for 30 minutes, 18˚C, and no brake. The PBMC layer was isolated and washed with PBS prior to lysis of red blood cells with ACK lysis buffer.

Fresh tumor samples were processed using Miltenyi Biotec human tumor dissociation kit and the Miltenyi GentleMACS Octo dissociator tough tumor dissociation program following manufacturer's instructions. The dissociated tumor was filtered with a 100 µM filter prior to red blood cell lysis with ACK lysis buffer. All tumor samples were used fresh the same day. $CD3^+$ T cells were isolated from human tumors via bead enrichment using the MojoSort human CD3 bead kit from BioLegend following manufacturer protocol. Cells were then

activated as outlined below for analysis by flow cytometry.

4.2.2 *in vitro* T cell assays

Generation of GVAX (whole cell vaccine)

B16-mOVA and B7H8-GM cell lines were irradiated with 100 Gy and mixed at a 10:1 ratio. The GVAX ratio was then resuspended such that the B16-mOVA cells were at a concentration of 10^7 cells/ml. 100 µl of the cell mixture was then injected subcutaneously in the flanks of mice for vaccination.

$CD4^+$ T cell skewing

One day prior to T cell skewing, 24 well flat bottom plates were coated with anti-mouse CD3 and CD28 antibodies at a concentration of 5 µg/ml and incubated at 4˚C overnight. Mouse $CD4^+$ were bead enriched as outlined above from healthy WT or inflammasome KO mice. Cells were plated at a concentration of 10^6/ml with the cytokine cocktail for the intended skewing (Tables 4.1-4.3). On day 5 post plating, cells were stimulated with 1x PMA and 0.5x monesin for 4 hours prior to flow cytometry analysis of cytokine production.

Table 4.1. Cytokine cocktail for $CD4^+$ skewing to Th1

Th1	Assay Concentration
Mouse IL-12	10 ng/ml
Anti-IL-4	10 µg/ml
Mouse IL-2	10 ng/ml
Anti-IFN-γ	1 µg/ml

Table 4.2. Cytokine cocktail for $CD4^+$ skewing to Th17

Th17	Assay Concentration
Mouse IL-6	50 ng/ml
Mouse IL-23	10 ng/ml
Mouse IL-1β	10 ng/ml
Human TGF-β	2 ng/ml
Anti-IFN-γ	10 µg/ml
Anti-IL-4	10 µg/ml

Table 4.3. Cytokine cocktail for $CD4^+$ skewing to T regulatory cells

Tregs	Assay Concentration
Human TGF-β	5 ng/ml
Mouse IL-2	10 ng/ml
Anti-IFN-γ	10 µg/ml
Anti-IL-4	10 µg/ml

T Cell Activation

$CD8^+$ T cells were isolated from the spleens of wildtype C57Bl/6 or knockout mice or from healthy human PBMCs by magnetic activated cell sorting. $CD8^+$ T cells were plated with equal numbers CD3/CD28 beads or 1 ng IL-7 at a concentration of 10^6 cells/ml. Human $CD8^+$ T cells were also plated with various inflammasome inhibitors and activators. After incubation at 37˚C for 5 days, cells were stimulated with 1x PMA and 0.5x monesin for 4 hours prior to flow cytometry analysis of perforin, granzyme, and IFN-γ production. T cells were also activated in the presence of 10 µg/ml Ac-YVAD-CHO (caspase-1 inhibitor).

T Cell Proliferation Assay

$CD3^+$ T cells were isolated from the spleens of wildtype C57Bl/6 or knockout mice by magnetic activated cell sorting and stained with 5 µM CFSE for 5 minutes in PBS + 5% FBS. Cells were washed twice with PBS + 10% FBS prior to plating. $CD3^+$ T cells were plated with equal numbers CD3/CD28 beads or 1 ng IL-7 at a concentration of 10^6 cells/ml. After

incubation at 37˚C for 3 days, the percentages of proliferating $CD3^+$ T cells were determined by CFSE dilution and PD-1 expression was assessed by flow cytometry analysis.

Phenotyping of tumor infiltrating T cells

Mice were sacrificed at day 16 post tumor injection and tumors were excised. Tumors were incubated with 1 mg/ml Collagenase II and 0.25 mg/ml DNase for 1 hour at 37˚C. Tumors were filtered with a 100 μM filter prior to red blood cell lysis with ACK lysis buffer. All tumor samples were used fresh the same day. Tumor samples were analyzed by flow cytometry for T cell memory markers, activation markers, $CD4^+$ subset markers, and checkpoint expression.

Caspase-1 activity assay

$CD3^+$, $CD4^+$, and $CD8^+$ T cells were isolated from WT or caspase-1 KO C57Bl/6 spleens or HNSCC patient tumors and PBMCs by magnetic activated cell sorting. Cells were plated at a concentration of 100,000 cells/well in 100 μl in a 96 well plate and stimulated with CD3/CD28 beads or 1 ng IL-7 overnight. In some conditions, cells were also treated with 10 μg/ml Ac-YVAD-CHO (caspase-1 inhibitor). Caspase 1 activity was determined using the Caspase 1 glo kit (Promega) according to manufacturer protocol.

4.2.3 *in vivo* T cell assays

In vivo T cell killing assay

Healthy WT or caspase-1 KO C57Bl/6 mice were vaccinated subcutaneously in the flank with GVAX. GVAX vaccine generated as described above. A cohort of non-vaccinated mice were used as a control. 7 days post vaccination, non-vaccinated WT mice were euthanized for splenocyte isolation. Splenocytes were resuspended in complete RPMI at a concentration of $5x10^6$ cells/ml and split in half. Half of the cells received 1 μl/ml of 1 mg/ml SIINFEKL

peptide and the other received equal volume PBS. Splenocytes were incubated at 37˚C for 1 hour. The cells receiving the SIINFEKL peptide were stained with 10 µM CFSE and the PBS treated cells were stained with 1 µM CFSE. After staining with CFSE, cells were mixed at equal ratios and resuspended to a concentration of 10^8 cells/ml in PBS. 100 µl of cells were adoptively transferred into the vaccinated mice and unvaccinated control mice as described above.

Mice receiving the adoptively transferred splenocytes were sacrificed 24 hours later and flow cytometry was performed of the spleens to access antigen-specific T cell killing. Percent specific killing was estimated by (1-target/control) x 100.

T cell tumor control

Antigen specific $CD3^+$ T cells were generated by vaccinating WT and caspase-1 KO mice with GVAX as described above. A total of 3 vaccinations were given each one week apart. Two days post final vaccination, B16-mOVA tumor cells were injected subcutaneously in the flanks of WT C57Bl/6 mice. One week post the final vaccination, vaccinated mice were sacrificed and $CD3^+$ cells were bead enriched from the spleens as outlined above. Isolated $CD3^+$ T cells were resuspended at a concentration of $2x10^7$ cells/ml and 100 µl were adoptively transferred into the B16-mOVA tumor bearing mice as outlined above. One cohort of tumor bearing mice received WT $CD3^+$ T cells, while the other received caspase-1 KO $CD3^+$ T cells. Further, half of each of these cohorts received 100 µg/mouse α-PD-1 2x/week which was started on the day of T cell adoptive transfer. Additionally, a control cohort received α-PD-1 only or PBS treatment only with no transfer of T cells. Tumor growth in these mice was monitored 3x/week for the remainder of the study until tumor endpoint.

in vivo checkpoint inhibitor treatment

To look at tumor growth in wildtype C57Bl/6 mice or caspase-1 KO mice, $1x10^5$ B16-mOVA cells were injected subcutaneously into the flanks of the mice. Tumors were measured 3x/week with calipers and tumor volumes were estimated using the formula V (cm3) = 3.14 × [largest diameter × (perpendicular diameter)2]/6. Mice were sacrificed when the tumors measured 2 cm in the largest diameter. Mice were treated 2x/week with depleting anti-PD-1 (100 μg/mouse) or PBS (100 μl/mouse) beginning once tumors became palpable (approximately day 7).

4.3 Results

4.3.1 T cell-intrinsic caspase-1 expression regulates T cell activation status

As described above, we have identified a myeloid-intrinsic pathway for inflammasome activation in the TME resulting in a pro-tumorigenic phenotype. While many recent studies identified T cell-intrinsic inflammasome gene expression within the context of various autoimmune and infectious disease models, the presence and role of the T cell-intrinsic inflammasome has yet to be investigated in cancer. [233, 242-244] We hypothesized that T cell-intrinsic inflammasome expression can alter T cell function in the TME.

We first wanted to determine if there was detectable caspase-1 activity in murine T cells. Here we found that *in vitro* $CD3^+$ T cells activated with CD3/CD28 beads have high caspase activity. This is primarily due to caspase-1 activity within the $CD8^+$ T cell population as $CD4^+$ T cells did not have a significant increase in caspase activity from those treated with the caspase-1 inhibitor, Ac-YVAD-cho (Figure 4.1a). We next sought to investigate if this finding translated to tumor infiltrating T cells. To determine this, we isolated $CD3^+$ T cells from both tumors and spleens of tumor bearing wildtype and caspase-1 KO mice. These cells were immediately used

for the caspase-1 activity assay to best capture what is happening *in vivo*. Here we found that $CD3^+$ T cells isolated from the TME had significant caspase-1 activity which was completely diminished in the splenic T cells (Figure 4.1b). Like what was observed within the tumor and spleen myeloid cell populations (Figure 2.9d), we concluded that T cell-intrinsic inflammasome activation is specific to stimuli within the TME.

Many groups have begun investigating the role of T cell intrinsic inflammasome expression on $CD4^+$ T cell differentiation. For example, NLRP3 expression in T cells was shown to promote skewing to a Th1 subtype.[244] Whereas other studies found that T cell-intrinsic AIM2 expression promotes T regulatory (Treg) cell skewing and survival to control autoimmune diseases.[244] Therefore, we sought to explore the role of T cell caspase-1 expression in the context of T cell skewing in cancer. Here we assessed the *in vitro* skewing potential of wildtype and caspase-1 KO $CD4^+$ T cells into Th1, Th17, Treg cell subsets. We observed that caspase-1 expression promotes $CD4^+$ differentiation into both Th17 and T regulatory cell subsets upon stimulation. We found no differences in Th1 skewing (Figure 4.1c). Both Th17 and Treg cell subsets have been shown to help generate a tumor-promoting TME,[245-247] indicating that T cell-intrinsic caspase-1 expression promotes an immunosuppressive TME to prevent an anti-tumor T cell response through increased Th17 and Treg skewing.

In addition to promotion of the pro-tumor $CD4^+$ subsets, we investigated whether caspase-1 expression played a similar role in inhibition of $CD8^+$ T cells to dampen an anti-tumor T cell response. We first sought to determine the role of T cell-intrinsic caspase-1 expression on cytotoxic T cell activation. Here we found that caspase-1 null $CD8^+$ T cells are functionally more activated *in vitro* and more highly produce perforin, granzyme, and IFN-γ (Figure 4.1d). These T cells also displayed a higher proliferative capacity *in vitro* (Figure 4.1e). Together this indicates

that T cell-intrinsic caspase-1 expression plays a key role in suppression of T cell activation. Similar to a previous study assessing T cell-intrinsic AIM2, this could likely be a mechanism for prevention of out of control T cell responses and autoimmunity.[242]

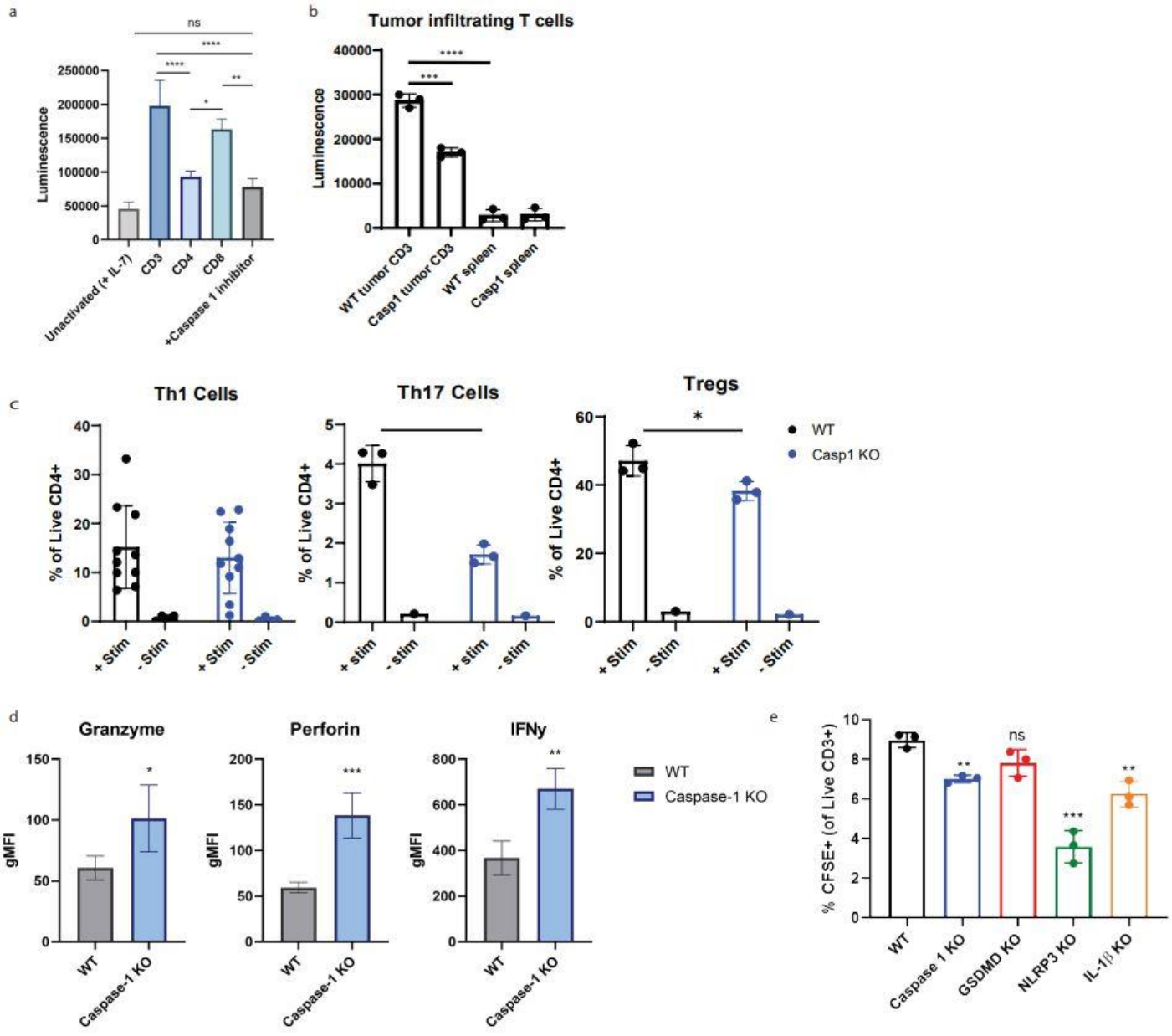
a
ns
****
****
**
*
Luminescence
250000
200000
150000
100000
50000
0
Unactivated (+ IL-7)
CD3
CD4
CD8
+Caspase 1 inhibitor
b
Tumor infiltrating T cells
****
***
Luminescence
40000
30000
20000
10000
0
WT tumor CD3
Casp1 tumor CD3
WT spleen
Casp1 spleen
c
Th1 Cells
Th17 Cells
Tregs
% of Live CD4+
40
30
20
10
0
5
4
3
2
1
60
40
20
*
+ Stim
- Stim
WT
Casp1 KO
d
Granzyme
Perforin
IFNy
gMFI
150
100
50
0
200
150
100
800
600
400
200
*
***
**
WT
Caspase-1 KO
e
% CFSE+ (of Live CD3+)
10
8
6
4
2
0
**
ns
***
**
WT
Caspase 1 KO
GSDMD KO
NLRP3 KO
IL-1β KO

Figure 4.1. T cell-intrinsic caspase-1 expression influences T cell activation and skewing

a) Wildtype murine $CD8^+$ T cells activated *in vitro* have highest caspase-1 activity upon CD3/CD28 bead stimulation. T cells were bead enriched from healthy wildtype mouse spleens and incubated for 5 days with CD3/CD28 activation beads (1:1 ratio of T cells and beads). After activation, T cells were used directly for caspase-1 activation assay. Caspase-1 inhibitor, Ac-YVAD-cho (10 μM) was used as a negative control. N=3. b) Tumor infiltrating $CD3^+$ T cells isolated from wildtype tumor-bearing mice have highest caspase-1 activity. $CD3^+$ T cells isolated from the spleens of tumor bearing mice show little caspase-1 activity. N=3. $CD3^+$ T cells were bead enriched from B16-mOVA tumors and matched spleens 2 weeks post tumor inoculation (100,000 B16-mOVA cells injected subcutaneously). T cells from tumors grown in caspase-1 KO mice were used as a negative control. After bead enrichment, $CD3^+$ T cells were used immediately for caspase-1 activity assay to best replicate what is happening *in vivo*. c) $CD4^+$ T cells bead enriched from healthy WT and caspase-1 KO mice differentially skew toward Th17 and Treg subsets when activated *in vitro* with cell skewing cocktail for 5 days (see methods tables 4.1-4.3). N=10 for Th1 skew and N=3 for Th17 and Treg skews. d) *in vitro* activation of WT and caspase-1 KO $CD8^+$ T cells. $CD8^+$ T cells were bead enriched from the spleens of healthy WT and caspase-1 KO mice and activated *in vitro* with CD3/CD28 beads at a 1:1 ratio. Flow cytometric analysis was used to measure expression of activation markers after a period of 5 days. N=3. e) *in vitro* proliferation of wildtype, caspase-1, GSDMD, NLRP3, and IL-1β KO $CD3^+$ T cells bead isolated from the spleens of C57Bl/6 mice. T cells were stained with 5 μM CFSE prior to incubation for 5 days. Proliferation was analyzed as a reduction in $CFSE^+$ T cells via flow cytometry. N=3. Statistics represent a one-way ANOVA with multiple comparisons and error bars represent SD. (*=$p<0.05$, **=$p<0.01$, ***=$p<0.001$, ****=$p<0.0001$, ns= not significant)

4.3.2 Caspase-1 negatively regulates T cell cytotoxicity and anti-tumor responses

We next sought to identify the functional role of T-cell intrinsic caspase-1 expression *in vivo*. The cytotoxic $CD8^+$ T cell population within the TME is crucial to facilitating an anti-tumor immune response. Further, tumors lacking T cell infiltration are considered "cold" tumors and thus have worse prognosis and poor response to checkpoint blockade therapy. Here we investigated if T cell intrinsic caspase-1 expression alters T cell-driven anti-tumor responses.

We first assessed functional differences between WT and caspase-1 KO T cells *in vivo*. To do so, we utilized a T cell killing assay in which the specific killing of target cells by $CD8^+$ cells can be monitored. The caspase-1 KO $CD8^+$ displayed an overall greater capacity to kill specific target cells with a specific lysis 5 times greater than that observed in the wildtype control (Figure 4.2a). This indicates that the antigen specific $CD8^+$ T cell response is more robust in caspase-1 KO mice, which could be attributed to increased clonal expansion and proliferation by caspase-1 KO T cells.

Since the inflammasome pathway is a well-known global pro-inflammatory signal, the impact on T cell trafficking to the tumor was also investigated. While, we have previously shown that general T cell trafficking to the tumor is unaltered in tumor bearing caspase-1 KO mice, we wanted to directly compare trafficking of WT and caspase-1 KO T cells within the same mouse (Figure 2.6d). Here we utilized a bone marrow chimera model in which wildtype mice were lethally irradiated and then received a bone marrow transplant containing an equal mixture of bone marrow from both wildtype and caspase-1 null mice (Figure 4.2b). In this model, caspase-1 KO $CD3^+$ cells were present in a much higher abundance in the tumor than the WT T cells (Figure 4.2c). However, we are unable to conclude whether this is due directly

to increased T cell trafficking, increased T cell survival within the TME, or increased clonal expansion and proliferation within the TME.

While we have demonstrated that caspase-1 KO T cells are phenotypically and functionally more activated *in vitro*, we wanted to investigate if this was also true in the TME and if it could translate to better anti-tumor responses by caspase-1 KO T cells. To do so, we first generated tumor specific T cells by vaccinating both WT and caspase-1 KO mice with GVAX a total of three times prior to harvesting the T cells. This method allowed us to generate both OVA-specific T cells and T cells specific for the B16 tumor model since GVAX is a whole-cell vaccine system. $CD3^+$ T cells were then harvested from the vaccinated mice and transferred to WT B16 tumor-bearing mice (Figure 4.2d). Mice receiving caspase-1 KO T cells but not WT T cells had significantly reduced tumor burden (Figure 4.2e). This shows caspase-1 KO T cells are better able to control tumor growth likely due to increased activation and killing capacity.

T cell-targeted immunotherapies are highly effective and long lasting in patients who respond to treatment. However, for a subset of patients, checkpoint blockade therapy is not effective due to a variety of innate and acquired resistance mechanisms.[248] One reason for checkpoint blockade failure is poor T cell activation and expansion. Therefore, we wanted to determine if combining inflammasome blockade and checkpoint blockade could overcome this obstacle. We first assessed checkpoint expression on tumor infiltrating T cells from WT and inflammasome KO mice. PD-1, Tim3, and Lag3 expression was significantly higher in T cells isolated from caspase-1 KO mice (Figure 4.2f). This data is normalized to checkpoint expression levels on T cells isolated from healthy spleens to account for alterations in baseline expression as healthy caspase-1 KO T cells tend to have lower checkpoint

expression than healthy WT T cells. After confirming that PD-1 expression was higher on caspase-1 KO T cells, we wanted to see if combination caspase-1 KO and PD-1 blockade would have an additive anti-tumor response. When B16 tumor bearing caspase-1 KO mice are treated with α-PD-1, tumor growth is diminished completely and with mice having no tumor growth or stable tumor burden throughout the duration of the experiment (Figure 4.2g). Taken together these data show that T cell-intrinsic caspase-1 expression acts as a checkpoint mechanism to dampen T cell activation and cytotoxic function. This can be targeted, along with PD-1, to increase T cell anti-tumor responses resulting in a reduction in tumor growth (Figure 4.3).

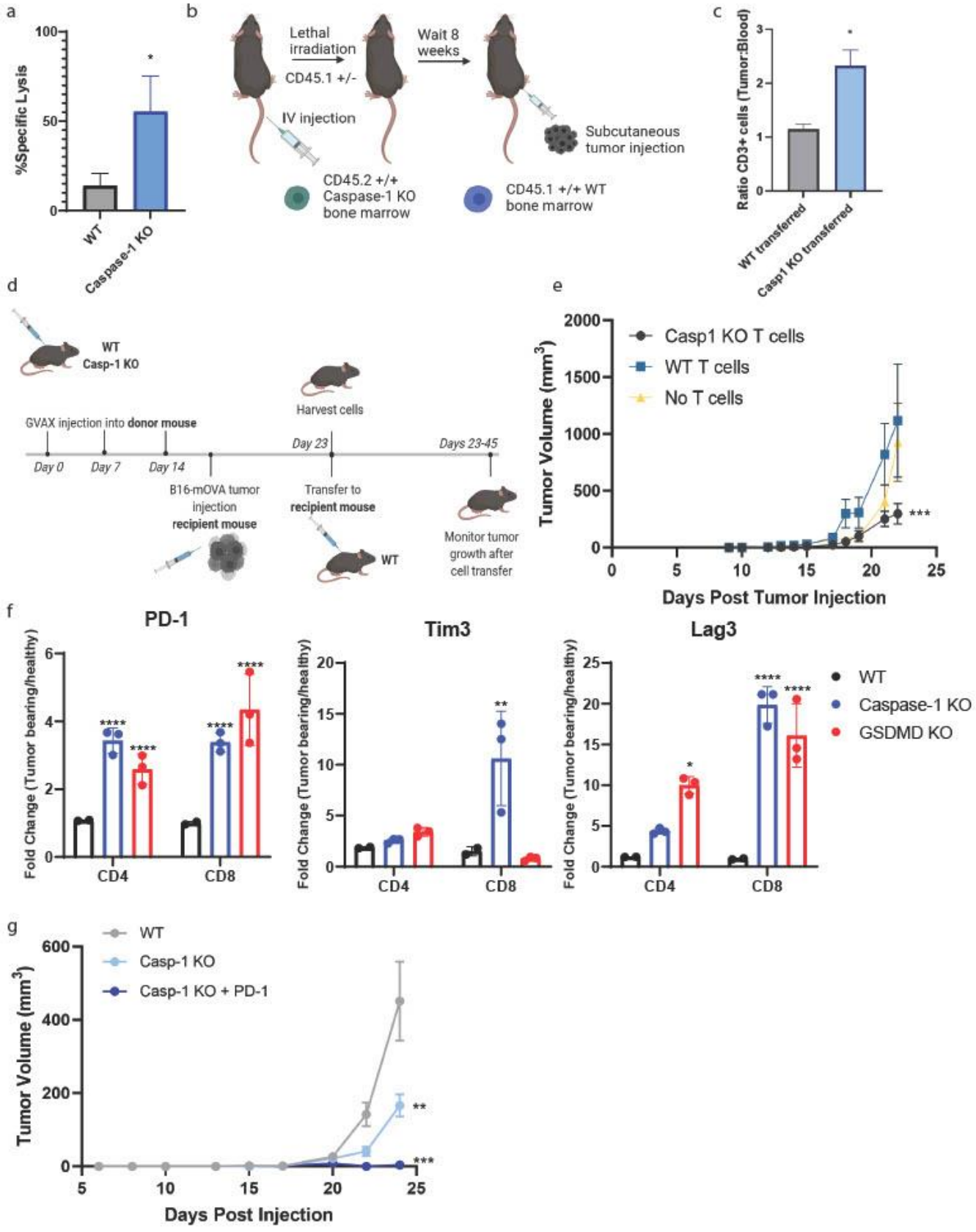
a
%Specific Lysis
100
50
0
*
WT
Caspase-1 KO
b
Lethal irradiation
CD45.1 +/-
IV injection
Wait 8 weeks
Subcutaneous tumor injection
CD45.2 +/+ Caspase-1 KO bone marrow
CD45.1 +/+ WT bone marrow
c
Ratio CD3+ cells (Tumor:Blood)
3
2
1
0
*
WT transferred
Casp1 KO transferred
d
WT
Casp-1 KO
GVAX injection into donor mouse
Day 0
Day 7
Day 14
B16-mOVA tumor injection recipient mouse
Harvest cells
Day 23
Transfer to recipient mouse
WT
Days 23-45
Monitor tumor growth after cell transfer
e
Tumor Volume (mm3)
2000
1500
1000
500
0
Casp1 KO T cells
WT T cells
No T cells
***
0
5
10
15
20
25
Days Post Tumor Injection
f
PD-1
Tim3
Lag3
Fold Change (Tumor bearing/healthy)
CD4
CD8
****
**
*
WT
Caspase-1 KO
GSDMD KO
g
Tumor Volume (mm3)
600
400
200
0
WT
Casp-1 KO
Casp-1 KO + PD-1
**
***
5
10
15
20
25
Days Post Injection

Figure 4.2. Inhibition of caspase-1 in T cells promotes cytotoxicity and tumor control

a) Cytotoxicity of murine $CD8^+$ T cells was assessed *in vivo*. WT and caspase-1 KO mice were vaccinated with the whole cell GVAX (see methods for GVAX description) 7 days prior to experiment. Vaccinated WT and caspase-1 KO mice were inoculated with 10^7 WT splenocytes target cells pulsed with1 µl/ml SINFEKL peptide + 10^7 unpulsed WT splenocyte target cells. The SINFEKL target cells were stained with 10 µM CFSE and the unpulsed cells were stained with 1 µM CFSE prior to transfer. 24 hours later, specific cell killing was assessed by ratios of CFSE low and high populations (1 µM vs 10 µM) via flow cytometry. (n=3 mice/group) b) Schematic showing experimental workflow for c. In brief, lethally irradiated $CD45.1^{+/-}$ mice were given a 50:50 $CD45.2^{+/+}$, caspase-1 KO: $CD45.1^{+/+}$, WT bone marrow transfer (total of 5-10x10^7 cells). After 8 week bone marrow engraftment period, B16-mOVA tumors were injected (100,000 cells/mouse subcutaneously). 3 weeks post tumor injection, tumors and matched PBMC were harvested for analysis by flow cytometry. c) WT and caspase-1 KO $CD3^+$ T cell abundance in the TME of the previously described bone marrow chimera mice. Data shown as a ratio to abundance in peripheral blood to adjust for any differences in bone marrow engraftment. (n=3 mice/group) d) Schematic showing experimental workflow for e. In brief, WT and caspase-1 mice were vaccinated 3 times (each one week apart) with GVAX (see methods for GVAX details). After the third GVAX vaccination, separate recipient WT mice were injected with 100,000 B16-mOVA cells/mouse subcutaneously. 7 days post third vaccination, 2x10^6 $CD3^+$ T cells were isolated and transferred to the tumor bearing WT mice. B16-mOVA tumor growth was measured 3x/week for the remainder of the study. (n=5 mice/group) e) Caspase-1 KO $CD3^+$ T cells control established tumor growth in the previously described experiment from d. f) Caspase-1 KO tumor infiltrating T cells express higher levels of PD-1 and Lag3. Data normalized to PD-1, Tim3, and Lag3 expression under basal conditions. B16-mOVA tumors were injected (100,000 cells/mouse subcutaneous) in WT, caspase-1 KO, and GSDMD KO mice. Tumors and matched spleens were harvested 2 weeks later for analysis by flow cytometry. N=3. g) Combination caspase-1 and PD-1 blockade synergizes to further reduce B16 tumor growth. WT and caspase-1 KO mice were injected with 100,000 B16-mOVA tumor cells subcutaneously. Tumor growth was monitored 3x/week for the duration of the study. Caspase-1 KO mice were treated 2x/week with 100 µg anti-PD-1. N=10 mice/group. Statistics represent a one-way ANOVA (a and c), two-way ANOVA (e and g), and a one-way ANOVA with multiple comparisons of the WT group to both the caspase-1 KO and GSDMD KO groups (f). Error bars represent SEM. (*=$p<0.05$, **=$p<0.01$, ***=$p<0.001$, ****=$p<0.0001$, ns=not significant)

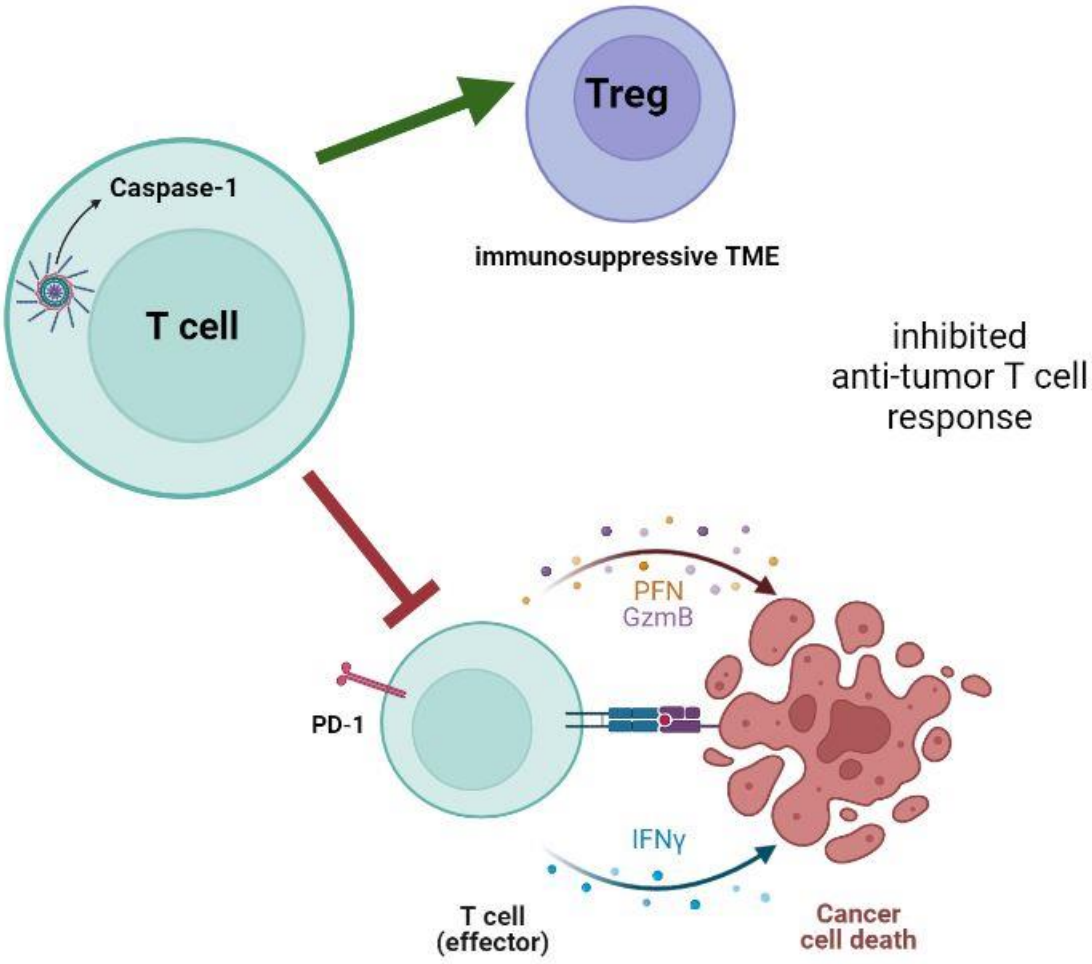

Figure 4.3. T cell-intrinsic caspase-1 expression dampens CD8$^+$ effector function and promotes CD4$^+$ skewing toward Tregs to inhibit an anti-tumor response and promote tumor growth.

Here we provide preliminary data that show T cell-intrinsic caspase-1 expression can act as a checkpoint pathway for T cell activation and function in the TME. We show *in vitro* that caspase-1 KO T cells have increased perforin, granzyme, and IFN-γ production as well as increased surface expression of PD-1. We further show that *in vitro* caspase-1 KO T cells have increased killing capacity of specific targets, increased trafficking to the TME, and greater ability to inhibit tumor growth.

4.4 Discussion

Here we have presented novel data showing an important role for T cell intrinsic caspase-1 expression and signaling in the TME. Data on the presence of inflammasome gene expression in T cells is newly emerging with some studies addressing role of this pathway in the context of infection (HIV) and autoimmunity.[233, 239, 242] However, to date there have been no studies addressing the T cell-intrinsic role of the inflammasome in cancer.

As T cell directed immunotherapies for cancer evolve, it is important to also consider potential resistance mechanisms as well. One of the major barriers to an effective immunotherapy response is an insufficient generation of anti-tumor T cells and an inadequate effector response from these cells.[249, 250] There are many mechanisms, both tumor-intrinsic and extrinsic, by which T cell function within the TME can be disrupted. Here we have identified a T cell intrinsic mechanism controlling T cell activation level and anti-tumor response. While this study is lacking in primary human data, it would be beneficial to explore the interplay of caspase-1 blockade and checkpoint blockade in human tumors. This pathway has the potential to increase efficacy of checkpoint blockade treatment for a larger population of patients.

This study also has a potential interesting role in CAR-T cell therapy for cancer patients. In CAR-T cell therapy, autologous T cells from the patient are transformed with the CAR receptor specific to a tumor antigen and expanded *ex vivo* prior to infusion into the patient.[251] However, CAR-T cells still experience exhaustion *in vivo* which impairs their overall persistence and killing capacity.[251] Therefore, it is important to identify mechanisms for enhancing CAR-T duration of activation while avoiding exhaustion to create more robust and long-lasting anti-tumor responses. Based on our findings, we suggest removing caspase-1

expression from the CAR-T cells using CRISPR to enhance activity and killing capacity of these cells.[252]

A recent study on the role of the inflammasome in T cells showed that AIM2 expression in Tregs acts as a control mechanism to suppress autoimmunity. Activation of AIM2 in Tregs alters their metabolic function resulting in enhanced Treg stability and effector function. As a result, these Tregs are more capable of dampening effector T cell response to prevent autoimmunity. [242] We propose that a similar mechanism could be regulating CTL function. It is possible that CTL-intrinsic caspase-1 expression can regulate the metabolic program of these T cells to alter their cytotoxic function.

We have identified a novel T-cell intrinsic signaling mechanism for control CTL activation and function. Here we show that upregulated T cell-intrinsic inflammasome signaling promotes CTL activation, proliferation, and anti-tumor function. While there are some new studies outlining functions of T cell-intrinsic inflammasome expression in autoimmune diseases and HIV infection, there are no published works on the T cell-intrinsic inflammasome in the context of cancer.

CHAPTER 5

Title of Chapter: Discussion and Future Directions

5.1 Implications

Increasing evidence supports that an inflammatory microenvironment drives tumor growth and metastases and alters the host immune landscape in favor of the tumor. One such inflammatory pathway is the NLRP3 inflammasome signaling cascade. However, the complex relationship between the inflammasome pathway and cancer progression has been highly contradictory and time, tissue, and context dependent.[253, 254] For example, one study in metastatic colorectal cancer demonstrated a protective role of inflammasome pathway via NK cell activity.[229] Conversely, NLRP3 dependent inflammasome signaling was triggered in macrophages by colorectal cancer cells and facilitated cancer cell migration and their metastatic potential *in vivo*.[255] Several other reports also identified a tumor aiding role of the inflammasome. For example, NLRP3 KO mice had fewer metastatic melanoma nodules in the lungs. Further, NLRP3 has also been shown to impair vaccine efficacy by enhancing the MDSCs in the TME.[256]

These data have several scientific and translational implications. First, our single-cell transcriptomic profile illustrates the heterogeneity and plasticity of the tumor infiltrating myeloid cells. Within the 5 macrophage subsets we identified, *NLRP3* and *IL1B* gene expression were predominant in 2 subsets, *NLPR3*$^{+}$ and *INHBA*$^{+}$, and our RNA velocity analysis suggests that these subsets may be derived from efferocytic myeloid cells. We also identified a *CD14*$^{+}$ monocyte population, which was highly enriched for MDSC-associated genes, but this population as well as the other two monocyte populations did not show an upregulation in inflammasome gene expression indicating that macrophages contribute most

significantly to this mechanism. Consistent with the current knowledge that questions the dichotomic M1/M2 nomenclature of macrophages, [257] we could not confirm or identify distinctly these polarized macrophage clusters in the human tumor milieu. Interestingly, we also detected high levels of *IL-1R1* expression in human HNSCC tumor infiltrating myeloid cells as well as murine macrophages post efferocytosis *in vitro*. IL-1β has been shown to act via its receptor and prime the inflammasome signaling pathway (signal 1). This suggests a paracrine signaling pathway where efferocytosis in one macrophage can potentially stimulate the inflammasome signaling in nearby myeloid cells, which remains to be investigated.

Efferocytosis is an important factor that needs to be considered during any cancer therapy. Cytotoxic therapies like radiation and chemotherapy greatly contribute to the clinical response and prognosis in many patients. However, systemic anticancer radiation or chemotherapy is often immunosuppressive and induces non-immunogenic modes of cell death, like apoptosis in the tumor cells. Therefore, therapy induced dying tumor cells can alter the dynamics of the TME and thus boost tumor repopulation, recruit more myeloid cells to trigger efferocytosis, [258, 259] and thereby orchestrate the anti-tumor immune response cascades to act as an "onco-regenerative niche."[223, 260] This was observed in a colorectal cancer study where following radiation, Mertk, Protein S and Gas6 expression increased in TAMs. In this study, Mertk KO mice had better survival after radiation therapy.[260] However, it is undeniable that different cytotoxic therapies may induce other forms of cell death. Therefore, in the TME, different forms of cell death may co-exist in different proportions giving rise to complex signaling cascades.[261, 262] Unfortunately, studies comparing the contribution of different forms of cell death co-existing in the TME remain scarce. Although earlier reports showed that cells undergoing apoptosis or autophagic death can activate

NLRP3 dependent inflammasome signaling,[131, 228] the relationship between efferocytosis of apoptotic tumor cells and the inflammasome pathway was not known.

Our report also underscores a targetable mechanism of non-immunogenic tumor cell death distinct from the immunogenic cell death induction paradigm that has shaped current clinical trials.[118, 263-269] While we did not see a role for the DNA sensing molecule AIM2 in our studies, others have noted a myeloid-intrinsic STING-dependent mechanism to render the tumor more responsive to immune checkpoint inhibitors. [270-274] Of note, while others have shown a mechanistic link between the inflammasome and STING signaling, there have been no studies linking efferocytosis with the STING pathway.[275-277] A translational implication from these studies is that both efferocytosis-dependent blockade of inflammasome signaling and myeloid-directed targeting of STING may be required for treatment of tumors that fail T cell-directed immune checkpoint inhibitor immunotherapies.

Several phagocytosis targeting agents that are hypothesized to shift the immunosuppressive TME towards an activated anti-tumor phenotype are being evaluated.[127, 259, 278] One example is the combination of bavituximab and pembrolizumab, which is currently in a phase 2 trial for pretreated advanced gastric or gastroesophageal junction cancer (NCT0409641). However, because efferocytosis involves many receptors, focusing on just one may be insufficient as illustrated by a compensatory increase in MerTK expression when Axl is targeted,[137] highlighting the importance of simultaneously targeting multiple efferocytosis related genes or downstream effector pathways.[279] Alternatively, our study suggests that instead of combining multiple efferocytosis blocking agents, targeting efferocytosis through inflammasome blockade may be more effective in reducing tumor burden. Furthermore, triple therapy targeting MerTK and PD-1 after radiotherapy-induced

abscopal anti-tumor immune responses indicates a possible use for targeting efferocytosis and the inflammasome post-radiotherapy. [206]

Our previous reports demonstrated a role for caspase-1 in monocytic MDSCs as a tumor growth mediator in a T cell-independent manner to warrant IL-1β blockade in cancer therapeutics.[75] Interestingly, the CANTOS trial showed that those treated with canakinumab (IL-1β blocking agent) had reduced lung cancer incidence and cancer-associated mortality.[84, 195] However, further trials investigating the efficacy of IL-1β blockade in cancer patients failed to meet the primary endpoints of overall survival and progression-free survival.[196, 197] These clinical studies suggest that IL-1β plays an important role in early carcinogenesis in humans. Thus, therapeutic targeting of inflammasome signaling may be more effective in patients with early-stage disease or as adjuvant therapy in patients with a high risk of recurrences.

Several preclinical studies have demonstrated that targeting efferocytosis receptors can reprogram TAMs towards an activated anti-tumor phenotype.[127] Multiple efferocytosis related molecules are currently being evaluated in clinical trials. Combinatorial targeting of efferocytosis related genes and IL-1β or NLRP3 to determine synergistic anti-tumor responses will be of interest. Although most solid tumor TMEs are infiltrated with immune suppressive lymphocytes and myeloid cells, some cancers are T cell poor. These non-inflamed “cold” tumors have been shown to be less responsive to checkpoint blockade therapies and thus may respond better to manipulation and reprogramming of the myeloid compartment. For instance, our earlier findings revealed a better response to checkpoint blockade when combined with myeloid depleting agents in HNSCC preclinical models.[280] Based on our findings, we speculate that the molecular cascade of efferocytosis induced IL-

1β secretion pathway is a valuable therapeutic tool in clinical setting to treat immune "cold" tumors.

In addition, our data for the first time identifies a T cell-intrinsic role for inflammasome signaling within the TME. While these data are still immature in nature, it has far reached implications for cancer immunotherapy treatments. The field of cancer immunotherapy is dominated by T cell driven therapeutics. While these treatments have long lasting effects for those who respond, both primary and acquired resistance mechanisms prevent a large portion of patients from having a sustained anti-tumor response. Overcoming these resistance mechanisms remains the first hurdle for improving therapeutic responses. Therefore, the identification of a targetable pathway regulating T cell activation is of great importance.

Reprogramming the tumor immune microenvironment is of great interest when it comes to efficacy of cancer immunotherapy. It is difficult to drive an anti-tumor CTL response when T cells are not present in the tumor or are having difficulty infiltrating due to a myeloid-dominated immunosuppressive TME. Therefore, development of combination strategies that both inhibit the pro-tumorigenic environment while also stimulating anti-tumor CTL responses are necessary. Currently, three major strategies for repolarizing the TME exist including targeting angiogenesis, myeloid cells, or Tregs. A recent phase III clinical trial investigating combination of angiogenesis inhibitors with checkpoint inhibitors in lung cancer showed success in reprogramming the TME and improved progression free survival and overall survival.[281] As TME reprogramming therapies become more prevalent, the field could move towards a more personalized approach where each patient's TME biomarkers are considered before selecting which combination of inhibitors are required to reprogram the TME.

Overall, our findings demonstrate a unique link between efferocytosis of tumor AC by tumor myeloid cells and activation of inflammasome signaling and subsequent IL-1β production. Further, we have identified a targetable pathway that can both inhibit T cell anti-tumor responses while also activating myeloid mediated responses and immunosuppression within the TME. Therefore, targeting inflammasome signaling has the potential to reprogram the TME from a tumor-promoting immunosuppressive environment to an anti-tumor CTL-driven environment.

5.2 Limitations

Our *in vitro* functional studies do not encompass a pure population due to the highly overlapping and complex nature of myeloid cells *in vivo* and the difficulty of purifying them in the absence of reliable unique markers. Our single-cell sequencing dataset identified a previously uncharacterized and highly complex myeloid landscape in HNSCC. However, it is difficult to predict or replicate *in vitro* the effects of inflammasome-rich macrophages on the other myeloid subsets that potentially exist *in vivo* due to the inability to sort out pure populations of each of these unique cell types. Additionally, since the inflammasome KO mouse models employed in this study are not lineage-specific deletions, the effect of gene knockouts occurring in different immune cell compartments must be considered and warrants additional exploration.

The NLRP3 dependent inflammasome pathway can be activated by a wide range of stimuli. The molecular mechanism of how cancer AC interacts with and activates NLRP3 in macrophages is currently unknown and requires further exploration to elucidate the full mechanism. Further, while we show that AIM2 has no *in vivo* tumorigenic role and that both

AIM2 and *NLRC4* have low expression in human tumor myeloid cells, we did not investigate the tumor promoting roles of other inflammasome sensors in this study. In line with this, little is known about the other inflammasome sensors in the context of cancer. A few studies have shown NLRP1 to have pro-tumor growth and anti-apoptotic roles in melanoma models.[282] Further, a tumor suppressive role of NLRC4 has been well documented in colon cancer models.[283]

Another limitation is the lack of specificity of caspase-1 reagents. It is well known that caspase-1 KO mice from Jackson Labs also harbor a caspase-4 mutation. Due to the proximity of the *Casp1* and *Casp4* genes, it is difficult to segregate them when creating KO mice.[284] Further, small molecule inhibitors for caspase-1 typically are not very specific and tend to have off target effects on other caspases.

The T cell inflammasome project is still limited and immature in nature. Here we show mostly *in vitro* findings validated with a few mouse experiments. There are no human data yet for this project, so it cannot yet be determined whether this is a relevant pathway in human tumor infiltrating T cells. This needs to be explored further in tumor infiltrating T cells from human tumors to determine if this pathway is upregulated. The molecular mechanism controlling the cross talk between T cell activation and inflammasome signaling pathways is still unknown. It is critical to explore this further to elucidate the mechanism by which inflammasome signaling regulates T cell effector function.

5.3 Future Directions

5.3.1 Elucidation of mechanism linking efferocytosis and NLRP3 inflammasome activation

One of the most important next steps for this project is to investigate the direct mechanism of efferocytosis-mediated inflammasome activation. Identification of the mechanism linking these two pathways could give us additional targetable molecules for cancer therapy. However, as mentioned previously, the NLRP3 inflammasome can be activated by many molecules and stimuli. This causes an issue when investigating the specific molecule stimulating NLRP3 activation in our model. Since the myeloid cells are efferocytosing apoptotic cancer cells to activate NLRP3, there are many stimuli present to activate this pathway. Further, it is possible that there is not only one mechanism by which NLRP3 is activated and that one method might be able to compensate if another one is blocked.

It is well known that lysosomal destabilization and rupture can activate the NLRP3 inflammasome.[203] Therefore, we hypothesize that destabilization of the phagolysosome post efferocytosis and subsequent leakage of AC cargo results in the activation of the NLRP3 inflammasome. To test this, we plan to investigate the role of cathepsins in efferocytosis-mediated inflammasome activation. Cathepsin B is important for degradation of phagolysosome cargo. Therefore, we plan on inhibiting cathepsin B with a small molecule inhibitor during efferocytosis to determine if it abolishes IL-1β production and speck formation post-efferocytosis.

If our hypothesis is incorrect, we can perform mass spectrometry-based proteomics to identify proteins released by apoptotic cells during efferocytosis.[285] We can then systematically investigate the functional role of the proteins identified on NLRP3 inflammasome activation.

5.3.2 Functional validation of RNA velocity findings

Another direction of interest is *in vitro* implications from our RNA velocity analysis. This analysis identified two macrophage populations enriched in efferocytosis genes (Macro_C1QC and Macro_SPP1) that can give rise to two inflammasome gene rich macrophage populations (Macro_INHBA and Macro_NLRP3). We plan to functionally validate this evolutionary trajectory *in vitro*. Our single cell RNAseq dataset identified a list of unique genes that define each of these macrophage populations. Therefore, we can use this as a gene signature to identify these populations in future RNAseq experiments.

To assess this, we plan to differentiate and expand human macrophages from PBMC from healthy human donors. We can then feed the macrophages apoptotic cancer cells to induce efferocytosis. We plan to perform RNAseq on macrophage samples from different time points in this experiment including prior to feeding with AC, post feeding with AC, and the 8-, 12-, and 24-hour time points during the rest period that were used for all previous experiments. With this experimental design, we should be able to see the transition from naïve macrophage to upregulation of efferocytosis genes post feeding with AC then to an upregulation of inflammasome genes during the rest period.

5.3.3 Cell specificity of efferocytosis-induced inflammasome activation

We are also interested in investigating the cell specificity of our model. All experiments presented here demonstrated the effect of efferocytosis of apoptotic tumor cells only. While we did see the same results with various tumor cell lines, we did not look outside of the tumor model. Within the TME, apoptosis of supportive stromal cells and immune cells also occurs in addition to apoptosis of the cancer cells. Therefore, we plan to investigate this by

feeding the macrophages apoptotic non-cancerous epithelial cells, apoptotic fibroblasts, or apoptotic T cells. With these experiments, the workflow from our previous experiments will remain the same with the only substitution being the type of apoptotic cell used. We plan to still use IL-1β production and speck formation as a readout for inflammasome activation post efferocytosis.

5.3.4 Inflammasome role in antigen specific T cell activation

Another interesting route of investigation with our T cell project is to determine the antigen specific nature of our findings. Our *in vivo* data showed that caspase-1 KO T cells initiate a better anti-tumor response. However, we did not explore the mechanism behind this. Our data suggest that caspase-1 KO T cells are more cytotoxic and proliferative which is likely what resulted in the better, more sustained anti-tumor response. However, it is also possible that more tumor specific T cells are being generated through GVAX vaccination in the caspase-1 KO mice than the WT mice. Therefore, with the caspase-1 KO mice we would be transferring in more effector T cells that are already primed to specifically target the tumor cells. Since we use a B16-mOVA line to generate GVAX, we can assess T cell specificity to OVA by staining for MHC-ova peptide (SINFEKL) complexes via flow cytometry. This will allow us to assess the abundance of T cells generated that are OVA specific as a surrogate marker for tumor-specific T cells. We can also repeat this experiment using a completely OVA specific model by generating OT-1/caspase-1 KO mice and using the OT-1 specific T cells for these experiments.

5.3.5 Inflammasome expression and functional profiling in human T cells

While our T cell findings are very exciting, they are still immature. Moving forward, it is important to also investigate this pathway in human T cells to confirm it is relevant in humans. While assessing *in vivo* alterations of T cell activation and function is not possible in humans, it is still important to confirm our phenotypic findings with human T cells. To do so, we first plan to confirm the presence of inflammasome signaling in human T cells using the caspase-1 activity assay. For this, we plan to isolate T cells from human PBMCs and activate them *in vitro* prior to use for this assay.

If we see caspase-1 activity in the human T cells, we can then move forward with phenotyping how the inflammasome affects activation. To do this, we would activate the human T cells *in vitro* in the presence of various inflammasome inhibitors and then assess perforin, granzyme, and IFN-γ production, checkpoint marker expression, and differences in proliferation.

5.4 Concluding Remarks

These findings are novel and for the first time show that efferocytosis of tumor AC creates a tumor permissive environment by activating the NLRP3 dependent inflammasome signaling and IL-1β secretion. Even though we demonstrate that the uptake of tumor AC can trigger the NLRP3 dependent inflammasome activity in myeloid cells and IL-1β secretion, the question of which factors derived from tumor AC prime and activate the inflammasome remains open for investigation. Further, our data suggest a novel T cell intrinsic pathway that regulates T cell activation and function. Together, our work identifies a targetable pathway that has the potential to both improve T cell responses and inhibit myeloid cell-mediated immunosuppression to improve tumor responses.

References

1. Hinshaw, D. C.; Shevde, L. A., The Tumor Microenvironment Innately Modulates Cancer Progression. *Cancer Res* **2019,** *79* (18), 4557-4566.
2. Anderson, N. M.; Simon, M. C., The tumor microenvironment. *Curr Biol* **2020,** *30* (16), R921-r925.
3. Hanahan, D.; Weinberg, Robert A., Hallmarks of Cancer: The Next Generation. *Cell* **2011,** *144* (5), 646-674.
4. Galon, J.; Costes, A.; Sanchez-Cabo, F.; Kirilovsky, A.; Mlecnik, B.; Lagorce-Pagès, C.; Tosolini, M.; Camus, M.; Berger, A.; Wind, P.; Zinzindohoué, F.; Bruneval, P.; Cugnenc, P. H.; Trajanoski, Z.; Fridman, W. H.; Pagès, F., Type, density, and location of immune cells within human colorectal tumors predict clinical outcome. *Science* **2006,** *313* (5795), 1960-4.
5. Galon, J.; Angell, H. K.; Bedognetti, D.; Marincola, F. M., The continuum of cancer immunosurveillance: prognostic, predictive, and mechanistic signatures. *Immunity* **2013,** *39* (1), 11-26.
6. Angell, H.; Galon, J., From the immune contexture to the Immunoscore: the role of prognostic and predictive immune markers in cancer. *Curr Opin Immunol* **2013,** *25* (2), 261-7.
7. Mlecnik, B.; Tosolini, M.; Kirilovsky, A.; Berger, A.; Bindea, G.; Meatchi, T.; Bruneval, P.; Trajanoski, Z.; Fridman, W. H.; Pagès, F.; Galon, J., Histopathologic-based prognostic factors of colorectal cancers are associated with the state of the local immune reaction. *J Clin Oncol* **2011,** *29* (6), 610-8.
8. Voskoboinik, I.; Whisstock, J. C.; Trapani, J. A., Perforin and granzymes: function, dysfunction and human pathology. *Nat Rev Immunol* **2015,** *15* (6), 388-400.
9. Wherry, E. J.; Kurachi, M., Molecular and cellular insights into T cell exhaustion. *Nat Rev Immunol* **2015,** *15* (8), 486-99.
10. Pardoll, D. M., The blockade of immune checkpoints in cancer immunotherapy. *Nat Rev Cancer* **2012,** *12* (4), 252-64.
11. Saravia, J.; Chapman, N. M.; Chi, H., Helper T cell differentiation. *Cell Mol Immunol* **2019,** *16* (7), 634-643.
12. Bailey, S. R.; Nelson, M. H.; Himes, R. A.; Li, Z.; Mehrotra, S.; Paulos, C. M., Th17 cells in cancer: the ultimate identity crisis. *Front Immunol* **2014,** *5*, 276.
13. Guéry, L.; Hugues, S., Th17 Cell Plasticity and Functions in Cancer Immunity. *Biomed Res Int* **2015,** *2015*, 314620.
14. Kim, I. S.; Gao, Y.; Welte, T.; Wang, H.; Liu, J.; Janghorban, M.; Sheng, K.; Niu, Y.; Goldstein, A.; Zhao, N.; Bado, I.; Lo, H.-C.; Toneff, M. J.; Nguyen, T.; Bu, W.; Jiang, W.; Arnold, J.; Gu, F.; He, J.; Jebakumar, D.; Walker, K.; Li, Y.; Mo, Q.; Westbrook, T. F.; Zong, C.; Rao, A.; Sreekumar, A.; Rosen, J. M.; Zhang, X. H. F., Immuno-subtyping of breast cancer reveals distinct myeloid cell profiles and immunotherapy resistance mechanisms. *Nature Cell Biology* **2019,** *21* (9), 1113-1126.
15. Wu, W.-C.; Sun, H.-W.; Chen, H.-T.; Liang, J.; Yu, X.-J.; Wu, C.; Wang, Z.; Zheng, L., Circulating hematopoietic stem and progenitor cells are myeloid-biased in cancer patients. *Proceedings of the National Academy of Sciences* **2014,** *111* (11), 4221-4226.
16. Ginhoux, F.; Schultze, J. L.; Murray, P. J.; Ochando, J.; Biswas, S. K., New insights into the multidimensional concept of macrophage ontogeny, activation and function. *Nature Immunology* **2016,** *17* (1), 34-40.
17. Singhal, S.; Stadanlick, J.; Annunziata, M. J.; Rao, A. S.; Bhojnagarwala, P. S.; O'Brien, S.; Moon, E. K.; Cantu, E.; Danet-Desnoyers, G.; Ra, H.-J.; Litzky, L.; Akimova, T.; Beier, U. H.; Hancock, W. W.; Albelda, S. M.; Eruslanov, E. B., Human tumor-associated monocytes/macrophages and their regulation of T cell responses in early-stage lung cancer. *Science Translational Medicine* **2019,** *11* (479), eaat1500.
18. Ma, R.-Y.; Black, A.; Qian, B.-Z., Macrophage diversity in cancer revisited in the era of single-cell omics. *Trends in Immunology* **2022,** *43* (7), 546-563.
19. Bronte, V.; Brandau, S.; Chen, S.-H.; Colombo, M. P.; Frey, A. B.; Greten, T. F.;

Mandruzzato, S.; Murray, P. J.; Ochoa, A.; Ostrand-Rosenberg, S.; Rodriguez, P. C.; Sica, A.; Umansky, V.; Vonderheide, R. H.; Gabrilovich, D. I., Recommendations for myeloid-derived suppressor cell nomenclature and characterization standards. *Nature Communications* **2016,** *7* (1), 12150.
20. Ugel, S.; De Sanctis, F.; Mandruzzato, S.; Bronte, V., Tumor-induced myeloid deviation: when myeloid-derived suppressor cells meet tumor-associated macrophages. *The Journal of Clinical Investigation* **2015,** *125* (9), 3365-3376.
21. Ugel, S.; Canè, S.; De Sanctis, F.; Bronte, V., Monocytes in the Tumor Microenvironment. *Annual Review of Pathology: Mechanisms of Disease* **2021,** *16* (1), 93-122.
22. Swann, J. B.; Smyth, M. J., Immune surveillance of tumors. *J Clin Invest* **2007,** *117* (5), 1137-46.
23. Hanahan, D., Hallmarks of Cancer: New Dimensions. *Cancer Discovery* **2022,** *12* (1), 31-46.
24. Gabrilovich, D., Mechanisms and functional significance of tumour-induced dendritic-cell defects. *Nature Reviews Immunology* **2004,** *4* (12), 941-952.
25. Gabrilovich, D. I.; Chen, H. L.; Girgis, K. R.; Cunningham, H. T.; Meny, G. M.; Nadaf, S.; Kavanaugh, D.; Carbone, D. P., Production of vascular endothelial growth factor by human tumors inhibits the functional maturation of dendritic cells. *Nature medicine* **1996,** *2* (10), 1096-1103.
26. Feng, M.; Jiang, W.; Kim, B. Y. S.; Zhang, C. C.; Fu, Y.-X.; Weissman, I. L., Phagocytosis checkpoints as new targets for cancer immunotherapy. *Nature Reviews Cancer* **2019,** *19* (10), 568-586.
27. Chen, L.; Deng, H.; Cui, H.; Fang, J.; Zuo, Z.; Deng, J.; Li, Y.; Wang, X.; Zhao, L., Inflammatory responses and inflammation-associated diseases in organs. *Oncotarget* **2018,** *9* (6), 7204-7218.
28. Bremnes, R. M.; Al-Shibli, K.; Donnem, T.; Sirera, R.; Al-Saad, S.; Andersen, S.; Stenvold, H.; Camps, C.; Busund, L. T., The role of tumor-infiltrating immune cells and chronic inflammation at the tumor site on cancer development, progression, and prognosis: emphasis on non-small cell lung cancer. *J Thorac Oncol* **2011,** *6* (4), 824-33.
29. Qian, B. Z.; Pollard, J. W., Macrophage diversity enhances tumor progression and metastasis. *Cell* **2010,** *141* (1), 39-51.
30. de Visser, K. E.; Eichten, A.; Coussens, L. M., Paradoxical roles of the immune system during cancer development. *Nat Rev Cancer* **2006,** *6* (1), 24-37.
31. DeNardo, D. G.; Andreu, P.; Coussens, L. M., Interactions between lymphocytes and myeloid cells regulate pro- versus anti-tumor immunity. *Cancer and Metastasis Reviews* **2010,** *29* (2), 309-316.
32. Grivennikov, S. I.; Greten, F. R.; Karin, M., Immunity, inflammation, and cancer. *Cell* **2010,** *140* (6), 883-899.
33. Karnoub, A. E.; Weinberg, R. A., Chemokine networks and breast cancer metastasis. *Breast disease* **2007,** *26* (1), 75-85.
34. Garner, H.; de Visser, K. E., Immune crosstalk in cancer progression and metastatic spread: a complex conversation. *Nature Reviews Immunology* **2020,** *20* (8), 483-497.
35. Nakamura, K.; Smyth, M. J., Myeloid immunosuppression and immune checkpoints in the tumor microenvironment. *Cellular & molecular immunology* **2020,** *17* (1), 1-12.
36. Wu, S.; Rhee, K. J.; Albesiano, E.; Rabizadeh, S.; Wu, X.; Yen, H. R.; Huso, D. L.; Brancati, F. L.; Wick, E.; McAllister, F.; Housseau, F.; Pardoll, D. M.; Sears, C. L., A human colonic commensal promotes colon tumorigenesis via activation of T helper type 17 T cell responses. *Nat Med* **2009,** *15* (9), 1016-22.
37. Mantovani, A.; Allavena, P.; Sica, A.; Balkwill, F., Cancer-related inflammation. *Nature* **2008,** *454* (7203), 436-44.
38. Zong, W. X.; Thompson, C. B., Necrotic death as a cell fate. *Genes Dev* **2006,** *20* (1), 1-15.
39. Kaplan, R. N.; Riba, R. D.; Zacharoulis, S.; Bramley, A. H.; Vincent, L.; Costa, C.; MacDonald, D. D.; Jin, D. K.; Shido, K.; Kerns, S. A.; Zhu, Z.; Hicklin, D.; Wu, Y.; Port, J. L.; Altorki, N.; Port, E. R.; Ruggero, D.; Shmelkov, S. V.; Jensen, K. K.; Rafii, S.; Lyden, D., VEGFR1-positive haematopoietic bone marrow progenitors initiate the pre-metastatic niche. *Nature* **2005,** *438* (7069), 820-7.

40. Lin, W. W.; Karin, M., A cytokine-mediated link between innate immunity, inflammation, and cancer. *J Clin Invest* **2007,** *117* (5), 1175-83.
41. Hargadon, K. M.; Johnson, C. E.; Williams, C. J., Immune checkpoint blockade therapy for cancer: An overview of FDA-approved immune checkpoint inhibitors. *Int Immunopharmacol* **2018,** *62*, 29-39.
42. Michot, J. M.; Bigenwald, C.; Champiat, S.; Collins, M.; Carbonnel, F.; Postel-Vinay, S.; Berdelou, A.; Varga, A.; Bahleda, R.; Hollebecque, A.; Massard, C.; Fuerea, A.; Ribrag, V.; Gazzah, A.; Armand, J. P.; Amellal, N.; Angevin, E.; Noel, N.; Boutros, C.; Mateus, C.; Robert, C.; Soria, J. C.; Marabelle, A.; Lambotte, O., Immune-related adverse events with immune checkpoint blockade: a comprehensive review. *Eur J Cancer* **2016,** *54*, 139-148.
43. Kantoff, P. W.; Higano, C. S.; Shore, N. D.; Berger, E. R.; Small, E. J.; Penson, D. F.; Redfern, C. H.; Ferrari, A. C.; Dreicer, R.; Sims, R. B.; Xu, Y.; Frohlich, M. W.; Schellhammer, P. F., Sipuleucel-T immunotherapy for castration-resistant prostate cancer. *N Engl J Med* **2010,** *363* (5), 411-22.
44. Andtbacka, R. H. I.; Collichio, F. A.; Amatruda, T.; Senzer, N. N.; Chesney, J.; Delman, K. A.; Spitler, L. E.; Puzanov, I.; Doleman, S.; Ye, Y.; Vanderwalde, A. M.; Coffin, R.; Kaufman, H., OPTiM: A randomized phase III trial of talimogene laherparepvec (T-VEC) versus subcutaneous (SC) granulocyte-macrophage colony-stimulating factor (GM-CSF) for the treatment (tx) of unresected stage IIIB/C and IV melanoma. *Journal of Clinical Oncology* **2013,** *31* (18_suppl), LBA9008-LBA9008.
45. Pan, C.; Liu, H.; Robins, E.; Song, W.; Liu, D.; Li, Z.; Zheng, L., Next-generation immuno-oncology agents: current momentum shifts in cancer immunotherapy. *Journal of Hematology & Oncology* **2020,** *13* (1), 29.
46. Grossman, J. G.; Nywening, T. M.; Belt, B. A.; Panni, R. Z.; Krasnick, B. A.; DeNardo, D. G.; Hawkins, W. G.; Goedegebuure, S. P.; Linehan, D. C.; Fields, R. C., Recruitment of CCR2(+) tumor associated macrophage to sites of liver metastasis confers a poor prognosis in human colorectal cancer. *Oncoimmunology* **2018,** *7* (9), e1470729.
47. Che, J.; Song, R.; Chen, B.; Dong, X., Targeting CXCR1/2: The medicinal potential as cancer immunotherapy agents, antagonists research highlights and challenges ahead. *Eur J Med Chem* **2020,** *185*, 111853.
48. Pyonteck, S. M.; Akkari, L.; Schuhmacher, A. J.; Bowman, R. L.; Sevenich, L.; Quail, D. F.; Olson, O. C.; Quick, M. L.; Huse, J. T.; Teijeiro, V.; Setty, M.; Leslie, C. S.; Oei, Y.; Pedraza, A.; Zhang, J.; Brennan, C. W.; Sutton, J. C.; Holland, E. C.; Daniel, D.; Joyce, J. A., CSF-1R inhibition alters macrophage polarization and blocks glioma progression. *Nat Med* **2013,** *19* (10), 1264-72.
49. Liu, X.; Pu, Y.; Cron, K.; Deng, L.; Kline, J.; Frazier, W. A.; Xu, H.; Peng, H.; Fu, Y. X.; Xu, M. M., CD47 blockade triggers T cell-mediated destruction of immunogenic tumors. *Nat Med* **2015,** *21* (10), 1209-15.
50. Grewal, I. S.; Flavell, R. A., CD40 and CD154 in cell-mediated immunity. *Annu Rev Immunol* **1998,** *16*, 111-35.
51. Li, T. T.; Ogino, S.; Qian, Z. R., Toll-like receptor signaling in colorectal cancer: carcinogenesis to cancer therapy. *World J Gastroenterol* **2014,** *20* (47), 17699-708.
52. Vonderheide, R. H.; Glennie, M. J., Agonistic CD40 antibodies and cancer therapy. *Clin Cancer Res* **2013,** *19* (5), 1035-43.
53. De Henau, O.; Rausch, M.; Winkler, D.; Campesato, L. F.; Liu, C.; Cymerman, D. H.; Budhu, S.; Ghosh, A.; Pink, M.; Tchaicha, J.; Douglas, M.; Tibbitts, T.; Sharma, S.; Proctor, J.; Kosmider, N.; White, K.; Stern, H.; Soglia, J.; Adams, J.; Palombella, V. J.; McGovern, K.; Kutok, J. L.; Wolchok, J. D.; Merghoub, T., Overcoming resistance to checkpoint blockade therapy by targeting PI3Kγ in myeloid cells. *Nature* **2016,** *539* (7629), 443-447.
54. Dawson, M. A.; Kouzarides, T., Cancer epigenetics: from mechanism to therapy. *Cell* **2012,** *150* (1), 12-27.
55. Woo, S. R.; Fuertes, M. B.; Corrales, L.; Spranger, S.; Furdyna, M. J.; Leung, M. Y.; Duggan, R.; Wang, Y.; Barber, G. N.; Fitzgerald, K. A.; Alegre, M. L.; Gajewski, T. F., STING-dependent cytosolic DNA sensing mediates innate immune recognition of immunogenic tumors.

Immunity **2014,** *41* (5), 830-42.
56. Watkins, S. K.; Egilmez, N. K.; Suttles, J.; Stout, R. D., IL-12 rapidly alters the functional profile of tumor-associated and tumor-infiltrating macrophages in vitro and in vivo. *J Immunol* **2007,** *178* (3), 1357-62.
57. Ham, B.; Fernandez, M. C.; D'Costa, Z.; Brodt, P., The diverse roles of the TNF axis in cancer progression and metastasis. *Trends Cancer Res* **2016,** *11* (1), 1-27.
58. Balahura, L. R.; Selaru, A.; Dinescu, S.; Costache, M., Inflammation and Inflammasomes: Pros and Cons in Tumorigenesis. *Journal of Immunology Research* **2020,** *2020*, 2549763.
59. Malik, A.; Kanneganti, T.-D., Inflammasome activation and assembly at a glance. *J Cell Sci* **2017,** *130* (23), 3955-3963.
60. Bergsbaken, T.; Fink, S. L.; Cookson, B. T., Pyroptosis: host cell death and inflammation. *Nature Reviews Microbiology* **2009,** *7* (2), 99-109.
61. Sharma, D.; Kanneganti, T.-D., The cell biology of inflammasomes: Mechanisms of inflammasome activation and regulation. *Journal of Cell Biology* **2016,** *213* (6), 617-629.
62. Gurung, P.; Anand, P. K.; Malireddi, R. K.; Vande Walle, L.; Van Opdenbosch, N.; Dillon, C. P.; Weinlich, R.; Green, D. R.; Lamkanfi, M.; Kanneganti, T. D., FADD and caspase-8 mediate priming and activation of the canonical and noncanonical Nlrp3 inflammasomes. *J Immunol* **2014,** *192* (4), 1835-46.
63. Gringhuis, S. I.; Kaptein, T. M.; Wevers, B. A.; Theelen, B.; van der Vlist, M.; Boekhout, T.; Geijtenbeek, T. B., Dectin-1 is an extracellular pathogen sensor for the induction and processing of IL-1β via a noncanonical caspase-8 inflammasome. *Nat Immunol* **2012,** *13* (3), 246-54.
64. Juliana, C.; Fernandes-Alnemri, T.; Kang, S.; Farias, A.; Qin, F.; Alnemri, E. S., Non-transcriptional priming and deubiquitination regulate NLRP3 inflammasome activation. *J Biol Chem* **2012,** *287* (43), 36617-22.
65. Kanneganti, T. D.; Ozören, N.; Body-Malapel, M.; Amer, A.; Park, J. H.; Franchi, L.; Whitfield, J.; Barchet, W.; Colonna, M.; Vandenabeele, P.; Bertin, J.; Coyle, A.; Grant, E. P.; Akira, S.; Núñez, G., Bacterial RNA and small antiviral compounds activate caspase-1 through cryopyrin/Nalp3. *Nature* **2006,** *440* (7081), 233-6.
66. Kuriakose, T.; Man, S. M.; Malireddi, R. K.; Karki, R.; Kesavardhana, S.; Place, D. E.; Neale, G.; Vogel, P.; Kanneganti, T. D., ZBP1/DAI is an innate sensor of influenza virus triggering the NLRP3 inflammasome and programmed cell death pathways. *Sci Immunol* **2016,** *1* (2).
67. Karki, R.; Man, S. M.; Malireddi, R. K. S.; Gurung, P.; Vogel, P.; Lamkanfi, M.; Kanneganti, T. D., Concerted activation of the AIM2 and NLRP3 inflammasomes orchestrates host protection against Aspergillus infection. *Cell Host Microbe* **2015,** *17* (3), 357-368.
68. Wei, M.; Wang, L.; Wu, T.; Xi, J.; Han, Y.; Yang, X.; Zhang, D.; Fang, Q.; Tang, B., NLRP3 Activation Was Regulated by DNA Methylation Modification during Mycobacterium tuberculosis Infection. *Biomed Res Int* **2016,** *2016*, 4323281.
69. Zheng, D.; Liwinski, T.; Elinav, E., Inflammasome activation and regulation: toward a better understanding of complex mechanisms. *Cell Discovery* **2020,** *6* (1), 36.
70. Rathinam, V. A. K.; Chan, F. K.-M., Inflammasome, Inflammation, and Tissue Homeostasis. *Trends in Molecular Medicine* **2018,** *24* (3), 304-318.
71. Dinarello, C. A., Immunological and inflammatory functions of the interleukin-1 family. *Annu Rev Immunol* **2009,** *27*, 519-50.
72. Miao, E. A.; Leaf, I. A.; Treuting, P. M.; Mao, D. P.; Dors, M.; Sarkar, A.; Warren, S. E.; Wewers, M. D.; Aderem, A., Caspase-1-induced pyroptosis is an innate immune effector mechanism against intracellular bacteria. *Nat Immunol* **2010,** *11* (12), 1136-42.
73. He, Q.; Fu, Y.; Tian, D.; Yan, W., The contrasting roles of inflammasomes in cancer. *Am J Cancer Res* **2018,** *8* (4), 566-583.
74. Guo, H.; Callaway, J. B.; Ting, J. P., Inflammasomes: mechanism of action, role in disease, and therapeutics. *Nat Med* **2015,** *21* (7), 677-87.
75. Zeng, Q.; Fu, J.; Korrer, M.; Gorbounov, M.; Murray, P. J.; Pardoll, D.; Masica, D. L.; Kim, Y. J., Caspase-1 from Human Myeloid-Derived Suppressor Cells Can Promote T Cell-Independent

Tumor Proliferation. *Cancer Immunol Res* **2018,** *6* (5), 566-577.
76. Zaki, M. H.; Boyd, K. L.; Vogel, P.; Kastan, M. B.; Lamkanfi, M.; Kanneganti, T. D., The NLRP3 inflammasome protects against loss of epithelial integrity and mortality during experimental colitis. *Immunity* **2010,** *32* (3), 379-91.
77. Allen, I. C.; TeKippe, E. M.; Woodford, R. M.; Uronis, J. M.; Holl, E. K.; Rogers, A. B.; Herfarth, H. H.; Jobin, C.; Ting, J. P., The NLRP3 inflammasome functions as a negative regulator of tumorigenesis during colitis-associated cancer. *J Exp Med* **2010,** *207* (5), 1045-56.
78. Zhang, W.; Borcherding, N.; Kolb, R., IL-1 Signaling in Tumor Microenvironment. *Adv Exp Med Biol* **2020,** *1240*, 1-23.
79. Tannenbaum, C. S.; Rayman, P. A.; Pavicic, P. G.; Kim, J. S.; Wei, W.; Polefko, A.; Wallace, W.; Rini, B. I.; Morris-Stiff, G.; Allende, D. S.; Hamilton, T.; Finke, J. H.; Diaz-Montero, C. M., Mediators of Inflammation-Driven Expansion, Trafficking, and Function of Tumor-Infiltrating MDSCs. *Cancer Immunol Res* **2019,** *7* (10), 1687-1699.
80. Bunt, S. K.; Yang, L.; Sinha, P.; Clements, V. K.; Leips, J.; Ostrand-Rosenberg, S., Reduced inflammation in the tumor microenvironment delays the accumulation of myeloid-derived suppressor cells and limits tumor progression. *Cancer Res* **2007,** *67* (20), 10019-26.
81. Guo, B.; Fu, S.; Zhang, J.; Liu, B.; Li, Z., Targeting inflammasome/IL-1 pathways for cancer immunotherapy. *Sci Rep* **2016,** *6*, 36107.
82. Das, S.; Shapiro, B.; Vucic, E. A.; Vogt, S.; Bar-Sagi, D., Tumor Cell-Derived IL1β Promotes Desmoplasia and Immune Suppression in Pancreatic Cancer. *Cancer Res* **2020,** *80* (5), 1088-1101.
83. Garlanda, C.; Mantovani, A., Interleukin-1 in tumor progression, therapy, and prevention. *Cancer Cell* **2021,** *39* (8), 1023-1027.
84. Crossman, D.; Rothman, A. M. K., Interleukin-1 beta inhibition with canakinumab and reducing lung cancer-subset analysis of the canakinumab anti-inflammatory thrombosis outcome study trial (CANTOS). *J Thorac Dis* **2018,** *10* (Suppl 26), S3084-s3087.
85. Lythgoe, M. P.; Prasad, V., Repositioning canakinumab for non-small cell lung cancer—important lessons for drug repurposing in oncology. *British Journal of Cancer* **2022,** *127* (5), 785-787.
86. Theivanthiran, B.; Evans, K. S.; DeVito, N. C.; Plebanek, M.; Sturdivant, M.; Wachsmuth, L. P.; Salama, A. K.; Kang, Y.; Hsu, D.; Balko, J. M.; Johnson, D. B.; Starr, M.; Nixon, A. B.; Holtzhausen, A.; Hanks, B. A., A tumor-intrinsic PD-L1/NLRP3 inflammasome signaling pathway drives resistance to anti-PD-1 immunotherapy. *J Clin Invest* **2020,** *130* (5), 2570-2586.
87. Chen, L.; Huang, C.-F.; Li, Y.-C.; Deng, W.-W.; Mao, L.; Wu, L.; Zhang, W.-F.; Zhang, L.; Sun, Z.-J., Blockage of the NLRP3 inflammasome by MCC950 improves anti-tumor immune responses in head and neck squamous cell carcinoma. *Cellular and Molecular Life Sciences* **2018,** *75* (11), 2045-2058.
88. Linder, A.; Hornung, V., Inflammasomes in T cells. *Journal of Molecular Biology* **2022,** *434* (4), 167275.
89. Roy, S.; Bag, A. K.; Dutta, S.; Polavaram, N. S.; Islam, R.; Schellenburg, S.; Banwait, J.; Guda, C.; Ran, S.; Hollingsworth, M. A.; Singh, R. K.; Talmadge, J. E.; Muders, M. H.; Batra, S. K.; Datta, K., Macrophage-Derived Neuropilin-2 Exhibits Novel Tumor-Promoting Functions. *Cancer Res* **2018,** *78* (19), 5600-5617.
90. Stanford, J. C.; Young, C.; Hicks, D.; Owens, P.; Williams, A.; Vaught, D. B.; Morrison, M. M.; Lim, J.; Williams, M.; Brantley-Sieders, D. M.; Balko, J. M.; Tonetti, D.; Earp, H. S., 3rd; Cook, R. S., Efferocytosis produces a prometastatic landscape during postpartum mammary gland involution. *J Clin Invest* **2014,** *124* (11), 4737-52.
91. Cunha, L. D.; Yang, M.; Carter, R.; Guy, C.; Harris, L.; Crawford, J. C.; Quarato, G.; Boada-Romero, E.; Kalkavan, H.; Johnson, M. D. L.; Natarajan, S.; Turnis, M. E.; Finkelstein, D.; Opferman, J. T.; Gawad, C.; Green, D. R., LC3-Associated Phagocytosis in Myeloid Cells Promotes Tumor Immune Tolerance. *Cell* **2018,** *175* (2), 429-441 e16.
92. Zhou, Y.; Fei, M.; Zhang, G.; Liang, W. C.; Lin, W.; Wu, Y.; Piskol, R.; Ridgway, J.; McNamara, E.; Huang, H.; Zhang, J.; Oh, J.; Patel, J. M.; Jakubiak, D.; Lau, J.; Blackwood, B.; Bravo, D. D.; Shi, Y.; Wang, J.; Hu, H. M.; Lee, W. P.; Jesudason, R.; Sangaraju, D.; Modrusan,

Z.; Anderson, K. R.; Warming, S.; Roose-Girma, M.; Yan, M., Blockade of the Phagocytic Receptor MerTK on Tumor-Associated Macrophages Enhances P2X7R-Dependent STING Activation by Tumor-Derived cGAMP. *Immunity* **2020,** *52* (2), 357-373 e9.
93. Morioka, S.; Maueroder, C.; Ravichandran, K. S., Living on the Edge: Efferocytosis at the Interface of Homeostasis and Pathology. *Immunity* **2019,** *50* (5), 1149-1162.
94. Boada-Romero, E.; Martinez, J.; Heckmann, B. L.; Green, D. R., The clearance of dead cells by efferocytosis. *Nat Rev Mol Cell Biol* **2020,** *21* (7), 398-414.
95. Poon, I. K.; Lucas, C. D.; Rossi, A. G.; Ravichandran, K. S., Apoptotic cell clearance: basic biology and therapeutic potential. *Nat Rev Immunol* **2014,** *14* (3), 166-80.
96. Elliott, M. R.; Ravichandran, K. S., Clearance of apoptotic cells: implications in health and disease. *J Cell Biol* **2010,** *189* (7), 1059-70.
97. Ravichandran, K. S., Find-me and eat-me signals in apoptotic cell clearance: progress and conundrums. *J Exp Med* **2010,** *207* (9), 1807-17.
98. Korns, D.; Frasch, S. C.; Fernandez-Boyanapalli, R.; Henson, P. M.; Bratton, D. L., Modulation of macrophage efferocytosis in inflammation. *Front Immunol* **2011,** *2*, 57.
99. Gordon, S.; Pluddemann, A., Macrophage Clearance of Apoptotic Cells: A Critical Assessment. *Front Immunol* **2018,** *9*, 127.
100. Green, D. R.; Oguin, T. H.; Martinez, J., The clearance of dying cells: table for two. *Cell Death Differ* **2016,** *23* (6), 915-26.
101. Elliott, M. R.; Koster, K. M.; Murphy, P. S., Efferocytosis Signaling in the Regulation of Macrophage Inflammatory Responses. *J Immunol* **2017,** *198* (4), 1387-1394.
102. Elliott, M. R.; Chekeni, F. B.; Trampont, P. C.; Lazarowski, E. R.; Kadl, A.; Walk, S. F.; Park, D.; Woodson, R. I.; Ostankovich, M.; Sharma, P.; Lysiak, J. J.; Harden, T. K.; Leitinger, N.; Ravichandran, K. S., Nucleotides released by apoptotic cells act as a find-me signal to promote phagocytic clearance. *Nature* **2009,** *461* (7261), 282-6.
103. Truman, L. A.; Ford, C. A.; Pasikowska, M.; Pound, J. D.; Wilkinson, S. J.; Dumitriu, I. E.; Melville, L.; Melrose, L. A.; Ogden, C. A.; Nibbs, R.; Graham, G.; Combadiere, C.; Gregory, C. D., CX3CL1/fractalkine is released from apoptotic lymphocytes to stimulate macrophage chemotaxis. *Blood* **2008,** *112* (13), 5026-36.
104. Lauber, K.; Bohn, E.; Kröber, S. M.; Xiao, Y. J.; Blumenthal, S. G.; Lindemann, R. K.; Marini, P.; Wiedig, C.; Zobywalski, A.; Baksh, S.; Xu, Y.; Autenrieth, I. B.; Schulze-Osthoff, K.; Belka, C.; Stuhler, G.; Wesselborg, S., Apoptotic cells induce migration of phagocytes via caspase-3-mediated release of a lipid attraction signal. *Cell* **2003,** *113* (6), 717-30.
105. Gude, D. R.; Alvarez, S. E.; Paugh, S. W.; Mitra, P.; Yu, J.; Griffiths, R.; Barbour, S. E.; Milstien, S.; Spiegel, S., Apoptosis induces expression of sphingosine kinase 1 to release sphingosine-1-phosphate as a "come-and-get-me" signal. *Faseb j* **2008,** *22* (8), 2629-38.
106. Werfel, T. A.; Cook, R. S., Efferocytosis in the tumor microenvironment. *Semin Immunopathol* **2018,** *40* (6), 545-554.
107. Fadok, V. A.; Voelker, D. R.; Campbell, P. A.; Cohen, J. J.; Bratton, D. L.; Henson, P. M., Exposure of phosphatidylserine on the surface of apoptotic lymphocytes triggers specific recognition and removal by macrophages. *J Immunol* **1992,** *148* (7), 2207-16.
108. Park, D.; Tosello-Trampont, A. C.; Elliott, M. R.; Lu, M.; Haney, L. B.; Ma, Z.; Klibanov, A. L.; Mandell, J. W.; Ravichandran, K. S., BAI1 is an engulfment receptor for apoptotic cells upstream of the ELMO/Dock180/Rac module. *Nature* **2007,** *450* (7168), 430-4.
109. Kobayashi, N.; Karisola, P.; Peña-Cruz, V.; Dorfman, D. M.; Jinushi, M.; Umetsu, S. E.; Butte, M. J.; Nagumo, H.; Chernova, I.; Zhu, B.; Sharpe, A. H.; Ito, S.; Dranoff, G.; Kaplan, G. G.; Casasnovas, J. M.; Umetsu, D. T.; Dekruyff, R. H.; Freeman, G. J., TIM-1 and TIM-4 glycoproteins bind phosphatidylserine and mediate uptake of apoptotic cells. *Immunity* **2007,** *27* (6), 927-40.
110. Park, S. Y.; Jung, M. Y.; Kim, H. J.; Lee, S. J.; Kim, S. Y.; Lee, B. H.; Kwon, T. H.; Park, R. W.; Kim, I. S., Rapid cell corpse clearance by stabilin-2, a membrane phosphatidylserine receptor. *Cell Death Differ* **2008,** *15* (1), 192-201.
111. Morizono, K.; Xie, Y.; Olafsen, T.; Lee, B.; Dasgupta, A.; Wu, A. M.; Chen, I. S., The

soluble serum protein Gas6 bridges virion envelope phosphatidylserine to the TAM receptor tyrosine kinase Axl to mediate viral entry. *Cell Host Microbe* **2011,** *9* (4), 286-98.
112. Hall, M. O.; Obin, M. S.; Heeb, M. J.; Burgess, B. L.; Abrams, T. A., Both protein S and Gas6 stimulate outer segment phagocytosis by cultured rat retinal pigment epithelial cells. *Exp Eye Res* **2005,** *81* (5), 581-91.
113. Caberoy, N. B.; Alvarado, G.; Bigcas, J. L.; Li, W., Galectin-3 is a new MerTK-specific eat-me signal. *J Cell Physiol* **2012,** *227* (2), 401-7.
114. Caberoy, N. B.; Zhou, Y.; Li, W., Tubby and tubby-like protein 1 are new MerTK ligands for phagocytosis. *Embo j* **2010,** *29* (23), 3898-910.
115. Brown, S.; Heinisch, I.; Ross, E.; Shaw, K.; Buckley, C. D.; Savill, J., Apoptosis disables CD31-mediated cell detachment from phagocytes promoting binding and engulfment. *Nature* **2002,** *418* (6894), 200-3.
116. Kojima, Y.; Volkmer, J. P.; McKenna, K.; Civelek, M.; Lusis, A. J.; Miller, C. L.; Direnzo, D.; Nanda, V.; Ye, J.; Connolly, A. J.; Schadt, E. E.; Quertermous, T.; Betancur, P.; Maegdefessel, L.; Matic, L. P.; Hedin, U.; Weissman, I. L.; Leeper, N. J., CD47-blocking antibodies restore phagocytosis and prevent atherosclerosis. *Nature* **2016,** *536* (7614), 86-90.
117. Vanden Berghe, T.; Vanlangenakker, N.; Parthoens, E.; Deckers, W.; Devos, M.; Festjens, N.; Guerin, C. J.; Brunk, U. T.; Declercq, W.; Vandenabeele, P., Necroptosis, necrosis and secondary necrosis converge on similar cellular disintegration features. *Cell Death Differ* **2010,** *17* (6), 922-30.
118. Green, D. R.; Ferguson, T.; Zitvogel, L.; Kroemer, G., Immunogenic and tolerogenic cell death. *Nat Rev Immunol* **2009,** *9* (5), 353-63.
119. de Jong, J. S.; Diest, P. J. v.; Baak, J. P. A., Number of apoptotic cells as a prognostic marker in invasive breast cancer. *British Journal of Cancer* **2000,** *82* (2), 368-373.
120. Soini, Y.; Pääkkö, P.; Lehto, V. P., Histopathological evaluation of apoptosis in cancer. *Am J Pathol* **1998,** *153* (4), 1041-1053.
121. Ucker, D. S.; Levine, J. S., Exploitation of Apoptotic Regulation in Cancer. *Frontiers in Immunology* **2018,** *9* (241).
122. Wyllie, A. H., Apoptosis and the regulation of cell numbers in normal and neoplastic tissues: an overview. *Cancer and Metastasis Reviews* **1992,** *11* (2), 95-103.
123. Gregory, C. D.; Pound, J. D., Microenvironmental influences of apoptosis in vivo and in vitro. *Apoptosis* **2010,** *15* (9), 1029-1049.
124. Linger, R. M.; Keating, A. K.; Earp, H. S.; Graham, D. K., TAM receptor tyrosine kinases: biologic functions, signaling, and potential therapeutic targeting in human cancer. *Advances in cancer research* **2008,** *100*, 35-83.
125. Verma, A.; Warner, S. L.; Vankayalapati, H.; Bearss, D. J.; Sharma, S., Targeting Axl and Mer Kinases in CancerAxl and Mer in Cancer. *Molecular cancer therapeutics* **2011,** *10* (10), 1763-1773.
126. Werfel, T. A.; Elion, D. L.; Rahman, B.; Hicks, D. J.; Sanchez, V.; Gonzales-Ericsson, P. I.; Nixon, M. J.; James, J. L.; Balko, J. M.; Scherle, P. A.; Koblish, H. K.; Cook, R. S., Treatment-Induced Tumor Cell Apoptosis and Secondary Necrosis Drive Tumor Progression in the Residual Tumor Microenvironment through MerTK and IDO1. *Cancer Res* **2019,** *79* (1), 171-182.
127. Myers, K. V.; Amend, S. R.; Pienta, K. J., Targeting Tyro3, Axl and MerTK (TAM receptors): implications for macrophages in the tumor microenvironment. *Mol Cancer* **2019,** *18* (1), 94.
128. Magge, R. S.; DeAngelis, L. M., The double-edged sword: neurotoxicity of chemotherapy. *Blood reviews* **2015,** *29* (2), 93-100.
129. Pisco, A. O.; Huang, S., Non-genetic cancer cell plasticity and therapy-induced stemness in tumour relapse:'What does not kill me strengthens me'. *British journal of cancer* **2015,** *112* (11), 1725-1732.
130. Jager, B.; Seeliger, B.; Terwolbeck, O.; Warnecke, G.; Welte, T.; Muller, M.; Bode, C.; Prasse, A., The NLRP3-Inflammasome-Caspase-1 Pathway Is Upregulated in Idiopathic Pulmonary Fibrosis and Acute Exacerbations and Is Inducible by Apoptotic A549 Cells. *Front Immunol* **2021,** *12*, 642855.

131. Ayna, G.; Krysko, D. V.; Kaczmarek, A.; Petrovski, G.; Vandenabeele, P.; Fesus, L., ATP release from dying autophagic cells and their phagocytosis are crucial for inflammasome activation in macrophages. *PLoS One* **2012,** *7* (6), e40069.
132. DeRose, P.; Thorpe, P. E.; Gerber, D. E., Development of bavituximab, a vascular targeting agent with immune-modulating properties, for lung cancer treatment. *Immunotherapy* **2011,** *3* (8), 933-44.
133. Ran, S.; Downes, A.; Thorpe, P. E., Increased exposure of anionic phospholipids on the surface of tumor blood vessels. *Cancer Res* **2002,** *62* (21), 6132-40.
134. Onken, J.; Torka, R.; Korsing, S.; Radke, J.; Krementeskaia, I.; Nieminen, M.; Bai, X.; Ullrich, A.; Heppner, F.; Vajkoczy, P., Inhibiting receptor tyrosine kinase AXL with small molecule inhibitor BMS-777607 reduces glioblastoma growth, migration, and invasion in vitro and in vivo. *Oncotarget* **2016,** *7* (9), 9876-89.
135. Zhu, C.; Wei, Y.; Wei, X., AXL receptor tyrosine kinase as a promising anti-cancer approach: functions, molecular mechanisms and clinical applications. *Mol Cancer* **2019,** *18* (1), 153.
136. Duan, Y.; Luo, L.; Qiao, C.; Li, X.; Wang, J.; Liu, H.; Zhou, T.; Shen, B.; Lv, M.; Feng, J., A novel human anti-AXL monoclonal antibody attenuates tumour cell migration. *Scand J Immunol* **2019,** *90* (2), e12777.
137. McDaniel, N. K.; Cummings, C. T.; Iida, M.; Hülse, J.; Pearson, H. E.; Vasileiadi, E.; Parker, R. E.; Orbuch, R. A.; Ondracek, O. J.; Welke, N. B.; Kang, G. H.; Davies, K. D.; Wang, X.; Frye, S. V.; Earp, H. S.; Harari, P. M.; Kimple, R. J.; DeRyckere, D.; Graham, D. K.; Wheeler, D. L., MERTK Mediates Intrinsic and Adaptive Resistance to AXL-targeting Agents. *Mol Cancer Ther* **2018,** *17* (11), 2297-2308.
138. Willingham, S. B.; Volkmer, J. P.; Gentles, A. J.; Sahoo, D.; Dalerba, P.; Mitra, S. S.; Wang, J.; Contreras-Trujillo, H.; Martin, R.; Cohen, J. D.; Lovelace, P.; Scheeren, F. A.; Chao, M. P.; Weiskopf, K.; Tang, C.; Volkmer, A. K.; Naik, T. J.; Storm, T. A.; Mosley, A. R.; Edris, B.; Schmid, S. M.; Sun, C. K.; Chua, M. S.; Murillo, O.; Rajendran, P.; Cha, A. C.; Chin, R. K.; Kim, D.; Adorno, M.; Raveh, T.; Tseng, D.; Jaiswal, S.; Enger, P.; Steinberg, G. K.; Li, G.; So, S. K.; Majeti, R.; Harsh, G. R.; van de Rijn, M.; Teng, N. N.; Sunwoo, J. B.; Alizadeh, A. A.; Clarke, M. F.; Weissman, I. L., The CD47-signal regulatory protein alpha (SIRPa) interaction is a therapeutic target for human solid tumors. *Proc Natl Acad Sci U S A* **2012,** *109* (17), 6662-7.
139. Chao, M. P.; Alizadeh, A. A.; Tang, C.; Myklebust, J. H.; Varghese, B.; Gill, S.; Jan, M.; Cha, A. C.; Chan, C. K.; Tan, B. T.; Park, C. Y.; Zhao, F.; Kohrt, H. E.; Malumbres, R.; Briones, J.; Gascoyne, R. D.; Lossos, I. S.; Levy, R.; Weissman, I. L.; Majeti, R., Anti-CD47 antibody synergizes with rituximab to promote phagocytosis and eradicate non-Hodgkin lymphoma. *Cell* **2010,** *142* (5), 699-713.
140. Clynes, R. A.; Towers, T. L.; Presta, L. G.; Ravetch, J. V., Inhibitory Fc receptors modulate in vivo cytotoxicity against tumor targets. *Nat Med* **2000,** *6* (4), 443-6.
141. Chung, C. H.; Parker, J. S.; Karaca, G.; Wu, J.; Funkhouser, W. K.; Moore, D.; Butterfoss, D.; Xiang, D.; Zanation, A.; Yin, X.; Shockley, W. W.; Weissler, M. C.; Dressler, L. G.; Shores, C. G.; Yarbrough, W. G.; Perou, C. M., Molecular classification of head and neck squamous cell carcinomas using patterns of gene expression. *Cancer Cell* **2004,** *5* (5), 489-500.
142. Sheeja, K.; Lakshmi, S., Nod-like receptor protein 3 inflammasome in head-and-neck cancer. *J Cancer Res Ther* **2020,** *16* (3), 405-409.
143. Ershaid, N.; Sharon, Y.; Doron, H.; Raz, Y.; Shani, O.; Cohen, N.; Monteran, L.; Leider-Trejo, L.; Ben-Shmuel, A.; Yassin, M.; Gerlic, M.; Ben-Baruch, A.; Pasmanik-Chor, M.; Apte, R.; Erez, N., NLRP3 inflammasome in fibroblasts links tissue damage with inflammation in breast cancer progression and metastasis. *Nat Commun* **2019,** *10* (1), 4375.
144. Privitera, G.; Rana, N.; Scaldaferri, F.; Armuzzi, A.; Pizarro, T. T., Novel Insights Into the Interactions Between the Gut Microbiome, Inflammasomes, and Gasdermins During Colorectal Cancer. *Front Cell Infect Microbiol* **2021,** *11*, 806680.
145. Zheng, G. X.; Terry, J. M.; Belgrader, P.; Ryvkin, P.; Bent, Z. W.; Wilson, R.; Ziraldo, S. B.; Wheeler, T. D.; McDermott, G. P.; Zhu, J.; Gregory, M. T.; Shuga, J.; Montesclaros, L.;

Underwood, J. G.; Masquelier, D. A.; Nishimura, S. Y.; Schnall-Levin, M.; Wyatt, P. W.; Hindson, C. M.; Bharadwaj, R.; Wong, A.; Ness, K. D.; Beppu, L. W.; Deeg, H. J.; McFarland, C.; Loeb, K. R.; Valente, W. J.; Ericson, N. G.; Stevens, E. A.; Radich, J. P.; Mikkelsen, T. S.; Hindson, B. J.; Bielas, J. H., Massively parallel digital transcriptional profiling of single cells. *Nat Commun* **2017,** *8*, 14049.
146. Dobin, A.; Davis, C. A.; Schlesinger, F.; Drenkow, J.; Zaleski, C.; Jha, S.; Batut, P.; Chaisson, M.; Gingeras, T. R., STAR: ultrafast universal RNA-seq aligner. *Bioinformatics* **2013,** *29* (1), 15-21.
147. Hao, Y.; Hao, S.; Andersen-Nissen, E.; Mauck, W. M., 3rd; Zheng, S.; Butler, A.; Lee, M. J.; Wilk, A. J.; Darby, C.; Zager, M.; Hoffman, P.; Stoeckius, M.; Papalexi, E.; Mimitou, E. P.; Jain, J.; Srivastava, A.; Stuart, T.; Fleming, L. M.; Yeung, B.; Rogers, A. J.; McElrath, J. M.; Blish, C. A.; Gottardo, R.; Smibert, P.; Satija, R., Integrated analysis of multimodal single-cell data. *Cell* **2021,** *184* (13), 3573-3587 e29.
148. Wolock, S. L.; Lopez, R.; Klein, A. M., Scrublet: Computational Identification of Cell Doublets in Single-Cell Transcriptomic Data. *Cell Syst* **2019,** *8* (4), 281-291 e9.
149. Stuart, T.; Butler, A.; Hoffman, P.; Hafemeister, C.; Papalexi, E.; Mauck, W. M., 3rd; Hao, Y.; Stoeckius, M.; Smibert, P.; Satija, R., Comprehensive Integration of Single-Cell Data. *Cell* **2019,** *177* (7), 1888-1902 e21.
150. Zilionis, R.; Engblom, C.; Pfirschke, C.; Savova, V.; Zemmour, D.; Saatcioglu, H. D.; Krishnan, I.; Maroni, G.; Meyerovitz, C. V.; Kerwin, C. M.; Choi, S.; Richards, W. G.; De Rienzo, A.; Tenen, D. G.; Bueno, R.; Levantini, E.; Pittet, M. J.; Klein, A. M., Single-Cell Transcriptomics of Human and Mouse Lung Cancers Reveals Conserved Myeloid Populations across Individuals and Species. *Immunity* **2019,** *50* (5), 1317-1334 e10.
151. Cheng, S.; Li, Z.; Gao, R.; Xing, B.; Gao, Y.; Yang, Y.; Qin, S.; Zhang, L.; Ouyang, H.; Du, P.; Jiang, L.; Zhang, B.; Yang, Y.; Wang, X.; Ren, X.; Bei, J. X.; Hu, X.; Bu, Z.; Ji, J.; Zhang, Z., A pan-cancer single-cell transcriptional atlas of tumor infiltrating myeloid cells. *Cell* **2021,** *184* (3), 792-809.e23.
152. Cortal, A.; Martignetti, L.; Six, E.; Rausell, A., Gene signature extraction and cell identity recognition at the single-cell level with Cell-ID. *Nat Biotechnol* **2021,** *39* (9), 1095-1102.
153. Liberzon, A.; Birger, C.; Thorvaldsdottir, H.; Ghandi, M.; Mesirov, J. P.; Tamayo, P., The Molecular Signatures Database (MSigDB) hallmark gene set collection. *Cell Syst* **2015,** *1* (6), 417-425.
154. Liberzon, A.; Subramanian, A.; Pinchback, R.; Thorvaldsdottir, H.; Tamayo, P.; Mesirov, J. P., Molecular signatures database (MSigDB) 3.0. *Bioinformatics* **2011,** *27* (12), 1739-40.
155. Subramanian, A.; Tamayo, P.; Mootha, V. K.; Mukherjee, S.; Ebert, B. L.; Gillette, M. A.; Paulovich, A.; Pomeroy, S. L.; Golub, T. R.; Lander, E. S.; Mesirov, J. P., Gene set enrichment analysis: a knowledge-based approach for interpreting genome-wide expression profiles. *Proc Natl Acad Sci U S A* **2005,** *102* (43), 15545-50.
156. Finak, G.; McDavid, A.; Yajima, M.; Deng, J.; Gersuk, V.; Shalek, A. K.; Slichter, C. K.; Miller, H. W.; McElrath, M. J.; Prlic, M.; Linsley, P. S.; Gottardo, R., MAST: a flexible statistical framework for assessing transcriptional changes and characterizing heterogeneity in single-cell RNA sequencing data. *Genome Biol* **2015,** *16*, 278.
157. La Manno, G.; Soldatov, R.; Zeisel, A.; Braun, E.; Hochgerner, H.; Petukhov, V.; Lidschreiber, K.; Kastriti, M. E.; Lönnerberg, P.; Furlan, A.; Fan, J.; Borm, L. E.; Liu, Z.; van Bruggen, D.; Guo, J.; He, X.; Barker, R.; Sundström, E.; Castelo-Branco, G.; Cramer, P.; Adameyko, I.; Linnarsson, S.; Kharchenko, P. V., RNA velocity of single cells. *Nature* **2018,** *560* (7719), 494-498.
158. Bergen, V.; Lange, M.; Peidli, S.; Wolf, F. A.; Theis, F. J., Generalizing RNA velocity to transient cell states through dynamical modeling. *Nat Biotechnol* **2020,** *38* (12), 1408-1414.
159. Wolf, F. A.; Hamey, F. K.; Plass, M.; Solana, J.; Dahlin, J. S.; Göttgens, B.; Rajewsky, N.; Simon, L.; Theis, F. J., PAGA: graph abstraction reconciles clustering with trajectory inference through a topology preserving map of single cells. *Genome Biology* **2019,** *20* (1), 59.
160. Liao, Y.; Smyth, G. K.; Shi, W., featureCounts: an efficient general purpose program for

assigning sequence reads to genomic features. *Bioinformatics* **2014,** *30* (7), 923-30.
161. Love, M. I.; Huber, W.; Anders, S., Moderated estimation of fold change and dispersion for RNA-seq data with DESeq2. *Genome Biol* **2014,** *15* (12), 550.
162. Yu, G.; Wang, L. G.; Han, Y.; He, Q. Y., clusterProfiler: an R package for comparing biological themes among gene clusters. *OMICS* **2012,** *16* (5), 284-7.
163. Sergushichev, A., An algorithm for fast preranked gene set enrichment analysis using cumulative statistic calculation. *bioRxiv* **2016**.
164. Hanzelmann, S.; Castelo, R.; Guinney, J., GSVA: gene set variation analysis for microarray and RNA-seq data. *BMC Bioinformatics* **2013,** *14*, 7.
165. Ritchie, M. E.; Phipson, B.; Wu, D.; Hu, Y.; Law, C. W.; Shi, W.; Smyth, G. K., limma powers differential expression analyses for RNA-sequencing and microarray studies. *Nucleic Acids Res* **2015,** *43* (7), e47.
166. Queen, M. M.; Ryan, R. E.; Holzer, R. G.; Keller-Peck, C. R.; Jorcyk, C. L., Breast cancer cells stimulate neutrophils to produce oncostatin M: potential implications for tumor progression. *Cancer Res* **2005,** *65* (19), 8896-904.
167. Zhang, L.; Li, Z.; Skrzypczynska, K. M.; Fang, Q.; Zhang, W.; O'Brien, S. A.; He, Y.; Wang, L.; Zhang, Q.; Kim, A.; Gao, R.; Orf, J.; Wang, T.; Sawant, D.; Kang, J.; Bhatt, D.; Lu, D.; Li, C. M.; Rapaport, A. S.; Perez, K.; Ye, Y.; Wang, S.; Hu, X.; Ren, X.; Ouyang, W.; Shen, Z.; Egen, J. G.; Zhang, Z.; Yu, X., Single-Cell Analyses Inform Mechanisms of Myeloid-Targeted Therapies in Colon Cancer. *Cell* **2020,** *181* (2), 442-459 e29.
168. Wu, F.; Fan, J.; He, Y.; Xiong, A.; Yu, J.; Li, Y.; Zhang, Y.; Zhao, W.; Zhou, F.; Li, W.; Zhang, J.; Zhang, X.; Qiao, M.; Gao, G.; Chen, S.; Chen, X.; Li, X.; Hou, L.; Wu, C.; Su, C.; Ren, S.; Odenthal, M.; Buettner, R.; Fang, N.; Zhou, C., Single-cell profiling of tumor heterogeneity and the microenvironment in advanced non-small cell lung cancer. *Nat Commun* **2021,** *12* (1), 2540.
169. Bischoff, P.; Trinks, A.; Obermayer, B.; Pett, J. P.; Wiederspahn, J.; Uhlitz, F.; Liang, X.; Lehmann, A.; Jurmeister, P.; Elsner, A.; Dziodzio, T.; Ruckert, J. C.; Neudecker, J.; Falk, C.; Beule, D.; Sers, C.; Morkel, M.; Horst, D.; Bluthgen, N.; Klauschen, F., Single-cell RNA sequencing reveals distinct tumor microenvironmental patterns in lung adenocarcinoma. *Oncogene* **2021,** *40* (50), 6748-6758.
170. Zhang, Y.; Narayanan, S. P.; Mannan, R.; Raskind, G.; Wang, X.; Vats, P.; Su, F.; Hosseini, N.; Cao, X.; Kumar-Sinha, C.; Ellison, S. J.; Giordano, T. J.; Morgan, T. M.; Pitchiaya, S.; Alva, A.; Mehra, R.; Cieslik, M.; Dhanasekaran, S. M.; Chinnaiyan, A. M., Single-cell analyses of renal cell cancers reveal insights into tumor microenvironment, cell of origin, and therapy response. *Proc Natl Acad Sci U S A* **2021,** *118* (24).
171. Gerhard, G. M.; Bill, R.; Messemaker, M.; Klein, A. M.; Pittet, M. J., Tumor-infiltrating dendritic cell states are conserved across solid human cancers. *J Exp Med* **2021,** *218* (1).
172. Chen, B.; Zhu, L.; Yang, S.; Su, W., Unraveling the Heterogeneity and Ontogeny of Dendritic Cells Using Single-Cell RNA Sequencing. *Front Immunol* **2021,** *12*, 711329.
173. Ren, X.; Zhang, L.; Zhang, Y.; Li, Z.; Siemers, N.; Zhang, Z., Insights Gained from Single-Cell Analysis of Immune Cells in the Tumor Microenvironment. *Annu Rev Immunol* **2021,** *39*, 583-609.
174. Grieshaber-Bouyer, R.; Radtke, F. A.; Cunin, P.; Stifano, G.; Levescot, A.; Vijaykumar, B.; Nelson-Maney, N.; Blaustein, R. B.; Monach, P. A.; Nigrovic, P. A.; ImmGen, C., The neutrotime transcriptional signature defines a single continuum of neutrophils across biological compartments. *Nat Commun* **2021,** *12* (1), 2856.
175. Ochocka, N.; Segit, P.; Walentynowicz, K. A.; Wojnicki, K.; Cyranowski, S.; Swatler, J.; Mieczkowski, J.; Kaminska, B., Single-cell RNA sequencing reveals functional heterogeneity of glioma-associated brain macrophages. *Nat Commun* **2021,** *12* (1), 1151.
176. Chen, K.; Wang, Q.; Li, M.; Guo, H.; Liu, W.; Wang, F.; Tian, X.; Yang, Y., Single-cell RNA-seq reveals dynamic change in tumor microenvironment during pancreatic ductal adenocarcinoma malignant progression. *EBioMedicine* **2021,** *66*, 103315.
177. Daley, D.; Mani, V. R.; Mohan, N.; Akkad, N.; Pandian, G.; Savadkar, S.; Lee, K. B.; Torres-Hernandez, A.; Aykut, B.; Diskin, B.; Wang, W.; Farooq, M. S.; Mahmud, A. I.; Werba, G.;

Morales, E. J.; Lall, S.; Wadowski, B. J.; Rubin, A. G.; Berman, M. E.; Narayanan, R.; Hundeyin, M.; Miller, G., NLRP3 signaling drives macrophage-induced adaptive immune suppression in pancreatic carcinoma. *J Exp Med* **2017,** *214* (6), 1711-1724.
178. Guo, J.; Liu, Y., INHBA promotes the proliferation, migration and invasion of colon cancer cells through the upregulation of VCAN. *J Int Med Res* **2021,** *49* (6), 3000605211014998.
179. Li, X.; Yang, Z.; Xu, S.; Wang, Z.; Jin, P.; Yang, X.; Zhang, Z.; Wang, Y.; Wei, X.; Fang, T.; Gao, Q., Targeting INHBA in Ovarian Cancer Cells Suppresses Cancer Xenograft Growth by Attenuating Stromal Fibroblast Activation. *Dis Markers* **2019,** *2019*, 7275289.
180. Seder, C. W.; Hartojo, W.; Lin, L.; Silvers, A. L.; Wang, Z.; Thomas, D. G.; Giordano, T. J.; Chen, G.; Chang, A. C.; Orringer, M. B.; Beer, D. G., Upregulated INHBA expression may promote cell proliferation and is associated with poor survival in lung adenocarcinoma. *Neoplasia* **2009,** *11* (4), 388-96.
181. Wang, C.; Yang, T.; Xiao, J.; Xu, C.; Alippe, Y.; Sun, K.; Kanneganti, T.-D.; Monahan Joseph, B.; Abu-Amer, Y.; Lieberman, J.; Mbalaviele, G., NLRP3 inflammasome activation triggers gasdermin D–independent inflammation. *Science Immunology 6* (64), eabj3859.
182. Kuriakose, T.; Kanneganti, T.-D., Gasdermin D Flashes an Exit Signal for IL-1. *Immunity* **2018,** *48* (1), 1-3.
183. Wang, M.; Chen, X.; Zhang, Y., Biological Functions of Gasdermins in Cancer: From Molecular Mechanisms to Therapeutic Potential. *Front Cell Dev Biol* **2021,** *9*, 638710.
184. Kaplanov, I.; Carmi, Y.; Kornetsky, R.; Shemesh, A.; Shurin, G. V.; Shurin, M. R.; Dinarello, C. A.; Voronov, E.; Apte, R. N., Blocking IL-1β reverses the immunosuppression in mouse breast cancer and synergizes with anti-PD-1 for tumor abrogation. *Proc Natl Acad Sci U S A* **2019,** *116* (4), 1361-1369.
185. Kiss, M.; Vande Walle, L.; Saavedra, P. H. V.; Lebegge, E.; Van Damme, H.; Murgaski, A.; Qian, J.; Ehling, M.; Pretto, S.; Bolli, E.; Keirsse, J.; Bardet, P. M. R.; Arnouk, S. M.; Elkrim, Y.; Schmoetten, M.; Brughmans, J.; Debraekeleer, A.; Fossoul, A.; Boon, L.; Raes, G.; van Loo, G.; Lambrechts, D.; Mazzone, M.; Beschin, A.; Wullaert, A.; Lamkanfi, M.; Van Ginderachter, J. A.; Laoui, D., IL1β Promotes Immune Suppression in the Tumor Microenvironment Independent of the Inflammasome and Gasdermin D. *Cancer Immunology Research* **2021,** *9* (3), 309-323.
186. Gabrilovich, D. I.; Nagaraj, S., Myeloid-derived suppressor cells as regulators of the immune system. *Nat Rev Immunol* **2009,** *9* (3), 162-74.
187. Youn, J. I.; Kumar, V.; Collazo, M.; Nefedova, Y.; Condamine, T.; Cheng, P.; Villagra, A.; Antonia, S.; McCaffrey, J. C.; Fishman, M.; Sarnaik, A.; Horna, P.; Sotomayor, E.; Gabrilovich, D. I., Epigenetic silencing of retinoblastoma gene regulates pathologic differentiation of myeloid cells in cancer. *Nat Immunol* **2013,** *14* (3), 211-20.
188. Weber, R.; Fleming, V.; Hu, X.; Nagibin, V.; Groth, C.; Altevogt, P.; Utikal, J.; Umansky, V., Myeloid-Derived Suppressor Cells Hinder the Anti-Cancer Activity of Immune Checkpoint Inhibitors. *Frontiers in immunology* **2018,** *9*, 1310-1310.
189. Martinez, F. O.; Gordon, S., The M1 and M2 paradigm of macrophage activation: time for reassessment. *F1000Prime Rep* **2014,** *6*, 13.
190. Azizi, E.; Carr, A. J.; Plitas, G.; Cornish, A. E.; Konopacki, C.; Prabhakaran, S.; Nainys, J.; Wu, K.; Kiseliovas, V.; Setty, M.; Choi, K.; Fromme, R. M.; Dao, P.; McKenney, P. T.; Wasti, R. C.; Kadaveru, K.; Mazutis, L.; Rudensky, A. Y.; Pe'er, D., Single-Cell Map of Diverse Immune Phenotypes in the Breast Tumor Microenvironment. *Cell* **2018,** *174* (5), 1293-1308 e36.
191. Borcherding, N.; Vishwakarma, A.; Voigt, A. P.; Bellizzi, A.; Kaplan, J.; Nepple, K.; Salem, A. K.; Jenkins, R. W.; Zakharia, Y.; Zhang, W., Mapping the immune environment in clear cell renal carcinoma by single-cell genomics. *Commun Biol* **2021,** *4* (1), 122.
192. Bi, K.; He, M. X.; Bakouny, Z.; Kanodia, A.; Napolitano, S.; Wu, J.; Grimaldi, G.; Braun, D. A.; Cuoco, M. S.; Mayorga, A.; DelloStritto, L.; Bouchard, G.; Steinharter, J.; Tewari, A. K.; Vokes, N. I.; Shannon, E.; Sun, M.; Park, J.; Chang, S. L.; McGregor, B. A.; Haq, R.; Denize, T.; Signoretti, S.; Guerriero, J. L.; Vigneau, S.; Rozenblatt-Rosen, O.; Rotem, A.; Regev, A.; Choueiri, T. K.; Van Allen, E. M., Tumor and immune reprogramming during immunotherapy in advanced renal

cell carcinoma. *Cancer Cell* **2021,** *39* (5), 649-661 e5.
193. Braun, D. A.; Street, K.; Burke, K. P.; Cookmeyer, D. L.; Denize, T.; Pedersen, C. B.; Gohil, S. H.; Schindler, N.; Pomerance, L.; Hirsch, L.; Bakouny, Z.; Hou, Y.; Forman, J.; Huang, T.; Li, S.; Cui, A.; Keskin, D. B.; Steinharter, J.; Bouchard, G.; Sun, M.; Pimenta, E. M.; Xu, W.; Mahoney, K. M.; McGregor, B. A.; Hirsch, M. S.; Chang, S. L.; Livak, K. J.; McDermott, D. F.; Shukla, S. A.; Olsen, L. R.; Signoretti, S.; Sharpe, A. H.; Irizarry, R. A.; Choueiri, T. K.; Wu, C. J., Progressive immune dysfunction with advancing disease stage in renal cell carcinoma. *Cancer Cell* **2021,** *39* (5), 632-648 e8.
194. Chen, Z.; Zhao, M.; Liang, J.; Hu, Z.; Huang, Y.; Li, M.; Pang, Y.; Lu, T.; Sui, Q.; Zhan, C.; Lin, M.; Guo, W.; Wang, Q.; Tan, L., Dissecting the single-cell transcriptome network underlying esophagus non-malignant tissues and esophageal squamous cell carcinoma. *EBioMedicine* **2021,** *69*, 103459.
195. Ridker, P. M.; MacFadyen, J. G.; Thuren, T.; Everett, B. M.; Libby, P.; Glynn, R. J., Effect of interleukin-1beta inhibition with canakinumab on incident lung cancer in patients with atherosclerosis: exploratory results from a randomised, double-blind, placebo-controlled trial. *Lancet* **2017,** *390* (10105), 1833-1842.
196. Garon, E. B.; Ardizzoni, A.; Barlesi, F.; Cho, B. C.; De Marchi, P.; Goto, Y.; Kowalski, D. M.; Lu, S.; Paz-Ares, L. G.; Spigel, D. R.; Spira, A. I.; Thomas, M.; Leung, M.; Baum, J.; Zhu, Z.; Oliveira Portella, M. d. S.; Yang, J. C.-H., CANOPY-A: A phase III, multicenter, randomized, double-blind, placebo-controlled trial evaluating canakinumab as adjuvant therapy in patients (pts) with completely resected non-small cell lung cancer (NSCLC). *Journal of Clinical Oncology* **2020,** *38* (15_suppl), TPS9075-TPS9075.
197. Garon, E. B.; Ardizzoni, A.; Barlesi, F.; Cho, B. C.; De Marchi, P.; Goto, Y.; Lu, S.; Paz-Ares, L. G.; Spigel, D. R.; Thomas, M.; Mookerjee, B.; Cazorla Arratia, P.; Baum, J.; Lau, Y.-Y. Y.; Zhu, Z.; Yang, J. C.-H., CANOPY-A: A phase III study of canakinumab as adjuvant therapy in patients with surgically resected non-small cell lung cancer (NSCLC). *Journal of Clinical Oncology* **2019,** *37* (15_suppl), TPS8570-TPS8570.
198. Swanson, K. V.; Deng, M.; Ting, J. P. Y., The NLRP3 inflammasome: molecular activation and regulation to therapeutics. *Nature Reviews Immunology* **2019,** *19* (8), 477-489.
199. Walev, I.; Reske, K.; Palmer, M.; Valeva, A.; Bhakdi, S., Potassium-inhibited processing of IL-1 beta in human monocytes. *Embo j* **1995,** *14* (8), 1607-14.
200. Murakami, T.; Ockinger, J.; Yu, J.; Byles, V.; McColl, A.; Hofer, A. M.; Horng, T., Critical role for calcium mobilization in activation of the NLRP3 inflammasome. *Proc Natl Acad Sci U S A* **2012,** *109* (28), 11282-7.
201. Tang, T.; Lang, X.; Xu, C.; Wang, X.; Gong, T.; Yang, Y.; Cui, J.; Bai, L.; Wang, J.; Jiang, W.; Zhou, R., CLICs-dependent chloride efflux is an essential and proximal upstream event for NLRP3 inflammasome activation. *Nat Commun* **2017,** *8* (1), 202.
202. Zhou, R.; Yazdi, A. S.; Menu, P.; Tschopp, J., A role for mitochondria in NLRP3 inflammasome activation. *Nature* **2011,** *469* (7329), 221-5.
203. Hornung, V.; Bauernfeind, F.; Halle, A.; Samstad, E. O.; Kono, H.; Rock, K. L.; Fitzgerald, K. A.; Latz, E., Silica crystals and aluminum salts activate the NALP3 inflammasome through phagosomal destabilization. *Nat Immunol* **2008,** *9* (8), 847-56.
204. Tzeng, T. C.; Schattgen, S.; Monks, B.; Wang, D.; Cerny, A.; Latz, E.; Fitzgerald, K.; Golenbock, D. T., A Fluorescent Reporter Mouse for Inflammasome Assembly Demonstrates an Important Role for Cell-Bound and Free ASC Specks during In Vivo Infection. *Cell Rep* **2016,** *16* (2), 571-582.
205. Lee-Sherick, A. B.; Jacobsen, K. M.; Henry, C. J.; Huey, M. G.; Parker, R. E.; Page, L. S.; Hill, A. A.; Wang, X.; Frye, S. V.; Earp, H. S.; Jordan, C. T.; DeRyckere, D.; Graham, D. K., MERTK inhibition alters the PD-1 axis and promotes anti-leukemia immunity. *JCI Insight* **2018,** *3* (21).
206. Caetano, M. S.; Younes, A. I.; Barsoumian, H. B.; Quigley, M.; Menon, H.; Gao, C.; Spires, T.; Reilly, T. P.; Cadena, A. P.; Cushman, T. R.; Schoenhals, J. E.; Li, A.; Nguyen, Q. N.; Cortez, M. A.; Welsh, J. W., Triple Therapy with MerTK and PD1 Inhibition Plus Radiotherapy Promotes

Abscopal Antitumor Immune Responses. *Clin Cancer Res* **2019,** *25* (24), 7576-7584.
207. Chen, C. J.; Liu, Y. P., MERTK Inhibition: Potential as a Treatment Strategy in EGFR Tyrosine Kinase Inhibitor-Resistant Non-Small Cell Lung Cancer. *Pharmaceuticals (Basel)* **2021,** *14* (2).
208. Lin, D.; Kang, X.; Shen, L.; Tu, S.; Lenahan, C.; Chen, Y.; Wang, X.; Shao, A., Efferocytosis and Its Associated Cytokines: A Light on Non-tumor and Tumor Diseases? *Mol Ther Oncolytics* **2020,** *17*, 394-407.
209. Bergen, V.; Soldatov, R. A.; Kharchenko, P. V.; Theis, F. J., RNA velocity-current challenges and future perspectives. *Mol Syst Biol* **2021,** *17* (8), e10282.
210. Cairo, C.; Webb, T. J., Effective Barriers: The Role of NKT Cells and Innate Lymphoid Cells in the Gut. *J Immunol* **2022,** *208* (2), 235-246.
211. Theocharidis, G.; Thomas, B. E.; Sarkar, D.; Mumme, H. L.; Pilcher, W. J. R.; Dwivedi, B.; Sandoval-Schaefer, T.; Sirbulescu, R. F.; Kafanas, A.; Mezghani, I.; Wang, P.; Lobao, A.; Vlachos, I. S.; Dash, B.; Hsia, H. C.; Horsley, V.; Bhasin, S. S.; Veves, A.; Bhasin, M., Single cell transcriptomic landscape of diabetic foot ulcers. *Nat Commun* **2022,** *13* (1), 181.
212. Vallelian, F.; Buzzi, R. M.; Pfefferle, M.; Yalamanoglu, A.; Dubach, I. L.; Wassmer, A.; Gentinetta, T.; Hansen, K.; Humar, R.; Schulthess, N.; Schaer, C. A.; Schaer, D. J., Heme-stress activated NRF2 skews fate trajectories of bone marrow cells from dendritic cells towards red pulp-like macrophages in hemolytic anemia. *Cell Death Differ* **2022**.
213. Wu, X.; Kasmani, M. Y.; Zheng, S.; Khatun, A.; Chen, Y.; Winkler, W.; Zander, R.; Burns, R.; Taparowsky, E. J.; Sun, J.; Cui, W., BATF promotes group 2 innate lymphoid cell-mediated lung tissue protection during acute respiratory virus infection. *Sci Immunol* **2022,** *7* (67), eabc9934.
214. Elliott, M. R.; Ravichandran, K. S., The Dynamics of Apoptotic Cell Clearance. *Dev Cell* **2016,** *38* (2), 147-160.
215. Lantz, C.; Radmanesh, B.; Liu, E.; Thorp, E. B.; Lin, J., Single-cell RNA sequencing uncovers heterogenous transcriptional signatures in macrophages during efferocytosis. *Sci Rep* **2020,** *10* (1), 14333.
216. Morioka, S.; Perry, J. S. A.; Raymond, M. H.; Medina, C. B.; Zhu, Y.; Zhao, L.; Serbulea, V.; Onengut-Gumuscu, S.; Leitinger, N.; Kucenas, S.; Rathmell, J. C.; Makowski, L.; Ravichandran, K. S., Efferocytosis induces a novel SLC program to promote glucose uptake and lactate release. *Nature* **2018,** *563* (7733), 714-718.
217. Zhang, S.; Weinberg, S.; DeBerge, M.; Gainullina, A.; Schipma, M.; Kinchen, J. M.; Ben-Sahra, I.; Gius, D. R.; Yvan-Charvet, L.; Chandel, N. S.; Schumacker, P. T.; Thorp, E. B., Efferocytosis Fuels Requirements of Fatty Acid Oxidation and the Electron Transport Chain to Polarize Macrophages for Tissue Repair. *Cell Metab* **2019,** *29* (2), 443-456 e5.
218. Zhou, T.; Damsky, W.; Weizman, O. E.; McGeary, M. K.; Hartmann, K. P.; Rosen, C. E.; Fischer, S.; Jackson, R.; Flavell, R. A.; Wang, J.; Sanmamed, M. F.; Bosenberg, M. W.; Ring, A. M., IL-18BP is a secreted immune checkpoint and barrier to IL-18 immunotherapy. *Nature* **2020,** *583* (7817), 609-614.
219. Chmielewski, M.; Abken, H., CAR T Cells Releasing IL-18 Convert to T-Bet(high) FoxO1(low) Effectors that Exhibit Augmented Activity against Advanced Solid Tumors. *Cell Rep* **2017,** *21* (11), 3205-3219.
220. McDonald, B.; Pittman, K.; Menezes, G. B.; Hirota, S. A.; Slaba, I.; Waterhouse, C. C.; Beck, P. L.; Muruve, D. A.; Kubes, P., Intravascular danger signals guide neutrophils to sites of sterile inflammation. *Science* **2010,** *330* (6002), 362-6.
221. Smith, J. P.; Lister, A. M.; Tew, J. G.; Szakal, A. K., Kinetics of the tingible body macrophage response in mouse germinal center development and its depression with age. *Anat Rec* **1991,** *229* (4), 511-20.
222. Yi, Y. S., Functional Role of Milk Fat Globule-Epidermal Growth Factor VIII in Macrophage-Mediated Inflammatory Responses and Inflammatory/Autoimmune Diseases. *Mediators Inflamm* **2016,** *2016*, 5628486.
223. Gregory, C. D.; Paterson, M., An apoptosis-driven 'onco-regenerative niche': roles of tumour-associated macrophages and extracellular vesicles. *Philos Trans R Soc Lond B Biol Sci* **2018,** *373*

(1737).
224. Lipponen, P., Apoptosis in breast cancer: relationship with other pathological parameters. *Endocr Relat Cancer* **1999,** *6* (1), 13-6.
225. Nishimura, R.; Nagao, K.; Miyayama, H.; Matsuda, M.; Baba, K.; Matsuoka, Y.; Yamashita, H.; Fukuda, M.; Higuchi, A., Apoptosis in breast cancer and its relationship to clinicopathological characteristics and prognosis. *J Surg Oncol* **1999,** *71* (4), 226-34.
226. Sinicrope, F. A.; Hart, J.; Hsu, H. A.; Lemoine, M.; Michelassi, F.; Stephens, L. C., Apoptotic and mitotic indices predict survival rates in lymph node-negative colon carcinomas. *Clin Cancer Res* **1999,** *5* (7), 1793-804.
227. Vaquero, J.; Zurita, M.; Aguayo, C.; Coca, S., Relationship between apoptosis and proliferation in secondary tumors of the brain. *Neuropathology* **2004,** *24* (4), 302-5.
228. Petrovski, G.; Ayna, G.; Majai, G.; Hodrea, J.; Benko, S.; Madi, A.; Fesus, L., Phagocytosis of cells dying through autophagy induces inflammasome activation and IL-1beta release in human macrophages. *Autophagy* **2011,** *7* (3), 321-30.
229. Dupaul-Chicoine, J.; Arabzadeh, A.; Dagenais, M.; Douglas, T.; Champagne, C.; Morizot, A.; Rodrigue-Gervais, I. G.; Breton, V.; Colpitts, S. L.; Beauchemin, N.; Saleh, M., The Nlrp3 Inflammasome Suppresses Colorectal Cancer Metastatic Growth in the Liver by Promoting Natural Killer Cell Tumoricidal Activity. *Immunity* **2015,** *43* (4), 751-63.
230. Beswick Ellen, J., Inflammasome activation to protect against colorectal cancer metastasis? *Science Translational Medicine* **2015,** *7* (314), 314ec196-314ec196.
231. Kumar, S.; Calianese, D.; Birge, R. B., Efferocytosis of dying cells differentially modulate immunological outcomes in tumor microenvironment. *Immunol Rev* **2017,** *280* (1), 149-164.
232. Rios-Doria, J.; Favata, M.; Lasky, K.; Feldman, P.; Lo, Y.; Yang, G.; Stevens, C.; Wen, X.; Sehra, S.; Katiyar, K.; Liu, K.; Wynn, R.; Harris, J. J.; Ye, M.; Spitz, S.; Wang, X.; He, C.; Li, Y.-L.; Yao, W.; Covington, M.; Scherle, P.; Koblish, H., A Potent and Selective Dual Inhibitor of AXL and MERTK Possesses Both Immunomodulatory and Tumor-Targeted Activity. *Front Oncol* **2020,** *10*, 598477-598477.
233. Caspase-1 Activity in CD4 T Cells Is Downregulated Following Antiretroviral Therapy for HIV-1 Infection. *AIDS Research and Human Retroviruses* **2017,** *33* (2), 164-171.
234. Doitsh, G.; Galloway, N. L.; Geng, X.; Yang, Z.; Monroe, K. M.; Zepeda, O.; Hunt, P. W.; Hatano, H.; Sowinski, S.; Muñoz-Arias, I., Cell death by pyroptosis drives CD4 T-cell depletion in HIV-1 infection. *Nature* **2014,** *505* (7484), 509-514.
235. Jin, X.; Zhou, R.; Huang, Y., Role of inflammasomes in HIV-1 infection and treatment. *Trends Mol Med* **2022,** *28* (5), 421-434.
236. Zhang, C.; Song, J.-W.; Huang, H.-H.; Fan, X.; Huang, L.; Deng, J.-N.; Tu, B.; Wang, K.; Li, J.; Zhou, M.-J., NLRP3 inflammasome induces CD4+ T cell loss in chronically HIV-1–infected patients. *The Journal of clinical investigation* **2021,** *131* (6).
237. Monroe, K. M.; Yang, Z.; Johnson, J. R.; Geng, X.; Doitsh, G.; Krogan, N. J.; Greene, W. C., IFI16 DNA sensor is required for death of lymphoid CD4 T cells abortively infected with HIV. *Science* **2014,** *343* (6169), 428-432.
238. Toksoy, A.; Sennefelder, H.; Adam, C.; Hofmann, S.; Trautmann, A.; Goebeler, M.; Schmidt, M., Potent NLRP3 inflammasome activation by the HIV reverse transcriptase inhibitor abacavir. *Journal of Biological Chemistry* **2017,** *292* (7), 2805-2814.
239. Martin, B. N.; Wang, C.; Zhang, C.-j.; Kang, Z.; Gulen, M. F.; Zepp, J. A.; Zhao, J.; Bian, G.; Do, J.-s.; Min, B., T cell–intrinsic ASC critically promotes TH17-mediated experimental autoimmune encephalomyelitis. *Nature immunology* **2016,** *17* (5), 583-592.
240. Javanmard Khameneh, H.; Leong, K. W. K.; Mencarelli, A.; Vacca, M.; Mambwe, B.; Neo, K.; Tay, A.; Zolezzi, F.; Lee, B.; Mortellaro, A., The inflammasome adaptor ASC intrinsically limits CD4+ T-cell proliferation to help maintain intestinal homeostasis. *Frontiers in immunology* **2019**, 1566.
241. Bruchard, M.; Rebé, C.; Derangère, V.; Togbé, D.; Ryffel, B.; Boidot, R.; Humblin, E.; Hamman, A.; Chalmin, F.; Berger, H., The receptor NLRP3 is a transcriptional regulator of TH 2 differentiation. *Nature immunology* **2015,** *16* (8), 859-870.

242. Chou, W.-C.; Guo, Z.; Guo, H.; Chen, L.; Zhang, G.; Liang, K.; Xie, L.; Tan, X.; Gibson, S. A.; Rampanelli, E.; Wang, Y.; Montgomery, S. A.; Brickey, W. J.; Deng, M.; Freeman, L.; Zhang, S.; Su, M. A.; Chen, X.; Wan, Y. Y.; Ting, J. P. Y., AIM2 in regulatory T cells restrains autoimmune diseases. *Nature* **2021,** *591* (7849), 300-305.
243. Chen, L.; Hou, W.; Liu, F.; Zhu, R.; Lv, A.; Quan, W.; Mao, S., Blockade of NLRP3/Caspase-1/IL-1β Regulated Th17/Treg Immune Imbalance and Attenuated the Neutrophilic Airway Inflammation in an Ovalbumin-Induced Murine Model of Asthma. *J Immunol Res* **2022,** *2022*, 9444227.
244. Arbore, G.; West, E. E.; Spolski, R.; Robertson, A. A. B.; Klos, A.; Rheinheimer, C.; Dutow, P.; Woodruff, T. M.; Yu, Z. X.; O'Neill, L. A.; Coll, R. C.; Sher, A.; Leonard, W. J.; Köhl, J.; Monk, P.; Cooper, M. A.; Arno, M.; Afzali, B.; Lachmann, H. J.; Cope, A. P.; Mayer-Barber, K. D.; Kemper, C., T helper 1 immunity requires complement-driven NLRP3 inflammasome activity in $CD4^+$ T cells. *Science* **2016,** *352* (6292), aad1210.
245. Salazar, Y.; Zheng, X.; Brunn, D.; Raifer, H.; Picard, F.; Zhang, Y.; Winter, H.; Guenther, S.; Weigert, A.; Weigmann, B.; Dumoutier, L.; Renauld, J. C.; Waisman, A.; Schmall, A.; Tufman, A.; Fink, L.; Brüne, B.; Bopp, T.; Grimminger, F.; Seeger, W.; Pullamsetti, S. S.; Huber, M.; Savai, R., Microenvironmental Th9 and Th17 lymphocytes induce metastatic spreading in lung cancer. *J Clin Invest* **2020,** *130* (7), 3560-3575.
246. Wilke, C. M.; Kryczek, I.; Wei, S.; Zhao, E.; Wu, K.; Wang, G.; Zou, W., Th17 cells in cancer: help or hindrance? *Carcinogenesis* **2011,** *32* (5), 643-9.
247. Protopsaltis, N. J.; Liang, W.; Nudleman, E.; Ferrara, N., Interleukin-22 promotes tumor angiogenesis. *Angiogenesis* **2019,** *22* (2), 311-323.
248. Jenkins, R. W.; Barbie, D. A.; Flaherty, K. T., Mechanisms of resistance to immune checkpoint inhibitors. *British Journal of Cancer* **2018,** *118* (1), 9-16.
249. Restifo, N. P.; Smyth, M. J.; Snyder, A., Acquired resistance to immunotherapy and future challenges. *Nat Rev Cancer* **2016,** *16* (2), 121-6.
250. Pitt, J. M.; Vétizou, M.; Daillère, R.; Roberti, M. P.; Yamazaki, T.; Routy, B.; Lepage, P.; Boneca, I. G.; Chamaillard, M.; Kroemer, G.; Zitvogel, L., Resistance Mechanisms to Immune-Checkpoint Blockade in Cancer: Tumor-Intrinsic and -Extrinsic Factors. *Immunity* **2016,** *44* (6), 1255-69.
251. Kouro, T.; Himuro, H.; Sasada, T., Exhaustion of CAR T cells: potential causes and solutions. *Journal of Translational Medicine* **2022,** *20* (1), 239.
252. Razeghian, E.; Nasution, M. K. M.; Rahman, H. S.; Gardanova, Z. R.; Abdelbasset, W. K.; Aravindhan, S.; Bokov, D. O.; Suksatan, W.; Nakhaei, P.; Shariatzadeh, S.; Marofi, F.; Yazdanifar, M.; Shamlou, S.; Motavalli, R.; Khiavi, F. M., A deep insight into CRISPR/Cas9 application in CAR-T cell-based tumor immunotherapies. *Stem Cell Research & Therapy* **2021,** *12* (1), 428.
253. Rakoff-Nahoum, S.; Medzhitov, R., Regulation of spontaneous intestinal tumorigenesis through the adaptor protein MyD88. *Science* **2007,** *317* (5834), 124-7.
254. Fabbi, M.; Carbotti, G.; Ferrini, S., Context-dependent role of IL-18 in cancer biology and counter-regulation by IL-18BP. *J Leukoc Biol* **2015,** *97* (4), 665-75.
255. Deng, Q.; Geng, Y.; Zhao, L.; Li, R.; Zhang, Z.; Li, K.; Liang, R.; Shao, X.; Huang, M.; Zuo, D.; Wu, Y.; Ma, Q., NLRP3 inflammasomes in macrophages drive colorectal cancer metastasis to the liver. *Cancer Lett* **2019,** *442*, 21-30.
256. van Deventer, H. W.; Burgents, J. E.; Wu, Q. P.; Woodford, R. M.; Brickey, W. J.; Allen, I. C.; McElvania-Tekippe, E.; Serody, J. S.; Ting, J. P., The inflammasome component NLRP3 impairs antitumor vaccine by enhancing the accumulation of tumor-associated myeloid-derived suppressor cells. *Cancer Res* **2010,** *70* (24), 10161-9.
257. Ginhoux, F.; Schultze, J. L.; Murray, P. J.; Ochando, J.; Biswas, S. K., New insights into the multidimensional concept of macrophage ontogeny, activation and function. *Nat Immunol* **2016,** *17* (1), 34-40.
258. Tajbakhsh, A.; Gheibi Hayat, S. M.; Movahedpour, A.; Savardashtaki, A.; Loveless, R.; Barreto, G. E.; Teng, Y.; Sahebkar, A., The complex roles of efferocytosis in cancer development,

metastasis, and treatment. *Biomed Pharmacother* **2021,** *140*, 111776.
259. Zhou, Y.; Yao, Y.; Deng, Y.; Shao, A., Regulation of efferocytosis as a novel cancer therapy. *Cell Commun Signal* **2020,** *18* (1), 71.
260. Crittenden, M. R.; Baird, J.; Friedman, D.; Savage, T.; Uhde, L.; Alice, A.; Cottam, B.; Young, K.; Newell, P.; Nguyen, C.; Bambina, S.; Kramer, G.; Akporiaye, E.; Malecka, A.; Jackson, A.; Gough, M. J., Mertk on tumor macrophages is a therapeutic target to prevent tumor recurrence following radiation therapy. *Oncotarget* **2016,** *7* (48), 78653-78666.
261. Martins, I.; Raza, S. Q.; Voisin, L.; Dakhli, H.; Allouch, A.; Law, F.; Sabino, D.; De Jong, D.; Thoreau, M.; Mintet, E.; Dugue, D.; Piacentini, M.; Gougeon, M. L.; Jaulin, F.; Bertrand, P.; Brenner, C.; Ojcius, D. M.; Kroemer, G.; Modjtahedi, N.; Deutsch, E.; Perfettini, J. L., Anticancer chemotherapy and radiotherapy trigger both non-cell-autonomous and cell-autonomous death. *Cell Death Dis* **2018,** *9* (7), 716.
262. Jiang, M. J.; Gu, D. N.; Dai, J. J.; Huang, Q.; Tian, L., Dark Side of Cytotoxic Therapy: Chemoradiation-Induced Cell Death and Tumor Repopulation. *Trends Cancer* **2020,** *6* (5), 419-431.
263. Kroemer, G.; Galluzzi, L.; Kepp, O.; Zitvogel, L., Immunogenic cell death in cancer therapy. *Annu Rev Immunol* **2013,** *31*, 51-72.
264. Galluzzi, L.; Buque, A.; Kepp, O.; Zitvogel, L.; Kroemer, G., Immunogenic cell death in cancer and infectious disease. *Nat Rev Immunol* **2017,** *17* (2), 97-111.
265. Pitt, J. M.; Kroemer, G.; Zitvogel, L., Immunogenic and Non-immunogenic Cell Death in the Tumor Microenvironment. *Adv Exp Med Biol* **2017,** *1036*, 65-79.
266. Fucikova, J.; Kepp, O.; Kasikova, L.; Petroni, G.; Yamazaki, T.; Liu, P.; Zhao, L.; Spisek, R.; Kroemer, G.; Galluzzi, L., Detection of immunogenic cell death and its relevance for cancer therapy. *Cell Death Dis* **2020,** *11* (11), 1013.
267. Fabian, K. P.; Wolfson, B.; Hodge, J. W., From Immunogenic Cell Death to Immunogenic Modulation: Select Chemotherapy Regimens Induce a Spectrum of Immune-Enhancing Activities in the Tumor Microenvironment. *Front Oncol* **2021,** *11*, 728018.
268. Ahmed, A.; Tait, S. W. G., Targeting immunogenic cell death in cancer. *Mol Oncol* **2020,** *14* (12), 2994-3006.
269. Zhou, J.; Wang, G.; Chen, Y.; Wang, H.; Hua, Y.; Cai, Z., Immunogenic cell death in cancer therapy: Present and emerging inducers. *J Cell Mol Med* **2019,** *23* (8), 4854-4865.
270. Ott, P. A.; Hu-Lieskovan, S.; Chmielowski, B.; Govindan, R.; Naing, A.; Bhardwaj, N.; Margolin, K.; Awad, M. M.; Hellmann, M. D.; Lin, J. J.; Friedlander, T.; Bushway, M. E.; Balogh, K. N.; Sciuto, T. E.; Kohler, V.; Turnbull, S. J.; Besada, R.; Curran, R. R.; Trapp, B.; Scherer, J.; Poran, A.; Harjanto, D.; Barthelme, D.; Ting, Y. S.; Dong, J. Z.; Ware, Y.; Huang, Y.; Huang, Z.; Wanamaker, A.; Cleary, L. D.; Moles, M. A.; Manson, K.; Greshock, J.; Khondker, Z. S.; Fritsch, E.; Rooney, M. S.; DeMario, M.; Gaynor, R. B.; Srinivasan, L., A Phase Ib Trial of Personalized Neoantigen Therapy Plus Anti-PD-1 in Patients with Advanced Melanoma, Non-small Cell Lung Cancer, or Bladder Cancer. *Cell* **2020,** *183* (2), 347-362.e24.
271. Pantelidou, C.; Sonzogni, O.; De Oliveria Taveira, M.; Mehta, A. K.; Kothari, A.; Wang, D.; Visal, T.; Li, M. K.; Pinto, J.; Castrillon, J. A.; Cheney, E. M.; Bouwman, P.; Jonkers, J.; Rottenberg, S.; Guerriero, J. L.; Wulf, G. M.; Shapiro, G. I., PARP Inhibitor Efficacy Depends on CD8(+) T-cell Recruitment via Intratumoral STING Pathway Activation in BRCA-Deficient Models of Triple-Negative Breast Cancer. *Cancer Discov* **2019,** *9* (6), 722-737.
272. Jiao, S.; Xia, W.; Yamaguchi, H.; Wei, Y.; Chen, M. K.; Hsu, J. M.; Hsu, J. L.; Yu, W. H.; Du, Y.; Lee, H. H.; Li, C. W.; Chou, C. K.; Lim, S. O.; Chang, S. S.; Litton, J.; Arun, B.; Hortobagyi, G. N.; Hung, M. C., PARP Inhibitor Upregulates PD-L1 Expression and Enhances Cancer-Associated Immunosuppression. *Clin Cancer Res* **2017,** *23* (14), 3711-3720.
273. Nakamura, T.; Sato, T.; Endo, R.; Sasaki, S.; Takahashi, N.; Sato, Y.; Hyodo, M.; Hayakawa, Y.; Harashima, H., STING agonist loaded lipid nanoparticles overcome anti-PD-1 resistance in melanoma lung metastasis via NK cell activation. *J Immunother Cancer* **2021,** *9* (7).
274. Li, A.; Yi, M.; Qin, S.; Song, Y.; Chu, Q.; Wu, K., Activating cGAS-STING pathway for the optimal effect of cancer immunotherapy. *J Hematol Oncol* **2019,** *12* (1), 35.

275. Wang, W.; Hu, D.; Wu, C.; Feng, Y.; Li, A.; Liu, W.; Wang, Y.; Chen, K.; Tian, M.; Xiao, F.; Zhang, Q.; Shereen, M. A.; Chen, W.; Pan, P.; Wan, P.; Wu, K.; Wu, J., STING promotes NLRP3 localization in ER and facilitates NLRP3 deubiquitination to activate the inflammasome upon HSV-1 infection. *PLoS Pathog* **2020,** *16* (3), e1008335.
276. Wan, D.; Jiang, W.; Hao, J., Research Advances in How the cGAS-STING Pathway Controls the Cellular Inflammatory Response. *Front Immunol* **2020,** *11*, 615.
277. Gaidt, M. M.; Ebert, T. S.; Chauhan, D.; Ramshorn, K.; Pinci, F.; Zuber, S.; O'Duill, F.; Schmid-Burgk, J. L.; Hoss, F.; Buhmann, R.; Wittmann, G.; Latz, E.; Subklewe, M.; Hornung, V., The DNA Inflammasome in Human Myeloid Cells Is Initiated by a STING-Cell Death Program Upstream of NLRP3. *Cell* **2017,** *171* (5), 1110-1124 e18.
278. Kumar, S.; Calianese, D.; Birge, R. B., Efferocytosis of dying cells differentially modulate immunological outcomes in tumor microenvironment. *Immunol Rev* **2017,** *280* (1), 149-164.
279. Rios-Doria, J.; Favata, M.; Lasky, K.; Feldman, P.; Lo, Y.; Yang, G.; Stevens, C.; Wen, X.; Sehra, S.; Katiyar, K.; Liu, K.; Wynn, R.; Harris, J. J.; Ye, M.; Spitz, S.; Wang, X.; He, C.; Li, Y. L.; Yao, W.; Covington, M.; Scherle, P.; Koblish, H., A Potent and Selective Dual Inhibitor of AXL and MERTK Possesses Both Immunomodulatory and Tumor-Targeted Activity. *Front Oncol* **2020,** *10*, 598477.
280. Clavijo, P. E.; Moore, E. C.; Chen, J.; Davis, R. J.; Friedman, J.; Kim, Y.; Van Waes, C.; Chen, Z.; Allen, C. T., Resistance to CTLA-4 checkpoint inhibition reversed through selective elimination of granulocytic myeloid cells. *Oncotarget* **2017,** *8* (34), 55804-55820.
281. Socinski, M. A.; Jotte, R. M.; Cappuzzo, F.; Orlandi, F.; Stroyakovskiy, D.; Nogami, N.; Rodríguez-Abreu, D.; Moro-Sibilot, D.; Thomas, C. A.; Barlesi, F.; Finley, G.; Kelsch, C.; Lee, A.; Coleman, S.; Deng, Y.; Shen, Y.; Kowanetz, M.; Lopez-Chavez, A.; Sandler, A.; Reck, M., Atezolizumab for First-Line Treatment of Metastatic Nonsquamous NSCLC. *N Engl J Med* **2018,** *378* (24), 2288-2301.
282. Zhai, Z.; Liu, W.; Kaur, M.; Luo, Y.; Domenico, J.; Samson, J. M.; Shellman, Y. G.; Norris, D. A.; Dinarello, C. A.; Spritz, R. A.; Fujita, M., NLRP1 promotes tumor growth by enhancing inflammasome activation and suppressing apoptosis in metastatic melanoma. *Oncogene* **2017,** *36* (27), 3820-3830.
283. Hu, B.; Elinav, E.; Huber, S.; Booth, C. J.; Strowig, T.; Jin, C.; Eisenbarth, S. C.; Flavell, R. A., Inflammation-induced tumorigenesis in the colon is regulated by caspase-1 and NLRC4. *Proc Natl Acad Sci U S A* **2010,** *107* (50), 21635-40.
284. Kayagaki, N.; Warming, S.; Lamkanfi, M.; Vande Walle, L.; Louie, S.; Dong, J.; Newton, K.; Qu, Y.; Liu, J.; Heldens, S.; Zhang, J.; Lee, W. P.; Roose-Girma, M.; Dixit, V. M., Non-canonical inflammasome activation targets caspase-11. *Nature* **2011,** *479* (7371), 117-21.
285. Tanzer, M. C.; Frauenstein, A.; Stafford, C. A.; Phulphagar, K.; Mann, M.; Meissner, F., Quantitative and Dynamic Catalogs of Proteins Released during Apoptotic and Necroptotic Cell Death. *Cell Reports* **2020,** *30* (4), 1260-1270.e5.